BENZODIAZEPINE COORDINATION CHEMISTRY AND NITROGEN HETEROCYCLIC COMPOUNDS FROM REACTIONS OF CARBONYL ALKYNES WITH *O*-PHENYLENEDIAMINES

by

DYLAN JOSEPH TWARDY

A dissertation submitted in partial fulfillment of the
requirements for the degree of

DOCTOR OF PHILOSOPHY IN
BIOMEDICAL SCIENCES

2022

Oakland University
Rochester, Michigan

Doctoral Advisory Committee:

Roman Dembinski, Ph.D., Chair
Ngong Kodiah Beyeh, Ph.D.
Ferman Chavez, Ph.D.
Kraig Wheeler, Ph.D.
Ziming Yang, Ph.D.

To my parents,

Marie A. Twardy and Daniel J. Twardy

ACKNOWLEDGMENTS

Dr. Roman Dembinski allowed me the privilege to work alongside him in his synthetic organic chemistry lab. I am forever grateful for the knowledge his experience imparted and the hand he always lent. Equally important, the research for this dissertation could not have been achieved without the persistent help of my team: Yousif, Fahro, Garrett, and Dr. Wheeler (Whitworth University).

I would like to thank Dr. Török and Dr. Mishra for our work in *Green Chemistry* and my committee at Oakland University: Dr. Chavez, Dr. Beyeh, and Dr. Yang.

I am grateful to Dr. Mukulesh Mondal and Dr. Manashi (Panda) Mondal for teaching me synthesis techniques. I thank Trevor, Owen, Sam, Katie, Dr. Ibrahim, and Dr. Mance for their intelligent influence and extend the remark to Dr. Kerrigan, Dr. Xia, and their students Dr. Chen, Dr. Peraino, Dr. Kahn, Dr. Mittelstaedt, and Dr. Badar.

Warm regards to Oakland University for funding me and to its chemistry department for these educational opportunities. Special thanks to Mr. Love, Managers Ms. Daly and Ms. Jones, Ms. Kosaski, and Ms. Bialke for a professional environment.

To my parents, Dan and Marie, my brothers Jordan and Dr. Brandon, my sister-in-law Kristen, and to the unnamed faculty, staff, or peers that in any way have helped me or inspired me over the past years, thank you from the bottom of my heart.

Dylan Joseph Twardy

ABSTRACT

BENZODIAZEPINE COORDINATION CHEMISTRY AND
NITROGEN HETEROCYCLIC COMPOUNDS
FROM REACTIONS OF CARBONYL ALKYNES WITH *O*-PHENYLENEDIAMINES

by

DYLAN JOSEPH TWARDY

Adviser: Roman Dembinski, Ph.D.

The presence of heterocyclic compounds in active pharmaceutical ingredients and natural products implicates their importance to synthetic chemistry. Moreover, their inherent structures offer potential as metal-chelators. This work involved the design of simple methods for the construction of new nitrogen-containing heterocycles and to explore examples of coordination complexes. Benzodiazepines and their derivatives are biologically active heterocycles often prescribed as a treatment for anxiety, epilepsy, and insomnia. In addition, benzimidazo[2,1-*a*]isoquinolines are another class of biologically active heterocycles that are composed of moieties inherent to a wide variety of active pharmaceutical ingredients. Herein, the microwave-assisted reaction in ethanol of *o*-phenylenediamines with either alk-2-ynones or 2-ethynyl benzaldehydes was found to yield 1,5-benzodiazepines and benzimidazo[2,1-*a*]isoquinolines, respectively. To facilitate selective coordination of benzodiazepines, new pyridine containing 1,5-benzodiazepine chelators were synthesized and combined with metal reagents to form new benzodiazepine metal complexes characterized by X-ray crystallography.

TABLE OF CONTENTS

TABLE OF CONTENTS—Continued

TABLE OF CONTENTS—Continued

TABLE OF CONTENTS—Continued

LIST OF TABLES

LIST OF TABLES—Continued

LIST OF FIGURES

LIST OF ABBREVIATIONS

Ac	Acetyl group
Anal	(Elemental) analysis
Calcd	Calculated
Cp*	Pentamethylcyclopentadienyl
d	Doublet (for NMR spectra) or day(s)
DCE	Dichloroethane
DMF	Dimethylformamide
DSC	Differential scanning calorimetry
ε	Extinction coefficient (UV-vis)
equiv.	Equivalent(s)
EPR	Electron paramagnetic resonance (spectroscopy)
Et	Ethyl group
GC-MS	Gas chromatography mass spectrometry
h	Hour(s)
HRMS	High-resolution mass spectrometry
IR	Infrared spectroscopy
LC-MS	Liquid chromatography mass spectrometry
m	Multiplet (for NMR spectra)
Me	Methyl group
MHz	Megahertz
MW	Microwave irradiation

m/z	Mass to charge ratio
N_{BZD}	Chelating diazepine-ring nitrogen
4-Nitro-*o*-phd	4-Nitro-*o*-phenylenediamine
NMR	Nuclear magnetic resonance (spectroscopy)
nm	Nanometer(s)
N_{py}	Chelating pyridine-ring nitrogen
PCy_3	Tricyclohexylphosphine
PivOH	Pivalic acid (2,2-dimethylpropanoic acid)
PMA	Phosphomolybdic acid
ppm	Parts per million
PTSA	*p*-Toluenesulfonic acid
rt	Room temperature
s	Singlet (for NMR spectra)
t	Triplet (for NMR spectra)
$TBAPF_6$	Tetrabutylammonium hexafluorophosphate
THF	Tetrahydrofuran
TLC	Thin layer chromatography
TMS	Tetramethylsilane
UV-vis	Ultraviolet-visible (spectroscopy)
λ_{max}	Wavelength of maximum absorbance in a UV-vis spectrum

CHAPTER ONE

SYNTHESIS OF PYRIDINE-SUBSTITUTED 1,5-BENZODIAZEPINES

1.1. Introduction

1.1.1. Significance of benzodiazepines

Benzodiazepines are a class of heterocyclic compounds that have received attention for their biological effects and medicinal applications.[1] Due to their varied structural features, these compounds offer different types of chemical and biological properties.[1] Benzodiazepines have also been applied as ligands in new bimetallic catalysts[2] and as complexing agents for metal-concentration measurement in samples.[3] Often cited as a treatment for anxiety and insomnia,[4] benzodiazepines are primarily utilized as active pharmaceutical ingredients.

The US Food and Drug Administration (FDA) has reported an estimated 92 million benzodiazepine prescriptions from U.S. pharmacies in 2019.[5,6] Although benzodiazepines are used often clinically and their abuse potential is lower as compared to other drug classes,[7] there are country-specific guidelines for their use that sometimes diverge.[6,8 9] Moreover, benzodiazepines' addictive qualities are well documented[10] and their long-term use has been associated with mental decline.[11,12] This compound class demonstrates useful properties but also adverse side effects, providing an impetus to examine their molecular structure more closely.

1.1.2. Important benzodiazepine isomers

Benzodiazepines are structurally distinguished by the presence of a benzene ring fused to a seven-membered heterocyclic ring containing two nitrogen atoms.[13]

Benzodiazepines are further classified based on the seven-membered ring's internal nitrogen atom positions relative to the benzene ring. In nomenclature, the benzodiazepine nitrogen closest to the benzene ring is given priority, followed by the adjacent carbon furthest from the benzene ring (Figures 1.1). [1] In addition, letter designations are sometimes given to indicate the position at which the two rings are fused (not depicted).[1]

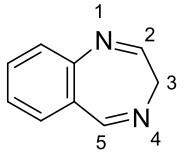

3*H*-1,4-benzodiazepine

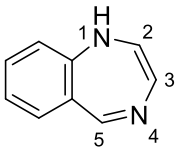

1*H*-1,4-benzodiazepine

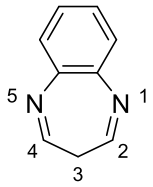

3*H*-1,5-benzodiazepine

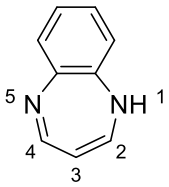

1*H*-1,5-beznodiazepine

Figure 1.1 The general structure of 1,4-benzodiazepines and 1,5-benzodiazepines.

A review of clinically used benzodiazepines showed that a substantial number of 1,4-benzodiazepines have been approved for medical use. Diazepam and alprazolam (Xanax and Valium respectively, Figure 1.2) are commonly prescribed to treat anxiety or insomnia.[13,14] In some countries, the pyridine-substituted bromazepam (Lexotan) is an approved anxiolytic.[15,16] Flumazenil (Romazicon) is FDA-approved to postoperatively

sedate patients that are under other benzodiazepine anesthetics or reverse the effects from a benzodiazepine overdose.[17] The American Psychiatric Association (APA) endorses the use of the 1,4-benzodiazepine lorazepam (Ativan, Figure 1.2) and the 1,5-benzodiazepine olanzapine (Zyprexa, Figure 1.3) in their list of antipsychotic treatments. Moreover, clozapine (Clozaril) is recommended by the APA to be carefully administered in the effective treatment of psychological disorders resistant to other medications (*e.g.*, severe schizophrenia).[18] Notably, clozapine is commonly referred to as a 1,4-benzodiazepine, but because its structure includes two aromatic rings fused to the seven-membered ring, opposite assignment of nitrogen priority would result in a 1,5-benzodiazepine designation instead.

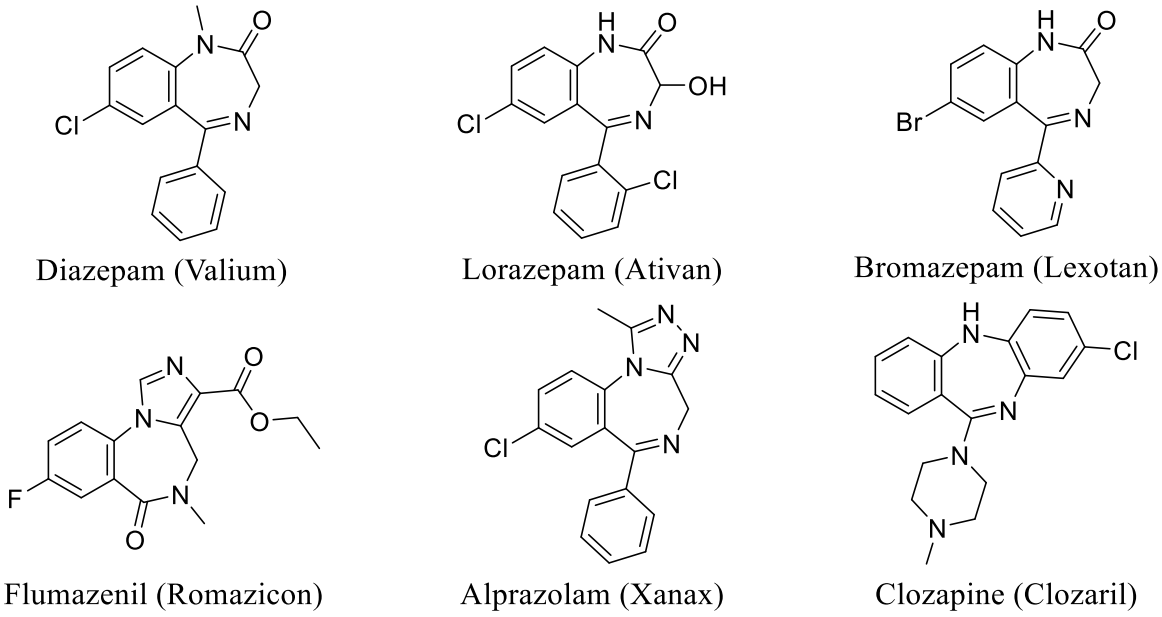

Figure 1.2 Examples of 1,4-benzodiazepines approved for medicinal use.

In determining which types of benzodiazepines to pursue, priority was placed on benzodiazepines that showed underutilized application. It was observed that, besides olanzapine, there are relatively few 1,5-benzodiazepines in clinical use (Figure 1.2) despite success in their clinical application. For instance, clobazam (Onfi), shown in Figure 1.3, was approved in 2011 by the FDA to treat Lennox-Gastaut syndrome and is used to treat refractory epilepsy.[19] Moreover, studies exemplify the antiviral, antibacterial, or antifungal activity of 1,5-benzodiazepines.[13,20,21] In an assay screening of over 10,000 compounds, Fader *et al.* have recently identified the 1,5-dihydrobenzo[*f*][1,5]diazepine-2,4-dione as an inhibitor of a unique step in the HIV life cycle (Figure 1.3).[21] One aim of this dissertation is to expand the variety of available 1,5-benzodiazepines because of their useful biological activity.

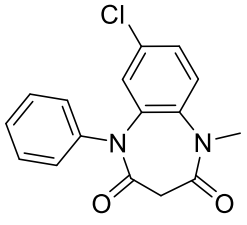

Clobazam (Onfi)

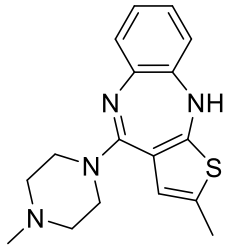

Olanzapine (Zyprexa)

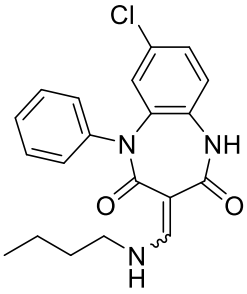

1,5-Dihydrobenzo[*f*] [1,5]diazepine-2,4-dione

Figure 1.3 Examples of pharmaceutically important 1,5-benzodiazepines.

1.1.3. 1,5-Benzodiazepines with pyridine substituents

In reviewing the present literature on benzodiazepine, insight was gained regarding useful substituents to include. Among the diverse 1,5-benzodiazepine substituents to consider, there is some indication that heterocyclic substituents may provide unique properties to the 1,5-benzodiazepine compound class.[21] For example, some studies investigated the synthesis and biological activity of heteroatomic ring-substituted 1,5-benzodiazepines.[21,22] Regarding biological activity, Nevirapine is an FDA approved non-nucleoside reverse transcriptase inhibitor for HIV treatment,[23] and An *et al*. found the pyridine ring had enhanced antifungal properties of a 1,5-benzodiazepine (Figure 1.4).[20] Both compounds (Figure 1.4) feature the fundamental 1,5-benzodiazepine structure along with connected pyridine rings, implicating pyridine as a key fragment.

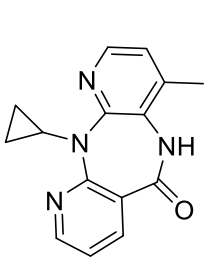

Nevirapine (Viramune)

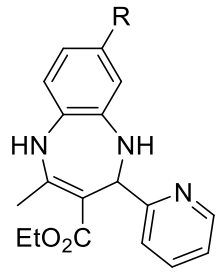

1,5-Benzodiazepine by An *et al.*

Figure 1.4 Nonnucleoside reverse transcriptase inhibitor 1,5-benzodiazepine and antibacterial/antifungal 1,5-benzodiazepine.

This dissertation includes the synthesis of pyridine-substituted 1,5-benzodiazepines containing two imine groups illustrated in Figure 1.5.

Attachment of a pyridine ring onto one of the imine carbons was chosen because of the limited synthetic reports of the specific scaffold, the implications of biological activity from the pyridine substituent,[21,22] and the potential coordination capabilities of the structure. Molecules such as these are intriguing from a synthetic standpoint due to the preparative challenges caused by the presence of the pyridine ring. A successful synthesis was also desirable in order to investigate such described ligands' metal-complexation properties.

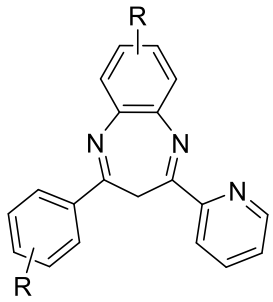

Figure 1.5 The core molecular framework of the 1,5-benzodiazepines investigated in this work.

1.1.4. Preparation of 1,5-benzodiazepines

In order to propose new methods, several 1,5-benzodiazepine preparations have been thoroughly examined,[24] with a recent preparative review by Arora *et al.*[13] Many of these protocols employ an imination reaction between a pair of amine functional groups and a pair of carbonyl functional groups. Other protocols utilize bifunctional starting materials in place of dicarbonyl compounds.[13] These methods differ in their yields and

research objectives, and these differences help define the direction of methods designed in this dissertation and demonstrate the value of simple reactions.

1.1.5. Synthesis of 1,5-benzodiazepines from dicarbonyl compounds

1,5-Benzodiazepine-2,4-dione derivatives have received special attention for their discovered potential as antiviral therapeutics,[21] among other uses,[19] and these compounds are readily synthesized through the reaction of amines and 1,3-dicarbonyl compounds. For example, 1,5-benzodiazepine-2,4-dione derivatives can be synthesized through the reaction of 1,3-propanedioic acid (malonic acid; Figure 1.6, X = OH).[25,26] This group of protocols is distinguished in that the hydroxyl group is replaced and the carbonyl groups are preserved in the final product, with contemporary studies reporting 45–73% yield.[26] Other 1,3-dicarbonyl compounds with better leaving groups are often employed to achieve similar outcomes via a substitution reaction.

Malonyl dichloride derivatives are more often employed in reactions with substituted *o*-phenylenediamines to produce 1,5-benzodiazepines. In this scenario, a substitution reaction occurs where an amine again displaces a leaving group (*e.g.*,

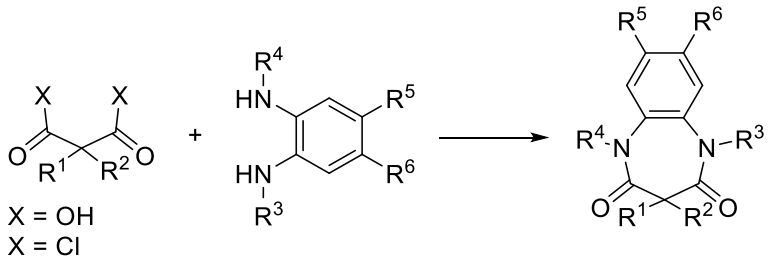

Figure 1.6 1,5-Benzodiazepine synthetic methods using 1,3-dicarbonyl starting materials.

chlorine, see Figure 1.6, X = Cl). Investigations that used the type of protocol illustrated in Figure 1.6 are appropriate strategies to synthesize a variety of symmetric and nonsymmetric 1,5-benzodiazepines (37–92% yields) and additionally allow optional diversification at C–3.[21,22,27–31]

Gümüş *et al*. reported diversification at C–2 and C–4 using specific 1,3-dicarbonyl starting materials.[32] The starting material consisted of two different functional groups that were used in the reaction: a ketone and an acyl halide (Figure 1.7). In using asymmetric diamines, the bifunctional reagent allowed regioselective synthesis, and the authors demonstrated this through the preparation of 1,5-benzodiazepines with diverse substituents (68–81% yield). This route is distinguished by the presence of both an imine and an amide function in the final benzodiazepine. The bifunctional carbonyl compound allows regioselective synthesis, and the acyl chloride-derived carbonyl function remains in the final structure (infer from Figure 1.7). Subsequent steps would be required to convert the benzodiazepine's carbonyl into a different substituent.

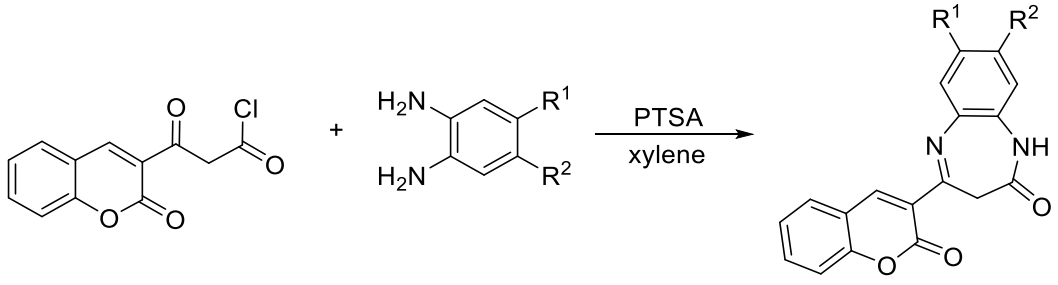

Figure 1.7 Tandem imination and substitution reaction using bifunctional compounds.

Dicarbonyl substrates can also be used in the preparation of pyridine substituents on 1,5-benzodiazepines, as demonstrated in the literature.[20,21] In one case, a 3-oxobutanoate is reacted with a diamine to form an enaminoate, which is reacted with pyridine-2-carbaldehyde in the presence of phosphomolybdic acid (PMA) to yield pyridine-substituted benzodiazepines.[20] In addition, it was found that a pyridine substituent (R = H, Me, Br, see Figure 1.8) had, on average, a larger zone of inhibition against *C. neoformans* (averages 23.1 mm vs. 6.00 mm) and *C. neoformans* clinical isolate (averages 24.0 mm vs. 15.2 mm) than having a phenyl substituent instead.[20]

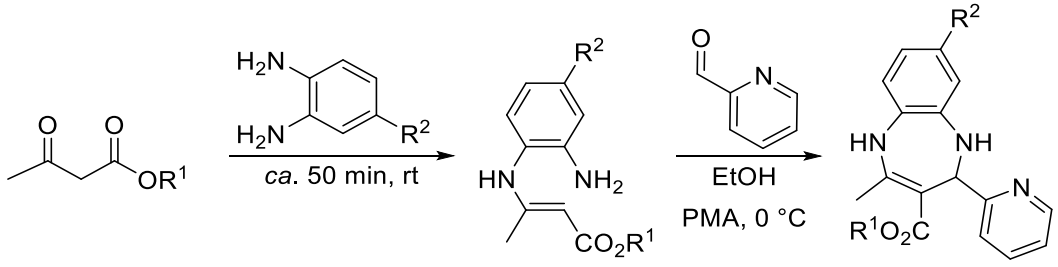

Figure 1.8 Acid catalyzed synthesis of pyridine-substituted 1,5-benzodiazepines.

A different type of 1,3-dicarbonyl compound, a 1,3-diketone, can also be used in the preparation of 1,5-benzodiazepines with > 90% yields, as reported in Vaddula *et al.*[33] The synthetic route is distinguished in that two amine groups are converted into imines via imination of the carbonyl groups (see Figure 1.9). Like malonyl dichloride-based protocols, this method can provide a route to diversification at C–3 and allow symmetrical substituents at either C–2 or C–4.

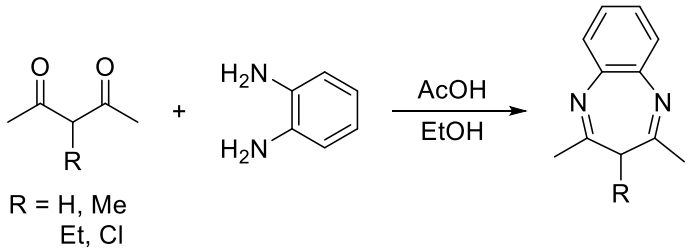

Figure 1.9 Representative synthesis of 1,5-benzodiazepines through a condensation reaction of acetylacetone derivatives with *o*-phenylenediamine.

A literature search indicated that protocols starting from 1,3-dicarbonyl compounds are not typically used to prepare nonsymmetric regioisomers (with regard to the *o*-phenylenediamine) in one step. The similar reactivity of the two carbonyl groups makes these routes prone to forming regioisomers in the presence of asymmetric *o*-phenylenediamines, and in some cases, multistep syntheses are employed to produce specific regioisomers. For example, An *et al*. studied the reaction of a functionalized enaminoate with 2-pyridinecarboxaldehyde catalyzed by PMA (Figure 1.8).[20] The authors' synthesis of a pyridine-substituted 1,5-benzodiazepine provided a protocol with yields of 85–95%.

1.1.6. Synthesis of 1,5-benzodiazepines from alkynones

Alkynones, or more informally alkynyl ketones, are versatile substrates used to prepare a library of organic compounds,[34] which includes 1,5-benzodiazepines.[24] Alk-2-ynones can react with *o*-phenylenediamines to produce benzodiazepines.[35] In an unspecific order, reactions generally proceed through a Michael addition by the nucleophilic amine function to the alkyne moiety and imination by the second amine function upon the ketone carbonyl group.[24,36,37]

A contemporary synthesis using alkynones was reported by Willy *et al*. in which a one-pot, two-step method combines a Sonogashira coupling and a cyclocondensation reaction (Figure 1.10).[35] The method produces alkynones *in situ* and reacts them subsequently with a variety of *o*-phenylenediamines. The resultant products are purified by column chromatography to provide benzodiazepines in 40–88% yields.[35] There are few other methods,[38] which offer the opportunity to improve the existing literature for the synthesis of benzodiazepines.

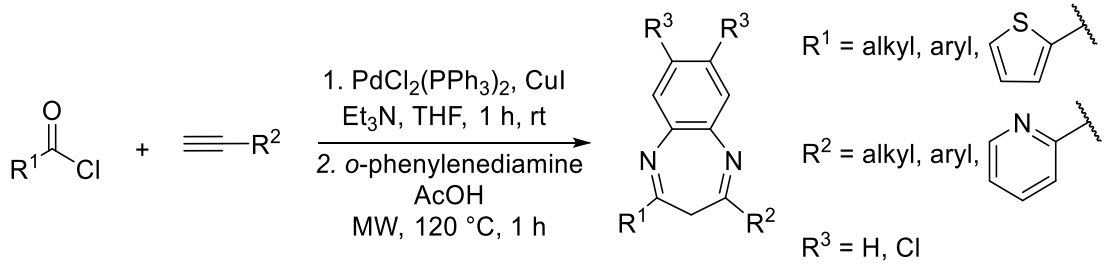

Figure 1.10 Synthesis of 1,5-benzodiazepines from acyl chlorides and terminal alkynes.

Solan *et al*. and Young *et al*. have developed a synthetic protocol for 1,5-benzodiazepines from alk-3-ynones and *o*-phenylenediamines (Figure 1.11).[36,37] The protocol is distinguished by the isolation of but-3-yn-1-ones and their subsequent reaction with *o*-phenylenediamines. The method was successfully applied to a variety of alkynones, with 70–99% yields for the corresponding 1,5-benzodiazepines, and avoided the use of column chromatography.

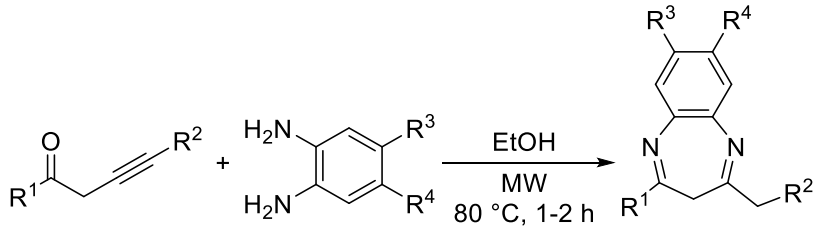

Figure 1.11 Synthesis of diversely substituted 1,5-benzodiazepines from but-3-yn-1-ones and *o*-phenylenediamines.

1.1.7. Synthetic design for the preparation of pyridine-substituted 1,5-benzodiazepines

The design of a simple protocol for preparing new pyridine-substituted 1,5-benzodiazepines, with keen interest in imine diazepine nitrogens, was presented here. Focus was placed on the inclusion of bifunctional starting materials and mild conditions. The retrosynthetic outline prepares a benzodiazepine from an alk-2-ynone and a *o*-phenylenediamine. Alkynones are advantageous in their ability to allow substitution at C–2 and C–4, so Willy *et al*.[35,38] and Young *et al*.'s[37] preparations were influential in the retrosynthetic design (Figure 1.12). The discussion shown below describes the reaction of alkynone and *o*-phenylenediamine and its ability to produce the target 1,5-benzodiazepine, which is proceeded by coupling of an acyl chloride to 2-ethynyl pyridine.

With regards to the substituents, the 1,5-benzodiazepine target molecules are designed to enhance crystallization for simple purification and to provide a convenient analytical marker to monitor the experiments. Aromatic ring substituents were specifically chosen to facilitate molecular packing in the solid-state. The target molecule in Figure 1.12 included an aliphatic group on the aromatic ring substituent to provide an

unobscured signal in the ^{1}H NMR. The methyl group in the product benzodiazepine is spectrally distinguished from the methyl group of its corresponding alkynone starting material.

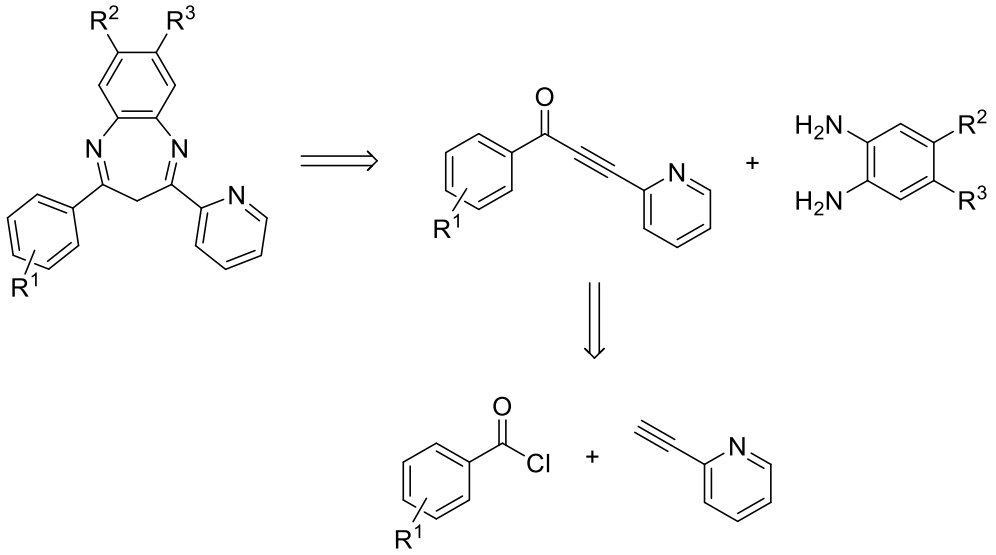

Figure 1.12 Retrosynthetic analysis of pyridine-substituted 1,5-benzodiazepines.

1.2. Results and discussion

1.2.1. Preparation of prop-2-yn-1-ones

To synthesize the pyridine-substituted alkynone substrate, a Sonogashira coupling was devised with the pyridine substituent delivered via reaction of a terminal acetylene with an aroyl chloride. Reviewing the literature, a variety of protocols to couple acyl chlorides and terminal acetylenes to form prop-2-yn-1-ones were found.[34,39–41] Within the literature, there were relatively few thorough reports focusing on the synthesis of a prop-

2-yn-1-one, or similar structures, from nicotinoyl chloride and an aryl terminal acetylene.[42–45] and this made the establishment of the outlined method (refer back to Figure 1.12) more valuable in terms of its novelty. Common to many of those reviewed protocols was a two-step procedure and/or the use of highly functionalized starting materials. However, an alternative combination of starting materials includes aroyl chlorides and 2-ethynyl pyridine, and Willy *et al*. produced pyridine-substituted alk-2-ynones *in situ* by this combination.[35]

A room-temperature reaction, with similar conditions to the protocols in Willy *et al*.,[35] was undertaken using 2-ethynyl pyridine and *p*-toluoyl chloride, but ^{1}H NMR analysis of the resultant product did not yield evidence that the targeted pyridine alk-2-ynone forms readily. Other protocols that involve amine-substituted acetylene substrates within a one-step, room-temperature Sonogashira coupling were also considered.[46,47] Specifically, Obulesu *et al.* reported the preparation of pyridine-substituted prop-2-yn-1-ones from 2-ethynyl pyridine and aroyl chlorides in the presence of zinc chloride (yields not reported).[47]

An experiment applying the protocol from Obulesu *et al.*[47] was undertaken, but the formation of the desired product was not observed by GC-MS. Zinc chloride, as a Lewis acid, may complex with the pyridine ring. Therefore, zinc chloride was omitted in subsequent attempts. Applying previously elaborated conditions by our group,[48] a slightly modified procedure was developed for the synthesis of pyridine-substituted prop-2-yn-1-ones by employing tetrakis(triphenylphosphine)palladium(0) in the absence of auxiliary metals[49] and increasing the reaction temperature to 70 °C (Figure 1.13). Moreover, a smaller mole percent of palladium was used as compared to similar palladium couplings

(1 mol% vs. 2 mol%);[50] the acetylene was used in slight excess to assist with complete consumption of the acyl chloride. Like most small acetylene molecules, 2-ethynyl pyridine is volatile and can be removed from the reaction much easier than acyl chlorides, thereby simplifying purification.

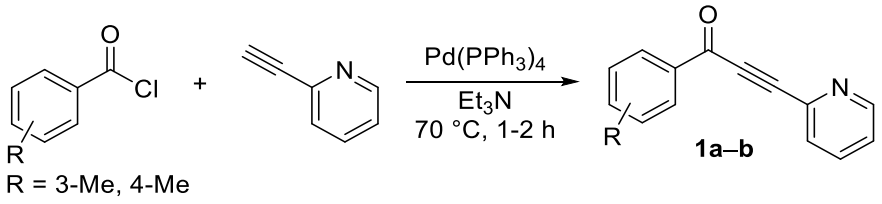

Figure 1.13 Synthesis of pyridine-substituted prop-2-yn-1-ones (**1a**–**b**).

With THF as a solvent, triethylamine can be added as a base to counteract the formation of HCl during the coupling, but it was found that the procedure is simpler using it as both the solvent and base. The reaction was monitored by GC-MS, and nearly complete depletion of the acyl chloride limiting reagent was observed, so complete conversion was assumed.

The prop-2-yn-1-ones (**1a**–**b**) were separated from the palladium catalyst by filtration, and its formation was confirmed by GC-MS. The ^{1}H and ^{13}C NMR of the product after solvent removal also confirmed formation of the prop-2-yn-1-one and the consumption of the acyl chloride but revealed the presence of triethylamine hydrochloride. Given the purity and the main objectives, no alternative protocol was

investigated, and the crude material was used in the subsequent step without further purification.

1.2.2. Preparation of 1,5-benzodiazepines

A general protocol was developed to form 1,5-benzodiazepines from prop-2-yn-1-ones (**1a**–**b**). Imination of the alkyne and ketone functional groups by *o*-phenylenediamine was found to proceed in ethanol when irradiated at 80 °C by a microwave reactor (Figure 1.14). The product was isolated readily through crystallization and in addition to GC-MS, consumption of the starting alkynone was observed by

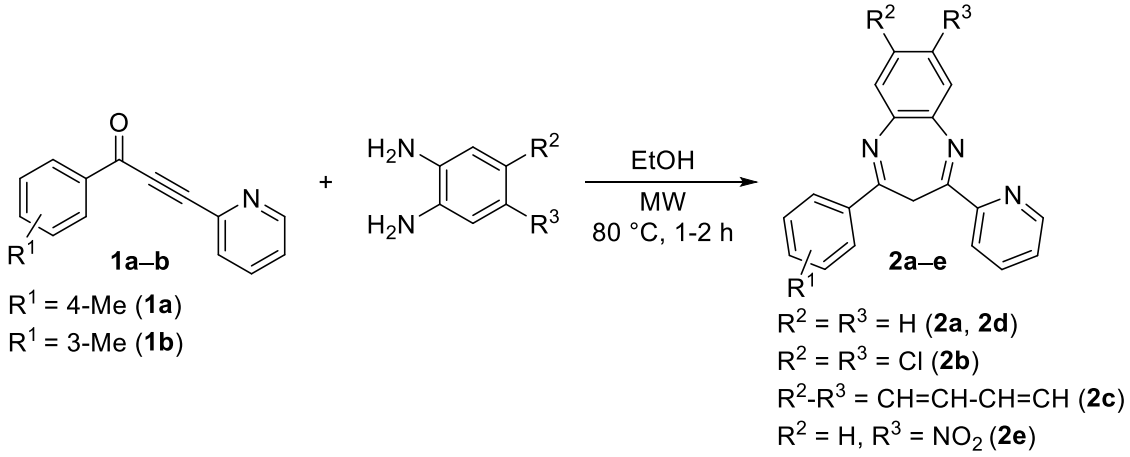

Figure 1.14 Synthesis of pyridine-substituted 1,5-benzodiazepines (refer to Table 1.1).

NMR (*e.g.*, 1.89 ppm for *p*-toluoyl derived alkynone **1a** aliphatic methyl group versus 2.36 ppm for the corresponding benzodiazepine **2a**, see Table 1.1, entry 1)

The brief screening conducted to probe the scope and limitations of the protocol is shown in Table 1.1. Comparing entry 1 to entries 2 and 3 demonstrates the protocol was

mildly sensitive to substituents on symmetrical diamines (66%, 67%, and 40%, respectively). For entry 4, a *m*-tolyl substituent caused differences in the resulting benzodiazepine. The recrystallized *m*-tolyl benzodiazepine **2d** appeared different in color, particle size, and density compared to the structurally similar *p*-tolyl benzodiazepine **2a**. Moreover, attempts were made at synthesizing nonsymmetrical derivatives with regards to the *o*-phenylenediamine (entries 5 and 6).

The implementation of nonsymmetrical *o*-phenylenediamines in a bifunctional benzodiazepine synthesis has precedence.[36,37] These preparations achieve regioselectivity through the formation and isolation of an enaminone intermediate. To check the inherent regioselectivity of the designed protocol, 4-nitro-*o*-phenylenediamine was used with this benzodiazepine synthesis and the result was a mixture of isomers (*ca*. 70:30 by ^{1}H NMR integration; Figure 1.15). To synthesize a single benzodiazepine regioisomer, the corresponding enaminone **3** was first isolated by hampering the imination reaction of the carbonyl group through the inclusion of triethylamine, resulting in a 60% yield (Figure 1.16). Subsequent cyclization of the enaminone under microwave conditions with catalytic amounts of acetic acid leads to a single 1,5-benzodiazepine regioisomer (Figure 1.17). The nitro substituted 1,5-benzodiazepine (**2e**) was isolated with 87% yield with respect to the starting enaminone **3** (overall yield of 52%).

Compounds **2a**–**e** (Table 1.1) were characterized by NMR, HRMS and UV-vis. The compounds' ^{1}H and ^{13}C NMR allowed for spectral assignment, with integrations and splitting patterns matching those expected from these structures. Compound masses were detected in HRMS and these matched theoretical molecular weights. Furthermore, the

Table 1.1 Synthesized benzodiazepines **2a**–**e**.

Entry	Alkynone		Diamine	Product		Yield[%][a]
1	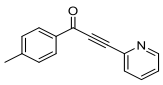	**1a**		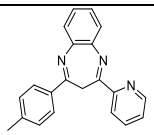	**2a**	66
2	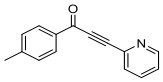	**1a**	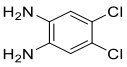	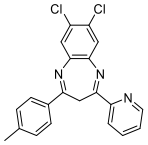	**2b**	67
3	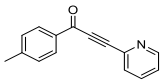	**1a**	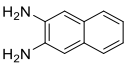	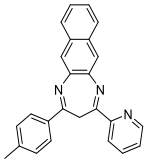	**2c**	40
4	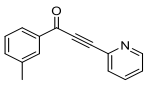	**1b**		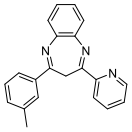	**2d**	82[b]
5	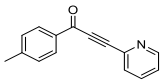	**1a**	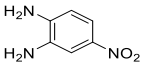	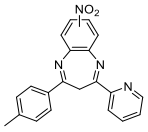	**n/a**	n.d.[c] *ca.* 70:30
6	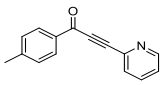	**1a**	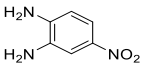	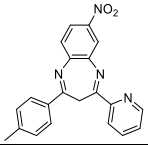	**2e**	52

a) Yields were calculated from the starting acyl chloride
b) Yield includes product from multiple recrystallizations of the mother liquor
c) Not determined (n.d.); a mixture of regioisomers was obtained

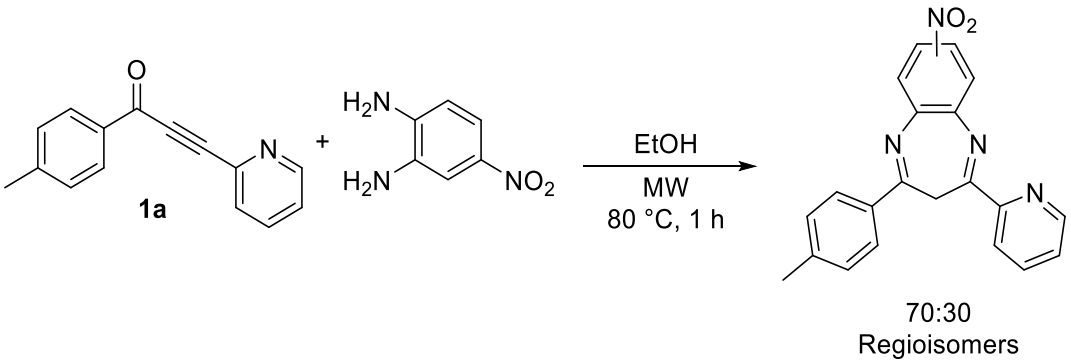

Figure 1.15 Preparation of regioisomer mixture of compound **2e**.

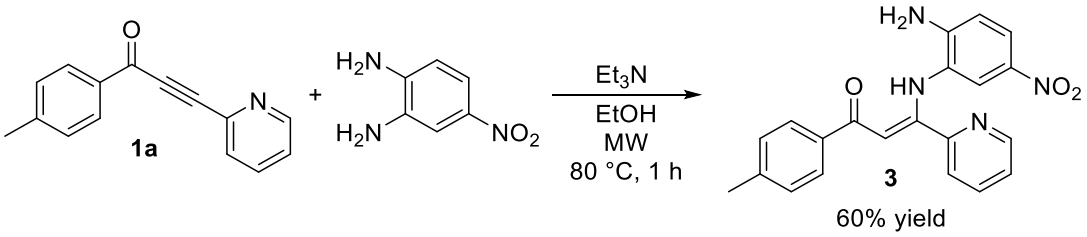

Figure 1.16 Preparation of enaminone intermediate **3**.

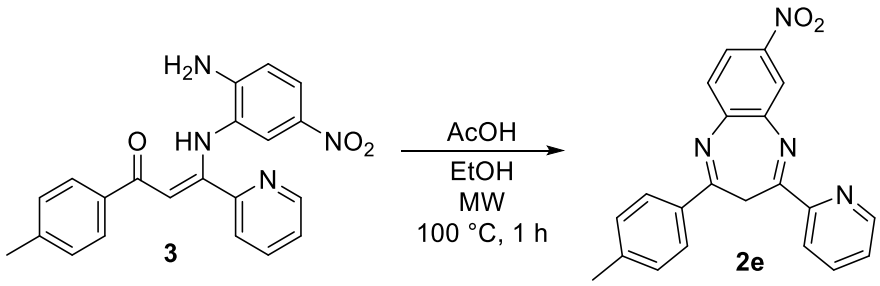

Figure 1.17 Preparation of nitro-substituted 1,5-benzodiazepine **2e**.

experimental UV-vis spectra consistently indicated at least one major absorbance maximum, occurring at the wavelength λ_{max}, for these compounds (Table 1.2). Compound **2e** had conspicuous absorbance peaks, where the peak observed at 295 nm had a larger absorbance than at 251 nm, which is illustrated in the molar extinction coefficient (28,100 vs. 23,800). On average, benzodiazepines **2a**–**e** had a λ_{max} of 284 nm (Table 1.2). The synthesized 1,5-benzodiazepines' pyridine and imine nitrogens could coordinate to a metal center, and thus form an optimal five-membered chelate ring. Another target for this dissertation was to explore metal complexes of these compounds since such interactions could take place *in vivo*.

Table 1.2 UV-vis absorbance maxima for benzodiazepines **2a**–**e** (CH_2Cl_2, 23 °C).

Structure	λ_{max} [nm]	ε [$M^{-1}cm^{-1}$]
2a	277	29,500
2b	282	27,300
2c	291	34,100
2d	273	31,200
2e	295	28,100

1.2.3. Attempted preparation of pyridine-substituted but-3-yn-1-ones

In preparing to investigate 1,5-benzodiazepine metal coordination compounds, consideration was made to the size of the ring that would theoretically form in a hypothesized coordination compound. Generally, five-membered chelation rings are balanced between ring flexibility and stability,[51] but attempts were made to synthesize 1,5-benzodiazepines that would allow larger ring chelation sizes.

A benzodiazepine with an additional carbon between its chelating nitrogens was designed, and its retrosynthesis is shown in Figure 1.18. A homopropargyl alcohol derivative was first synthesized as depicted in Figure 1.19. 2-Ethynylpyridine reacted with lithium diisopropylamine to form a lithium acetylide. Nucleophilic attack of the acetylide on styrene oxide led to the but-3-yn-1-ol product **4** in *ca.* 50% yield. Conversion of the starting materials into but-3-yn-1-ol **4** was confirmed by GC-MS and ^{1}H and ^{13}C NMR.

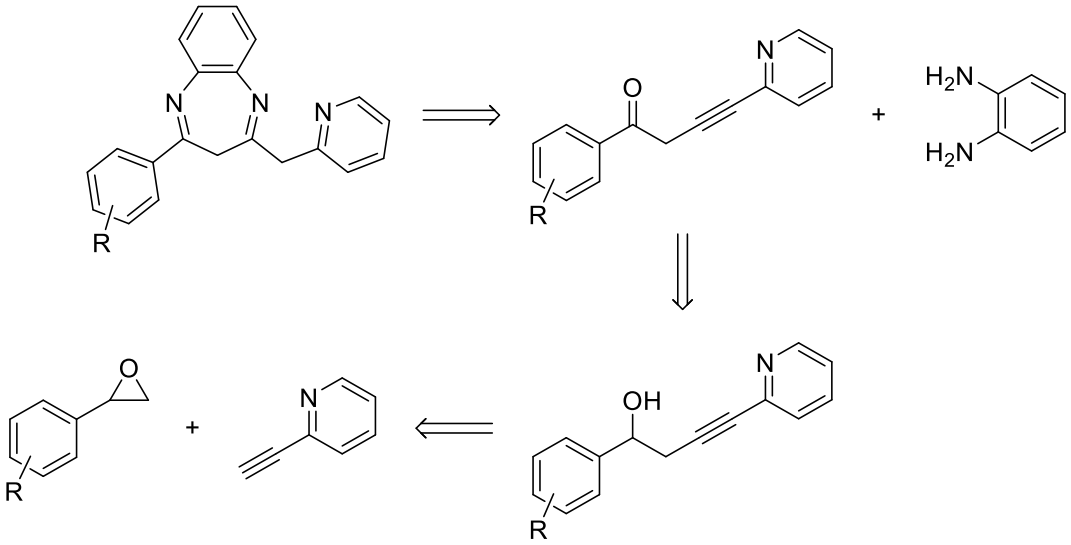

Figure 1.18 Retrosynthesis of pyridine methylene substituted 1,5-benzodiazepines.

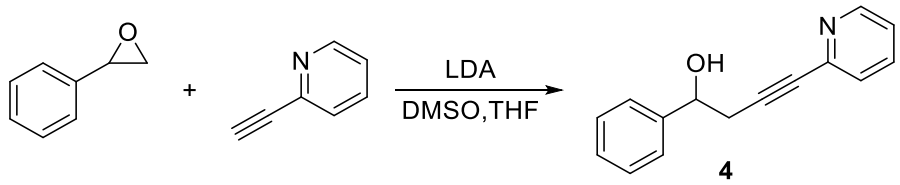

Figure 1.19 Synthesis of but-3-yn-1-ol **4**.

The next objective was to synthesize a pyridine propargyl ketone **5** from its but-3-yn-1-ol precursor, compound **4** (Figure 1.20). Propargyl ketones have been prepared from but-3-yn-1-ols using either Jones reagent or Dess-Martin periodinate.[52] However, neither oxidant appeared to produce the desired product. The Jones reagent was initially thought to oxidize the alcohol, and thereby provide complete conversion of the alcohol into its corresponding ketone, but the proton NMR signals did not indicate the presence of the

methylene group adjacent to the carbonyl carbon. In a previous work from our laboratory, the molecular ion of aryl-substituted alk-3-ynone **5** was detected by

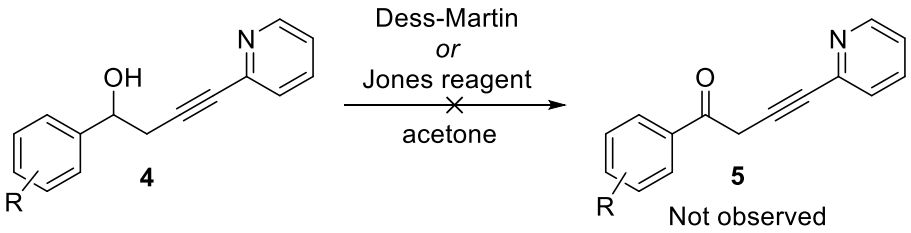

Figure 1.20 Attempted synthesis of but-3-yn-1-ones.

GC-MS, but the pyridine-containing molecular ion was not found in the GC-MS analysis of current experiments. Given the preparation of similar structures without the pyridine ring,[52] it was thought the pyridine nitrogen's lone pair was involved in deviation from the desired outcome. The rich aromatic region in the proton NMR was also indicative of the formation of either a furan ring or an allene. In the absence of progress after several oxidation attempts, exploration of this synthesis was not pursued further.

1.3. Summary

A general two-step synthesis of 1,5-benzodiazepines incorporating a pyridine ring has been developed. The protocol allows the production of nonsymmetric 1,5-benzodiazepines **2a**–**e**, and avoids column chromatography, providing 40–82% yield. The final step of the synthesis requires no metal catalyst and proceeds in a renewable organic solvent, ethanol.

1.4. Experimental

1.4.1. Materials and methods

Triethylamine was distilled twice from phosphorus pentoxide and once from calcium hydride. *p*-Toluoyl chloride and *m*-toluoyl chloride were distilled under an oil-pump vacuum into Schlenk flasks, which were sealed under inert atmosphere and were stored in a –20 °C freezer. Unless otherwise noted, reagent-grade solvents were used without further purification. Microwave reactions were carried out in a Biotage Initiator reactor. NMR measurements were carried out on a Bruker Avance III or a Bruker Ascend 400 spectrometer operating at 400 MHz for ^{1}H and 100 MHz for ^{13}C, and on a Bruker Avance spectrometer operating at 200 MHz for ^{1}H and 50 MHz for ^{13}C, all at 20–25 °C. High-resolution mass spectra (HRMS) were recorded on an Agilent 6520 Q-TOF LC-MS. FT-IR spectra were recorded on a Bruker Alpha-P ATR spectrometer. Electronic absorbance was measured using a Cary-100 UV-vis spectrophotometer (Agilent) in double-beam mode (sample and solvent blank) using a 10 mm path quartz cuvette (Starna 23-Q-10 cell with a Teflon stopper) and appropriate background subtraction to compensate for the solvent cutoff. Melting points were recorded in evacuated and sealed capillaries using either a Mel-Temp model no. 1201D or a Stuart SMP10 Digital Melting Point apparatus.

1.4.2. Synthesis of prop-2-yn-1-ones **1a**–**b**; general procedure

An oven-dried Schlenk flask (25 mL) equipped with a stir bar was charged with tetrakis(triphenylphosphine)palladium(0) (0.0346 g, 0.0299 mmol). The flask was connected to an oven-dried condenser affixed with a septum, and the system was evacuated and flushed with nitrogen. Triethylamine (18.0 mL) was added via syringe,

and the mixture was stirred for 15 min. The corresponding acyl chloride (3.0 mmol) was added, followed by 2-ethynylpyridine (3.2 mmol), using syringes. The reaction was placed into an oil bath preheated to 70 °C, stirred, and monitored by GC-MS, which showed nearly full conversion of the acyl chloride after 2 h. Further conversion with longer heating times was not observed. The mixture was allowed to cool to rt and was filtered through a celite pad (3 cm; medium porosity fritted funnel). The celite was washed with portions of dichloromethane (*ca.* 3 × 5 mL) until the eluent was colorless. The solvent was removed using rotary evaporation, and the solid was dried with an oil-pump vacuum. The ^{1}H NMR of the crude product showed the presence of signals attributed to the desired product along with triethylamine hydrochloride.[53] The material was used without further purification for subsequent reactions.

1.4.3. 1-(4-Methylphenyl)-3-(pyridin-2-yl)prop-2-yn-1-one (**1a**)

From 2-ethynylpyridine (0.32 mL, 3.2 mmol) and *p*-toluoyl chloride (0.39 mL, 3.0 mmol), analytically pure material was isolated by column chromatography (hexanes:ethyl acetate 60:40), mp: 68 °C. NMR (δ, ppm): ^{1}H (200 MHz; $CDCl_3$) 8.71 (ddd, 1H, *J* = 4.9, 1.5, 1.2 Hz), 8.15 (AA′XX′, 2H, *J* = 8.3 Hz), 7.77 (virtual dt, 1H, *J* = 7.6, 1.7 Hz), 7.69 (ddd, 1H, *J* = 7.9, 1.6, 0.9 Hz), 7.38 (ddd, 1H, *J* = 7.1, 5.0, 1.2 Hz), 7.31 (AA′XX′, 2H, *J* = 8.0 Hz), 2.45 (s, 3H); ^{1}H (200 MHz; C_6D_6): 8.31 (partially obscured ddd, 1H, *J* = 4.8, 1.8, 1.0 Hz), 8.28 (AA′XX′, 2H, *J* = 8.2 Hz), 6.98 (virtual td, 1H, *J* = 8.0, 1.1 Hz), 6.82 (AA′XX′, 2H, *J* = 7.9 Hz), 6.74 (virtual dt, 1H, *J* = 7.7, 1.8 Hz), 6.44 (ddd, 1H, *J* = 7.7, 4.8, 1.2 Hz), 1.89 (s, 3H); ^{13}C{^{1}H} (50 MHz; $CDCl_3$) 177.44, 150.65, 145.80, 141.11, 136.54, 134.25, 129.96 (2C), 129.50 (2C), 128.99, 124.73, 90.05,

84.91, 21.95. HRMS (ESI-TOF) $[M+H]^+$ calcd for $C_{15}H_{12}NO^+$ 222.0914, found 222.0913.

1.4.4. 1-(3-Methylphenyl)-3-(pyridin-2-yl)prop-2-yn-1-one (**1b**)

From 2-ethynylpyridine (0.43 mL, 4.3 mmol) and *m*-toluoyl chloride (0.52 mL, 4.0 mmol). NMR (δ, ppm; $CDCl_3$): ^1H (200 MHz) 8.72 (ddd, 1H, *J* = 4.9, 1.6, 1.0 Hz), 8.12–8.02 (m, 2H), 7.78 (virtual dt, 1H, *J* = 7.4, 1.8 Hz), 7.70 (ddd, 1H, *J* = 7.8, 1.8, 1.1 Hz), 7.46–7.34 (m, 3H), 2.42 (s, 3H); $^{13}C\{^1H\}$ (50 MHz) 178.03, 150.69, 141.15, 138.72, 136.59, 136.55, 135.47, 129.96, 129.04, 128.72, 127.50, 124.77, 90.31, 85.00, 21.40. HRMS (ESI-TOF) $[M+H]^+$ calcd for $C_{15}H_{12}NO^+$ 222.0914, found 222.0913.

1.4.5. Synthesis of 1,5-benzodiazepines **2a**–**e**; general procedure

A microwave vial (20 mL) was charged with a diamine derivative (1.20 equiv.), a stir bar, and the corresponding alkynone (**1a**–**b**) (*ca.* 1.0 equiv.) in ethanol (3 mL per 1.0 equiv.). The vial was sealed, and the reaction was irradiated in the microwave reactor at 80 °C for 1 h. The vial was allowed to cool to rt and was stored at –20°C (freezer) for 24 h. The solid was filtered off, washed with cold methanol (3 × 2 mL), and dried with an oil-pump vacuum to give the corresponding benzodiazepine.

1.4.6. 2-(4-Methylphenyl)-4-(pyridin-2-yl)-3*H*-1,5-benzodiazepine (**2a**)

From *o*-phenylenediamine (0.518 g, 4.80 mmol) and **1a** (theoretical 4.0 mmol) compound **2a** was obtained as a white solid (0.821 g, 2.64 mmol; 66%), mp: 159–160 °C. NMR (δ, ppm; $CDCl_3$): ^1H (200 MHz) 8.74 (ddd, 1H, *J* = 4.8, 1.6, 0.85 Hz), 8.28 (td, 1H, *J* = 8.1, 1.0 Hz), 8.25 (AA′XX′, 2H, *J* = 8.3 Hz), 7.74 (dt, 1H, *J* = 7.7, 1.8 Hz), 7.6 (dd, 2H, *J* = 6.7, 2.8 Hz), 7.39–7.29 (m, 3H), 7.21 (d, 2H, *J* = 8.1 Hz), 2.36 (s, 3H); $^{13}C\{^1H\}$ (50, MHz) 155.6, 155.2, 153.5, 148.7, 141.5, 140.9, 140.6, 136.6, 134.6, 129.1 (2C),

128.79, 128.76 (2C), 128.7, 125.9, 125.1, 125.8, 123.3, 32.8, 21.4. IR: (ν, cm^{-1}): 3090 w, 3059 w, 1598 w, 1583 w, 1563 m, 1471 m, 1430 m, 1327 m, 1306 w, 1257 m, 1186 w, 815 w, 752 s, 743 s, 521 m. UV-vis (CH_2Cl_2, 17.0 μM): λ_{max} 277 nm (29,500 $M^{-1}cm^{-1}$), (MeOH:CH_2Cl_2 (98:2), 35.6 μM) λ_{max} 275 nm (21,100 $M^{-1}cm^{-1}$). HRMS (ESI-TOF): $[M+H]^+$ calcd for $C_{21}H_{17}N_3^+$ 312.1495, found 312.1496.

1.4.7. 7,8-Dichloro-2-(4-methylphenyl)-4-(pyridin-2-yl)-3*H*-1,5-benzodiazepine (**2b**)

From 4,5-dichloro-*o*-phenylenediamine (0.4249 g, 2.400 mmol) and **1a** (theoretical 2.0 mmol) compound **2b** was obtained as a white solid (0.5067 g, 1.332 mmol, 67%), mp: 220–222 °C. NMR (δ, ppm; C_6D_6): ^1H (200 MHz) 8.47 (d, 2H, *J* = 8.3 Hz), 8.43 (ddd, 1H, *J* = 4.8, 1.8, 0.9 Hz), 8.13 (td, 1H, *J* = 8.0, 1.0 Hz), 7.76 (s, 1H), 7.74 (s, 1H), 7.01 (d, 2H, *J* = 8.03 Hz), 6.96 (dt, 1H, *J* = 7.5, 4.8, 1.2 Hz), 3.85 (br s, 2H), 2.10 (s, 3H); $^{13}C\{^1H\}$ (50 MHz) 156.55, 156.25, 153.74, 148.67, 141.61, 141.57, 140.47, 136.44, 134.64, 130.45, 130.37, 129.58 (2C), 129.46 (2C), 124.95, 123.65, 32.20, 21.29. IR (ν, cm^{-1}): 3028 br w, 2917 w, 1594 w, 1559 m, 1446 s, 1318 m, 1294 s, 1196 m, 1122 s, 1092 w, 944 w, 887 w, 813 m, 786 m, 709 m, 742 m, 709 m, 572 w, 537 m, 521 m. UV-vis (CH_2Cl_2, 16.6 μM): λ_{max} 282 nm (27,300 $M^{-1}cm^{-1}$), (MeOH:CH_2Cl_2 (98:2), 29.2 μM) λ_{max} 280 nm (30,800 $M^{-1}cm^{-1}$). HRMS (ESI-TOF): $[M + H]^+$ calcd for $C_{21}H_{16}Cl_2N_3^+$ 380.07158, found 380.07350.

1.4.8. 2-(4-Methylphenyl)-4-(pyridin-2-yl)-3*H*-naphtho[2,3-*b*][1,4]diazepine (**2c**)

From 2,3-diaminonaphthalene (0.4792 g, 3.029 mmol) and **1a** (theoretical 3.0 mmol) compound **2c** was obtained as a fluffy yellow solid (0.4349 g, 1.203 mmol, 40%), mp: 189–193 °C. NMR (δ, ppm; C_6D_6): ^1H (200 MHz) 8.48 (ddd, 1H, *J* = 1.7, 0.9 Hz), 8.63 (td, 2H, *J* = 8.3, 1.9 Hz), 8.38 (td, 1H, *J* = 8.0, 1.0 Hz), 8.29 (d, 2H, *J* = 2.9 Hz),

7.81–7.70 (m, 2H), 7.31–7.20 (m, 2H), 6.61 (ddd, 1H, *J* = 7.5, 4.8, 1.2 Hz), 4.10 (s, 2H), 2.04 (s, 3H); $^{13}C\{^{1}H\}$ (50 MHz): 160.63, 160.54, 154.57, 148.62, 141.48, 141.02, 140.81, 136.37, 135.70, 132.29, 131.67, 129.44 (2C), 129.26 (2C), 127.24, 126.91, 126.31, 125.99, 124.71, 123.04, 31.27, 21.29. IR (ν, cm^{-1}): 3053 br w, 1603 w, 1584 w, 1561 m, 1431 m, 1294 m, 1240 w, 1191 w, 876 s, 816 m, 774 m, 740 s, 622 m, 469 m. UV-vis (CH_2Cl_2, 16.0 μM): λ_{max} 291 nm (34,100 $M^{-1}cm^{-1}$). HRMS (ESI-TOF) $[M+H]^+$ calcd for $C_{25}H_{20}N_3^+$ 362.1652, found 362.1656.

1.4.9. 2-(3-Methylphenyl)-4-(pyridin-2-yl)-3*H*-1,5-benzodiazepine (**2d**)

From *o*-phenylenediamine (0.4547 g, 4.205 mmol) and **1b** (theoretical 4.2 mmol) and after multiple recrystallization of the mother liquor from methanol was obtained compound **2d** as reddish lumps (0.7847 g, 2.520 mmol, 75%), mp: 132–137 °C. NMR (δ, ppm; $CDCl_3$): ^{1}H (200 MHz) 8.76 (ddd, 1H, *J* =4.9, 1.5, 0.9 Hz), 8.29 (td, 1H, *J* = 8.0, 0.9 Hz), 8.21 (br s, 1H), 8.19 (partially obscured td, 1H), 7.76 (dt, 1H, *J* = 7.8, 1.8 Hz), 7.66–7.56 (m, 2H), 7.43–7.18 (m, 5H), 2.39 (s, 3H); $^{13}C\{^{1}H\}$ (50 MHz) 156.01, 155.27, 153.89, 148.72, 141.52, 140.78, 138.14, 137.39, 136.77, 131.50, 129.49, 128.93, 128.88, 128.41, 126.02 (2C), 125.32, 124.96, 123.46, 32.47, 21.58. IR (ν, cm^{-1}): 3055 w, 1576 w, 1561 w, 1467 w, 1426 w, 1324 m, 1307 m, 1255 w, 1198 w, 790 m, 763 s, 699 s, 515 m, 475 w. UV-vis (CH_2Cl_2, 18.1 μM): λ_{max} 273 nm (31,200 $M^{-1}cm^{-1}$). HRMS (ESI-TOF) $[M+H]^+$ calcd for $C_{21}H_{18}N_3^+$ 312.1496, found 312.1495.

1.4.10. (2*Z*)-3-(2-Amino-5-nitroanilino)-1-(4-methylphenyl)-3-(pyridin-2-yl)prop-2-en-1-one (**3**)

A 20 mL microwave vial equipped with a stir bar was charged with **1a** (theoretical 2.0 mmol), 4-nitro-*o*-phenylenediamine (0.3063 g, 2.000 mmol),

triethylamine (0.40 mL, 3.0 mmol), and ethanol (9.5 mL). The vial was sealed, and the reaction was irradiated in the microwave reactor at 50 °C for 1 h. The vial was kept at –20 °C for 18 h after which the solid was filtered off (medium porosity fritted funnel) and washed with ether (2 × 1.5 mL) and cold methanol (2 × 3.0 mL). The solid was dried over an oil-pump vacuum for 6 h to give compound **3** as a yellow (gold colored) solid (0.4535 g, 1.211 mmol, 60%), mp: 218–219 °C. NMR (δ, ppm; $CDCl_3$): ^1H (200 MHz) 11.89 (s, 1H), 8.58 (ddd, 1H), 7.95 (AA′XX′, 2H, *J* = 8.2 Hz), 7.84 (dt, 1H, *J* = 7.7, 1.8 Hz), 7.73 (dd, 1H, 9.0, 2.6 Hz), 7.56 (td, 1H, *J* = 7.9, 1.0 Hz), 7.40 (ddd, 1H, *J* = 7.5, 4.8, 1.1 Hz), 7.33 (AA′XX′, 2H, *J* = 8.0 Hz), 7.06 (d, 1H, *J* = 2.5 Hz), 6.89 (s, 2H), 6.76 (d, 1H, *J* = 9.0 Hz), 6.55 (s, 1H), 2.39 (s, 3H); $^{13}C\{^1H\}$ (50 MHz) 189.07, 159.61, 153.02, 150.11, 149.55, 142.17, 137.13, 136.23, 135.42, 129.25 (2C), 127.47 (2C), 124.75, 124.34, 123.74, 122.81, 121.45, 113.52, 97.97, 21.08. IR (ν, cm^{-1}) 3464 w, 3341 w, 1610 m, 1574 w, 1559 w, 1547 m, 1510 w, 1449 w, 1284 s, 1215 s, 1206 s, 1178 m, 1090 w, 1055 m, 772 s, 744 m, 643 m, 439 br m. UV-vis (CH_2Cl_2, 15.4 μM): λ_{max} 373 nm (28,589 $M^{-1}cm^{-1}$), 270 nm (16,700 $M^{-1}cm^{-1}$). HRMS (ESI-TOF): $[M + H]^+$ calcd for $C_{21}H_{18}N_4O_3^+$ 375.1451, found 375.1449.

1.4.11. 2-(4-Methylphenyl)-7-nitro-4-(pyridin-2-yl)-3*H*-1,5-benzodiazepine (**2e**)

A microwave vial (20 mL) equipped with a stir bar was charged with enaminone **3** (0.4094 g, 1.094 mmol), acetic acid (6 mL), and ethanol (6 mL). The vial was sealed, and the reaction was irradiated in the microwave at 100 °C for 1 h with stirring. The vial was kept at –20 °C for 18 h. A yellow-colored precipitate was filtered off (medium porosity frit funnel) and washed with cold methanol (2 × 3 mL). The solid was dried over

an oil-pump vacuum to give compound **2e** as a yellow solid (0.3391 g, 0.9515 mmol, 87%), mp: 247–248 °C. NMR (δ, ppm; $CDCl_3$): ^1H (200 MHz) 8.75 (ddd, 1H, *J* = 4.8, 1.6, 1.0 Hz), 8.50 (d, 1H, *J* = 2.6 Hz), 8.33 (td, 1H, *J* = 8.0, 1.0 Hz), 8.31 (AA′XX′, 2H, *J* = 8.3 Hz), 8.15 (dd, 1H, *J* = 9.0, 2.6 Hz), 7.90 (dt, 1H, *J* = 7.6, 1.7 Hz,), 7.67 (d, 1H, *J* = 9.0 Hz), 7.39 (ddd, 1H, *J* = 7.5, 4.8, 1.1 Hz), 7.24 (AA′XX′, 2H, *J* = 7.7 Hz), 2.38 (s, 3H); $^{13}C\{^1H\}$ (50 MHz) 158.35, 157.53, 153.21, 148.97, 146.37, 144.28, 142.40, 140.27, 137.00, 133.79, 129.77, 129.49 (2C), 129.46 (2C), 125.58, 125.09, 123.71, 120.18, 32.88, 21.66. IR (ν, cm^{-1}): 3104 w, 3070 w, 2920 w, 1550 m, 1505 s, 1433 br w, 1337 s, 1306 s, 1185 m, 1148 w, 1083 m, 992 w, 817 br w, 787 m, 744 m, 702 m, 532 w, 515 m, 406 w. UV-vis (CH_2Cl_2, 18.9 μM): λ_{max} 295 nm (28,100 $M^{-1}cm^{-1}$), 251 nm (23,800 $M^{-1}cm^{-1}$), (MeOH:CH_2Cl_2 (98:2), 35.1 μM): λ_{max} 291 nm (19,200 $M^{-1}cm^{-1}$), 250 nm (15,055 $M^{-1}cm^{-1}$). HRMS (ESI-TOF): $[M + H]^+$ calcd for $C_{21}H_{17}N_4O_2^+$ 357.1346, found 357.1346.

1.4.12. 1-Phenyl-4-(pyridin-2-yl)but-3-yn-1-ol (**4**)

A 250 mL Schlenk flask, equipped with a magnetic stirring bar and fitted with a septum, was charged with THF (35 mL) and 2-ethynyl pyridine (2.35 mL, 23.3 mmol) via syringes. The reaction vessel was placed in a dry ice acetone bath. After 10 min, lithium diisopropylamide solution (LDA) (*ca*. 1.8 M; 13 mL, 23 mmol) was added within 5 min via syringe to the stirred reaction mixture. The mixture was allowed to stir for 10 min after which time the bath is removed and the reaction vessel is allowed to warm to room temperature. Dimethyl sulfoxide (DMSO) (54.0 mL) was added via syringe to the reaction vessel, followed by a solution of styrene oxide (2.05 mL, 18.0 mmol) in THF (3.7 mL) via syringe. The reaction mixture acquired a dark red wine color and was stirred

at rt for 16 h. Then, the reaction flask was placed in an ice-bath and quenched with saturated aqueous ammonium chloride (70 mL). The mixture was transferred to a 250 mL separatory funnel using saturated aqueous ammonium chloride (100 mL) as a rinse. The aqueous phase was extracted with ether (200 mL and 3 × 150 mL). The combined ether extracts were transferred to a 1-L separatory funnel and washed with saturated aqueous sodium chloride (2 × 200 mL). The organic phase was dried with anhydrous sodium sulfate and filtered through a fritted-glass funnel of medium porosity. The solvent was removed via rotary evaporation followed by drying with an oil-pump vacuum. The crude solid was recrystallized from ethyl acetate and the mother liquor was subjected to silica gel column chromatography (ethyl acetate:hexanes) to give **4** as a dark solid (2.092 g, 9.370 mmol, 52%). NMR (δ, ppm; $CDCl_3$): ^1H (200 MHz) 8.53 (ddd, 1H, *J* = 5.0, 1.8, 0.9 Hz), 8.28 (dt, 1H, *J* = 7.7, 1.8 Hz), 7.49–7.17 (m, 8H), 5.02 (t, 1H, *J* = 6.3 Hz), 2.89 (d, 2H, *J* = 6.3 Hz); $^{13}C\{^1H\}$ (50 MHz) 175.40, 149.22, 142.98 and 142.86, 136.81, 128.50 (2C), 127.84, 127.04, 125.89 (2C), 122.91, 88.54, 81.76, 72.31, 21.35.

1.4.13. Attempted synthesis of 1-phenyl-4-(pyridin-2-yl)but-3-yn-1-one (**5**)

A 25 mL round-bottomed flask equipped with a rubber septum and a magnetic stirring bar is charged with but-3-yn-1-ol (0.1358 g, 0.6083 mmol) and acetone (6.37 mL). Jones reagent (3.00 M; 0.255 mL, 0.765 mmol) is added by syringe over 5 min at 5 °C (ice-water bath) to the stirred mixture. The bath is removed, and the reaction mixture is allowed to stir for an additional 15 min, then ether (5 mL) and isopropanol (0.2 mL) were added. The blue-green solid is filtered off through a medium porosity fritted-glass funnel and the filtrate is transferred to a separatory funnel filled with 4 mL of ice water. Three extractions with ether are carried out (3 × 10 mL) and the combined organic phases

were washed twice with saturated sodium bicarbonate (2 × 6 mL), dried over sodium sulfate, filtered, and concentrated at reduced pressure on a rotary evaporator. The resulting solid was transferred to a round bottomed flask and dried under an oil-pump vacuum. The GC-MS analysis indicated a molecular ion of m/z 222.0 and gave a base peak of m/z 179.0, whereas the compound's mass is 221.3 g/mol and its alcohol starting material is 223.1 g/mol. Further analysis by ^{1}H NMR did not indicate signals in the region 3.00 ppm to 5.00 ppm, in which there was expected to be a signal for the ketone's methylene protons. The starting material was absent as evidenced by the missing triplet at 5.02 ppm and doublet at 2.89 ppm.

CHAPTER TWO

SIX-COORDINATE 1,5-BENZODIAZEPINE METAL COMPLEXES WITH BISCHELATE LIGANDS

2.1. Introduction

2.1.1. Benzodiazepines as a ligand for metal ions

Benzodiazepines can serve as chelating ligands for metal cations, and benzodiazepine metal complexes have been previously synthesized using second and third row transition metals in order to propose new medicinal compounds or enhance chemical manufacturing.[54] The specific pyridine-substituted 1,5-benzodiazepines synthesized in the previous chapter have not been investigated in regards to their coordination abilities. The pyridine ring could facilitate the formation of a five-membered chelate ring with a metal cation (Figure 2.1), which provides optimal stability.[51] In this chapter, the synthesis of benzodiazepine complexes derived from metal dichloride starting materials was explored to better understand the chelating behavior of the pyridine-substituted 1,5-benzodiazepines illustrated in Figure 2.1.

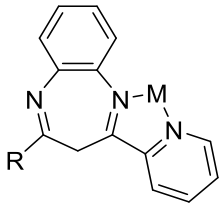

Figure 2.1 Target pyridine-substituted 1,5-benzodiazepine metal complex structure.

2.1.2. Benzodiazepine metal complexes

So far, most reports have concentrated on the metal complexation of 1,4-benzodiazepines, with several studies focusing on bromazepam, the pyridine-fused 1,4-benzodiazepine (Figure 1.2, page 3). Characterization by elemental analysis, polarimetry, IR spectroscopy, UV-vis spectroscopy, electron paramagnetic resonance spectroscopy, cyclic voltammetry, molar conductivity, or in some cases X-ray crystallography were carried out. X-Ray crystallography has been particularly underutilized in this area,[54] so focus in this dissertation was placed on structure determination.

Several metal-coordinated 1,4-benzodiazepines have been examined for the purpose of describing new metal coordinated complexes.[54] For example, Mosset *et al.* determined the X-ray crystal structure of two molecules of diazepam complexed to a copper(II) ion in a square-planar geometry, as depicted in Figure 2.2.[55] The structure is distinguished in that only one nitrogen on each benzodiazepine molecule is available for coordination.

In a series of studies, nickel 1,4-benzodiazepine complexes[3] and, separately, chromium, iron, and ruthenium tris-chelated complexes[56] have been described, providing a larger set of metals for benzodiazepine ligands, and specifically pyridine-substituted benzodiazepine ligands, *e.g.* bromazepam (Figure 2.2). The nickel, ruthenium, chromium, and iron complexes depicted in Figure 2.2 are different than those pursued in this dissertation by the position of the benzene ring relative to the chelating diazepine nitrogen atom (compare with Figure 2.1). Moreover, three molecules of pyridine-substituted benzodiazepine ligand each provided two chelating nitrogen atoms forming

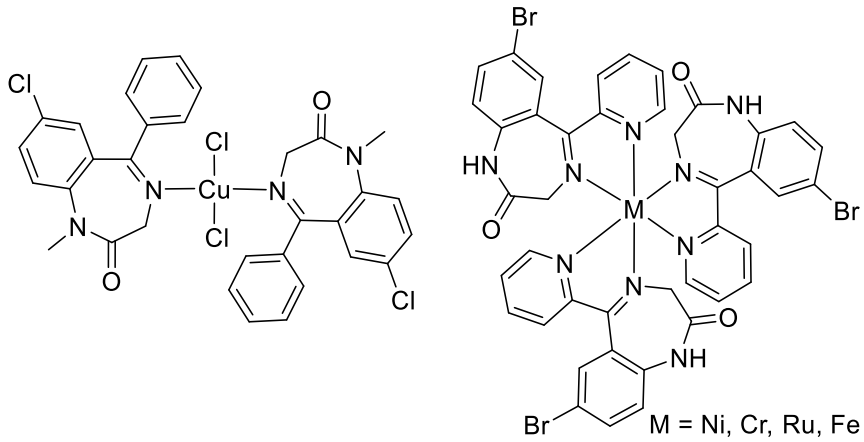

Figure 2.2 Selected examples of 1,4-benzodiazepine metal complexes.

hexacoordinate complexes. The nickel complex's structure was proposed based on a continuous variation methodology using UV-vis measurements,[3] and the proposed structures of the chromium, iron, and ruthenium complexes were justified primarily by elemental analysis and infrared spectroscopy measurements (Figure 2.2).[56] In addition to these studies on metals coordinated by 1,4-benzodiazepine, 1,5-benzodiazepine metal complexes have been investigated as well.[57]

Studies seeking to improve chemical manufacturing have included the 1,5-benzodiazepine scaffold. For example, olefins represent a key ingredient in the production of chemical products and the maintenance of polyolefins' microstructural properties and their synthesis are of particular importance to relevant industries.[57,58] Within this context, Sun's group sought to emulate the tridentate ligands previously established for catalysis through the synthesis of new 1,5-benzodiazepine centered bimetallic catalysts (Figure 2.3).[2,57–59] The 1,5-benzodiazepines used in these studies

(Figure 2.3) differ from those pursued in this dissertation (Figure 2.1 and Figure 1.14) by including only one imine nitrogen in the benzodiazepine body, as opposed to two imine nitrogen atoms in compounds **2a**, **2b**, **2d**, and **2e**. Moreover, the ligands in Figure 2.3 feature a tridentate system on each metal ion. The authors studied the polymerization activity and resulting oligomer distribution under different conditions using these metal complexes and successfully characterized these new materials.[2,57–59] Homometallic structures included nickel, cobalt, or iron centers, which featured three coordinating nitrogen atoms per metal ion (Figure 2.3, a and b).[57,58] Sun's group also made complexes with bridging chlorides (Figure 2.3, a and c),[58,59] and heteronuclear systems also with three coordinating nitrogen-donors per metal ion (M1 ≠ M2, Figure 2.3, b).[2] The nickel, iron, and cobalt structures were characterized primarily as powders through IR, though there were cases where analysis of an X-ray crystal structure was provided.[2,57–59] X-ray structures were provided for nickel complex R^1 = Me, R^2 = H (Figure 2.3, a), cobalt complex M1 = M2 = Co, R^1 = *i*-Pr, R^2 = H, (Figure 2.3, b), the bimetallic complex M1 = Co, M2 = Ni, R^1 = *i*-Pr, R^2 = H, (Figure 2.3, b), and the bridged chlorine nickel complex (Figure 2.3, c).

Within medicinal chemistry, 1,5-benzodiazepines have also been examined for their chelating abilities. The protonated 2,4-dimethyl-1,5-benzodiazepine and quinoline derivatives of 1,5-benzodiazepines (Figure 2.4) have been investigated for their potential as ligands to transition metals (cobalt, nickel, copper, zinc, cadmium) in the exploration of novel pharmaceuticals.[60–62] These medicinal studies were, however, less thorough in determining the final products' structure than the aforementioned benzodiazepine metal-

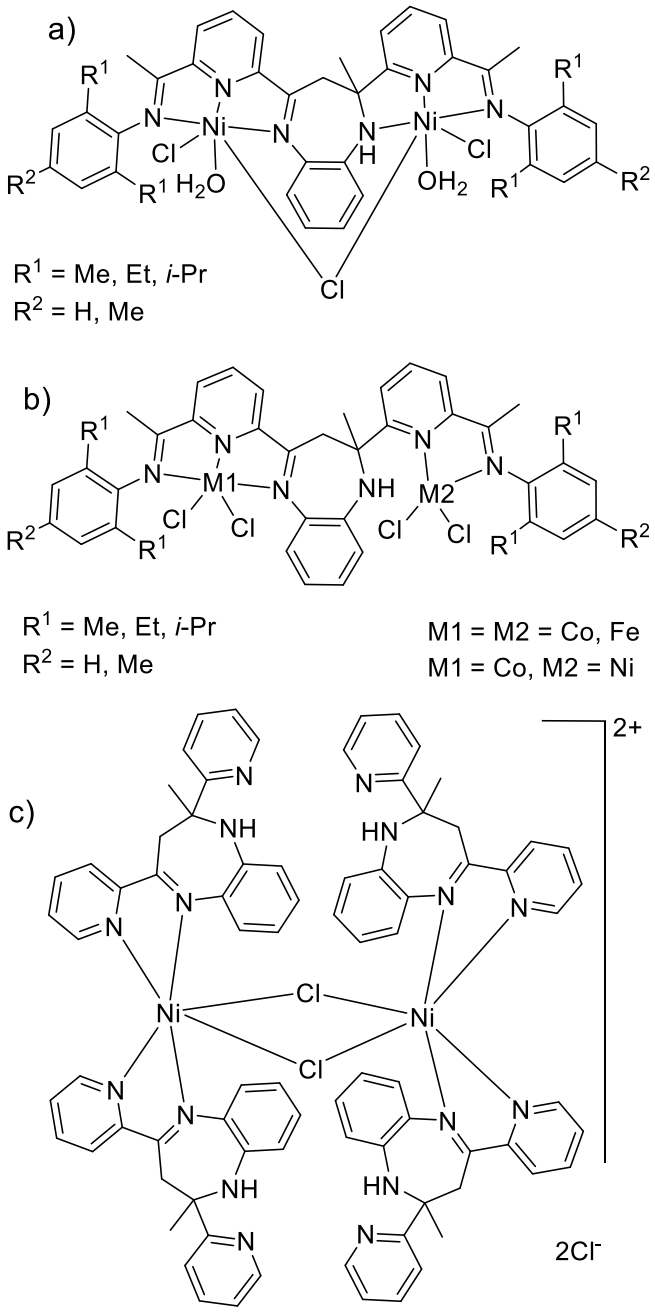

Figure 2.3 Nickel, iron, and cobalt 1,5-benzodiazepine complexes.

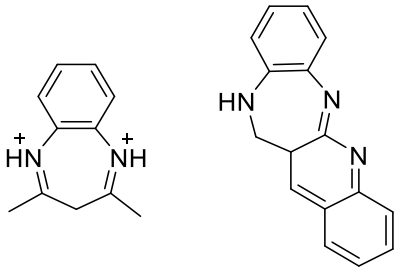

Figure 2.4 2,4-Dimethyl-1,5-benzodiazepinium ion and quinolino[3,2-*b*]benzodiazepine used in complexation studies.

complex studies. Unambiguous structures of the complexes were not proposed, indicating a scarcity of research in this area. Consideration of the pyridine-substituted 1,5-benzodiazepine scaffold as a ligand led to studies that were carried out by investigating its interaction with metal ions: nickel, cobalt, and manganese.

2.2. Results and discussion

2.2.1. 1,5-Benzodiazepine nickel and cobalt complexes

Having demonstrated an effective synthesis of 1,5-benzodiazepines substituted with a pyridine moiety (Chapter 1), the coordination capabilities of their bidentate structure was investigated next. The metals nickel, cobalt, and manganese were chosen due to their relevance to biological processes (*e.g.*, metabolic systems)[63] and the ability of nickel(II), cobalt(II), and manganese(II) to form coordination complexes.[64] Regarding biological processes, manganese is involved in the oxidation of water in photosystem II and is important in preventing oxidative damage in multicellular organisms.[65] Nickel is more common to anaerobic organisms, and is essential for human gut flora.[66] Cobalt is integral to vitamin B12 in humans, which is essential for different biochemical transformations.[65] In addition, while transition metals with –1, 0, +1, +2, +3, and +4

oxidation states can bind to nitrogen, the reported synthesis of nickel and cobalt complexes[2] (Figure 2.3) specifically indicates binding 1,5-benzodiazepines to transition metals with a +2 oxidation state is feasible.

The complexation of selected metals with pyridine-substituted 1,5-benzodiazepines was designed and carried out as depicted in Figure 2.5, where a bischelate complex forms using either 1 or 2 equivalents of benzodiazepine. The binding of metals by benzodiazepines indicated that these complexes might form through

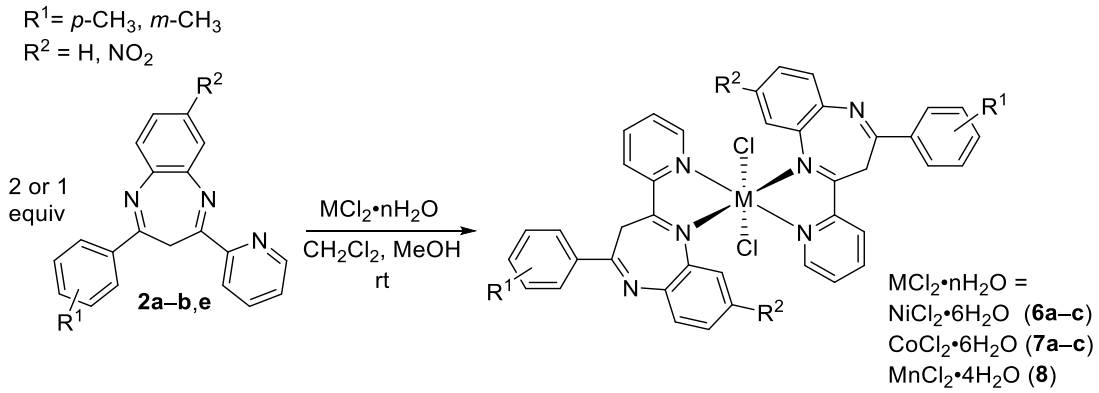

Figure 2.5 General synthesis of benzodiazepine metal complexes. The Λ isomer is shown although racemic mixtures are obtained.

association of the ligand and a metal starting material in solution,[3,55,67] so it was reasoned that common commercial reagents like nickel(II) chloride hexahydrate, cobalt(II) chloride hexahydrate, and manganese(II) chloride tetrahydrate could serve as starting reagents. Experiments were carried out to test the feasibility of this method at room temperature since the formation of benzodiazepine metal complexes at room temperature

have been reported.[3,55,67] Subsequent crystallization were designed to purify and verify the formation of the complexes.

The benzodiazepine **2** (2 equiv.) was dissolved in dichloromethane, as it was found to be soluble, and likewise, the metal chloride hydrate (1 equiv.) was dissolved in alcohol (methanol or ethanol) because of its good solubility. After mixing the metal solution with the benzodiazepine solution for *ca*. 1 h, crystallization was carried out by the slow diffusion of a third, highly volatile solvent, such as ether or pentane (24–48 h). As shown in Table 2.1, the crystalline material of nickel compounds **6a**, **6b**, and **6c** was isolated with yields of 92%, 86%, and 95%, respectively. Likewise, crystalline material of cobalt compounds **7a**, **7b**, and **7c** were also isolated with yields of 83%, 91%, and 81%, respectively. These compounds were characterized primarily by elemental analysis and X-ray crystallography.

The elemental analysis (Table 2.1) of the dried crystalline materials (**6a**–**c** and **7a**–**c**) gave evidence that the samples used to determine the structures shown in Table 2.1 were indeed representative of all of the material produced. In general, the elemental analysis of the material, dried for several hours by oil-pump vacuum, matched within 0.3% of the expected elemental percentages when the presence of water molecules, likely from the hydrated starting material, was taken into account. An O–H stretch in the infrared spectra of the crystalline material (*ca.* 3400 cm^{-1}) was observed and confirmed the presence of water, with the exception of nickel complex **6c**. In the case of **6c**, the elemental analysis was within 2% of the expected percentages of carbon, hydrogen, and nitrogen (Table 2.1). Results from crystallographic information obtained for compound

6c showed solvation by dichloromethane, so the elemental analysis calculations include dichloromethane.

The X-ray crystal structures for compounds **6a** and **6b** are presented in Figure 2.6. Nickel chloride is chelated by two molecules of benzodiazepine **2a** and **2d** respectively, and, in the case of compound **6a**, hydrogen bonding was detected between a molecule of methanol and a chloride anion, with the O1–Cl2 distance measuring at 2.27(3) Å (Figure 2.6, top). The preparation was further extended to the nitro-substituted 1,5-benzodiazepine **2e** (compounds **6c**, Figure 2.7). Analogous X-ray structures were observed with cobalt chloride hexahydrate (compounds **7a**, **7b**, and **7c**, Figure 2.8 to 2.10). These X-ray structures were determined with high accuracy as shown by the low *R*1 (< 0.050). The *R*1 of compound **6a** is 0.036, of compound **6b** is 0.028, and of compound **6c** is 0.040 (see appendix A). This structural integrity is also present in the cobalt compounds: 0.029, 0.030, 0.042 for compounds **7a**, **7b**, and **7c** respectively.

To investigate whether a monochelate complex may form in equimolar amounts of benzodiazepine and metal, experiments were carried out. These studies also resulted in bischelate formation (structure determined by X-ray crystallography) instead of monochelate complexes (yields from equimolar experiments were not quantified).

The X-ray structures obtained from the nickel complexes **6a**–**c** revealed that each complex had a distorted octahedral geometry, with the distances between the nickel ion and the ligands' respective pyridine nitrogen atom (Ni–N2) having a range of 2.07 to 2.09 Å. The Ni–N distances between the nickel ion and the nitrogen atom of the benzodiazepines range from 2.14 to 2.17 Å (Table 2.2). The ORTEP depiction of nickel

Table 2.1 Synthesized nickel and cobalt complexes with analytical data.

Entry	Metal Complex	Elemental Analysis	Yield [%]
6a	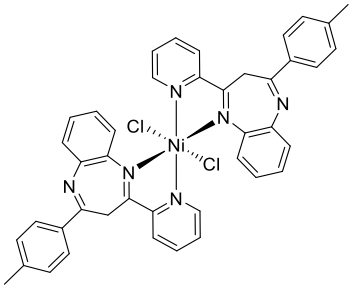	$C_{42}H_{34}N_6Cl_2Ni \bullet 1.5\ H_2O$ Calculated C: 64.72, H: 4.79, N: 10.79 Found C: 64.86, H: 4.69, N: 10.72	92
6b	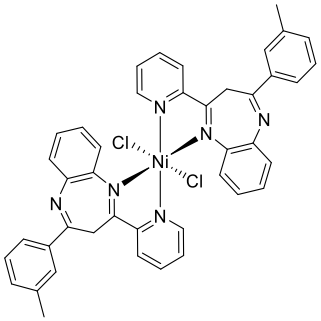	$C_{42}H_{34}Cl_2N_6Ni \bullet 2.5\ H_2O$ Calculated C: 63.26, H: 4.93, N: 10.54. Found C: 63.43, H: 4.73, N: 10.51	86
6c	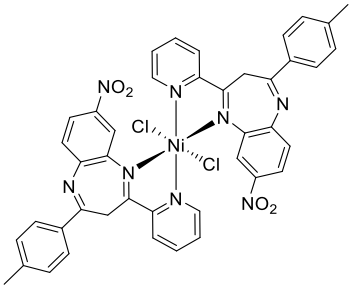	$C_{42}H_{32}Cl_2NiN_8O_4 \bullet 0.5\ CH_2Cl_2$ Calculated C: 58.02, H: 4.06, N: 12.89 Found C: 57.85, H: 4.07, N: 12.73	95
7a	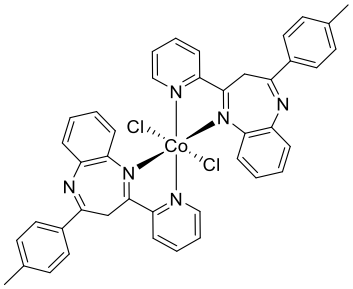	$C_{42}H_{34}N_6Cl_2Co \bullet 1.5\ H_2O$ Calculated C: 64.70, H: 4.78, N: 10.78 Found C: 64.55, H: 4.78, N: 10.80	83

Table 2.1 Synthesized nickel and cobalt complexes with analytical data—Continued

Entry	Metal Complex	Elemental Analysis	Yield [%]
7b	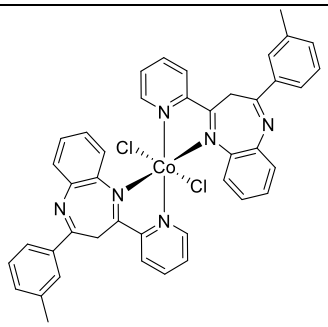	$C_{42}H_{34}Cl_2N_6Co•1.5\ H_2O$ Calculated C: 64.71, H: 4.78, N: 10.78 Found C: 64.61, H: 4.57, N: 10.86	91
7c	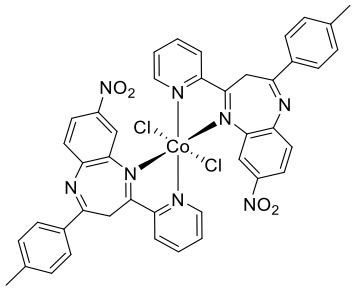	$C_{42}H_{32}Cl_2CoN_8O_4•H_2O$ Calculated C: 58.61, H: 3.98, N: 13.02 Found C: 58.61, H: 4.05, N: 12.88	81

complex **6a** showed hydrogen bonding between one of the complex's chlorides and a molecule of methanol, with a distance of 2.27(3) Å between the chlorine and the methanol hydrogen. Sun's group provided X-ray structures of six-coordinate nickel complexes and these were compared with Table 2.2.[58,59] Sun *et al*.'s complex had an average Ni–N_{py} of 2.03 Å (range of 2.02 to 2.03 Å); N_{py} refers to a pyridine substituent's nitrogen. These complexes had an average Ni–N_{BZD} distance of 2.18 Å (range of 2.13 to 2.23 Å); N_{BZD} refers to the coordinating diazepine nitrogen.[58] In addition, a six-coordinate nickel within a second cobalt/nickel compound (M1 = Ni, M2 = Co, R^1 = *i*-Pr, R^2 = H Figure 2.3, b) exhibits a Ni–N_{py} bond distance of 2.061(1) Å and Ni–N_{BZD} bond distance of 2.312(1) Å.[2]

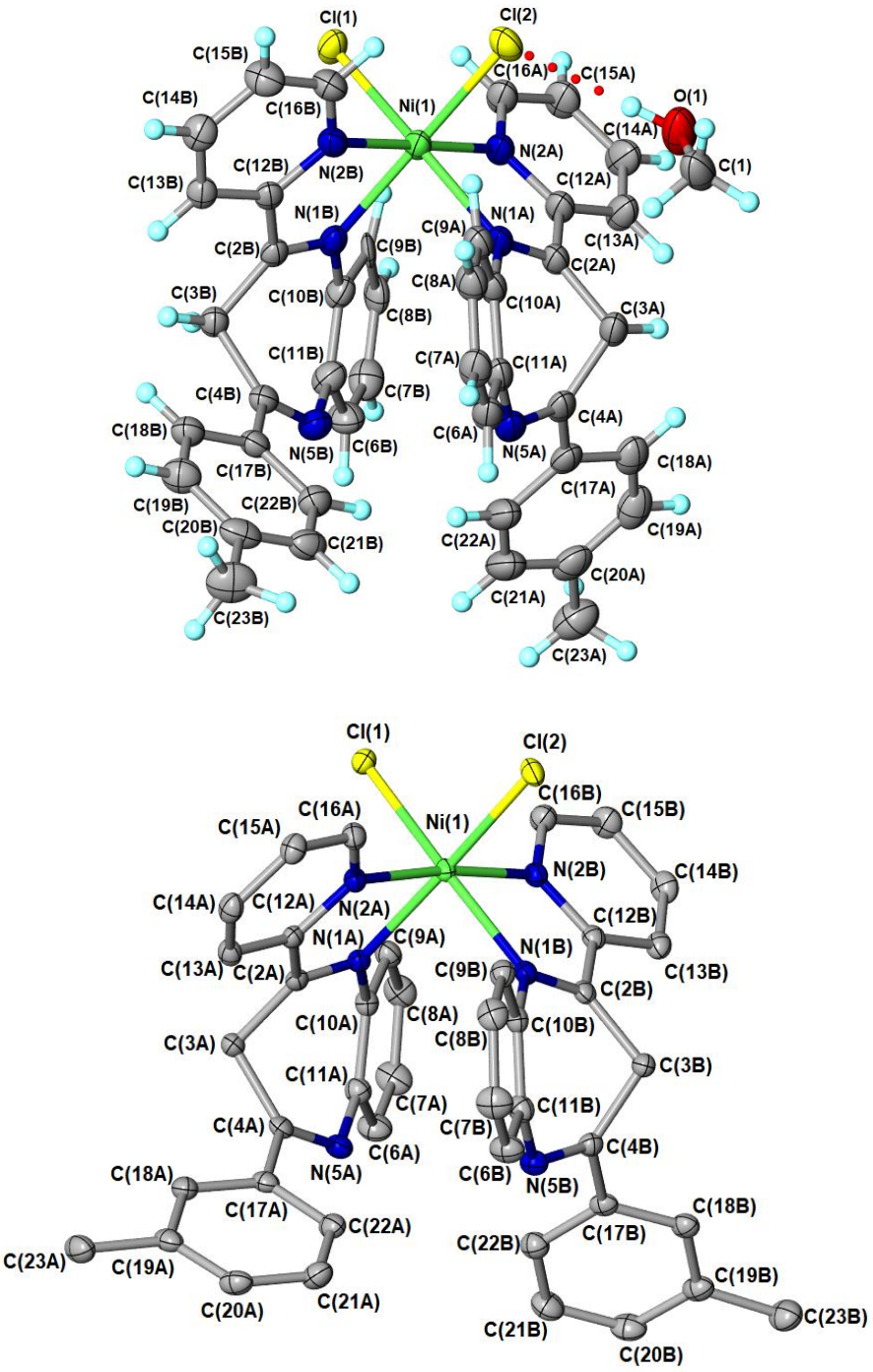

Figure 2.6 Crystal structures (50% probability thermal ellipsoids) of nickel complexes **6a** (top) and **6b** (bottom, hydrogen atoms omitted for clarity).

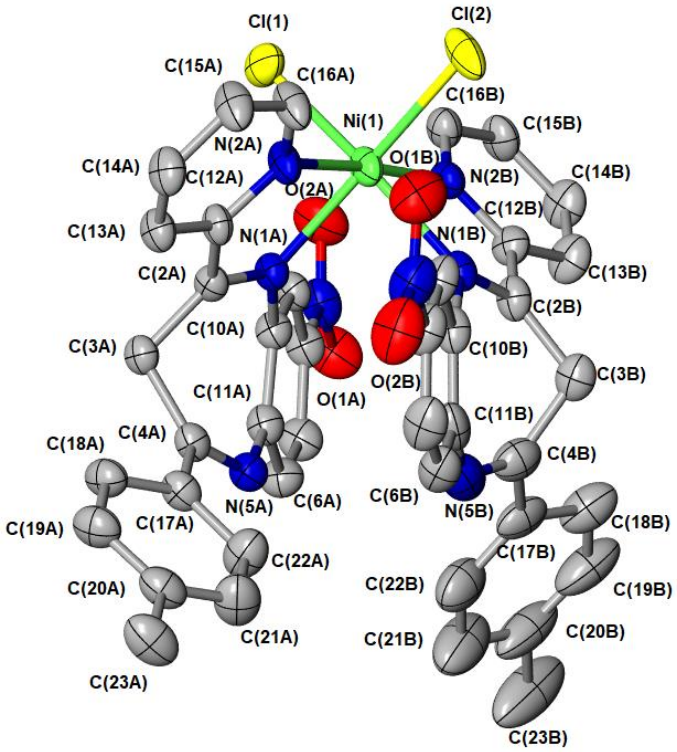

Figure 2.7 Crystal structure (50% probability thermal ellipsoids) of nickel complex **6c** (hydrogen atoms omitted for clarity).

The X-ray structures of the cobalt complexes **7a**–**c** (Figures 2.8 to 2.10) had distorted octahedral geometries similar to **6a**–**c**, but the cobalt complexes had longer nitrogen to metal bonds. The cobalt ion to the pyridine nitrogen atom (Co–N2) distances were in the range of 2.14 to 2.17 Å, and the distance between the cobalt atom and the benzodiazepine nitrogen atom (Co–N1) are in the range of 2.19 to 2.23 Å. Reports of X-ray crystal structures of similar benzodiazepine cobalt complexes exist.[2,57] For example, Figure 2.3, b (M1 = M2 = Co, R^1 = *i*-Pr, R^2 = H) includes two cobalt ions, one of which is complexed in an octahedral environment that includes three chelating nitrogen atoms and one chelating ethanol molecule.

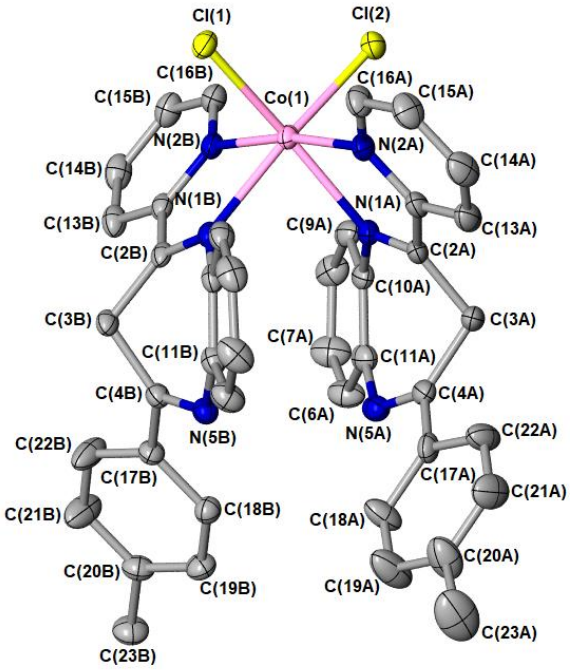

Figure 2.8 Crystal structure (50% probability thermal ellipsoids) of cobalt complex **7a** (hydrogen atoms omitted for clarity).

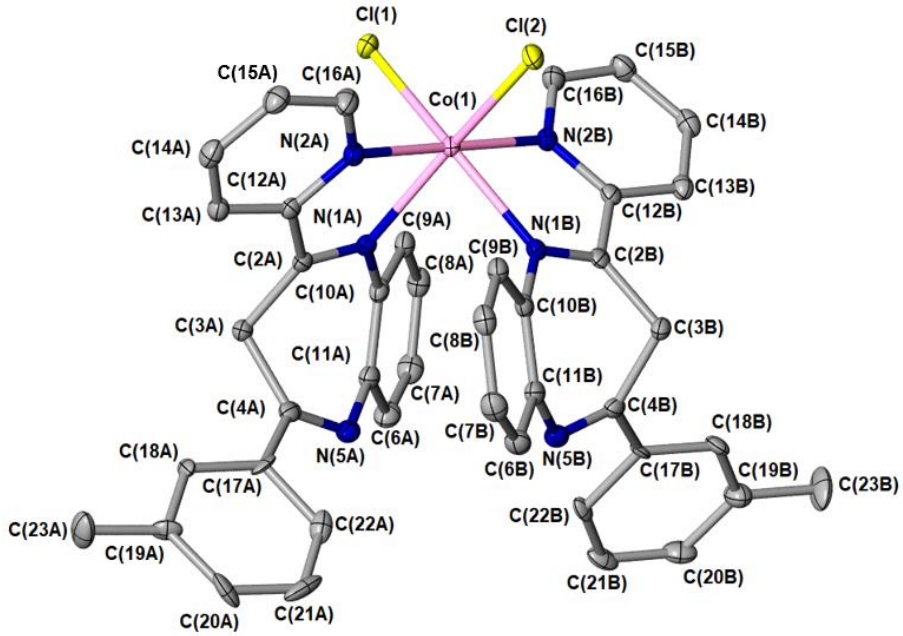

Figure 2.9 Crystal structure (50% probability thermal ellipsoids) of cobalt complex **7b** (hydrogen atoms omitted for clarity).

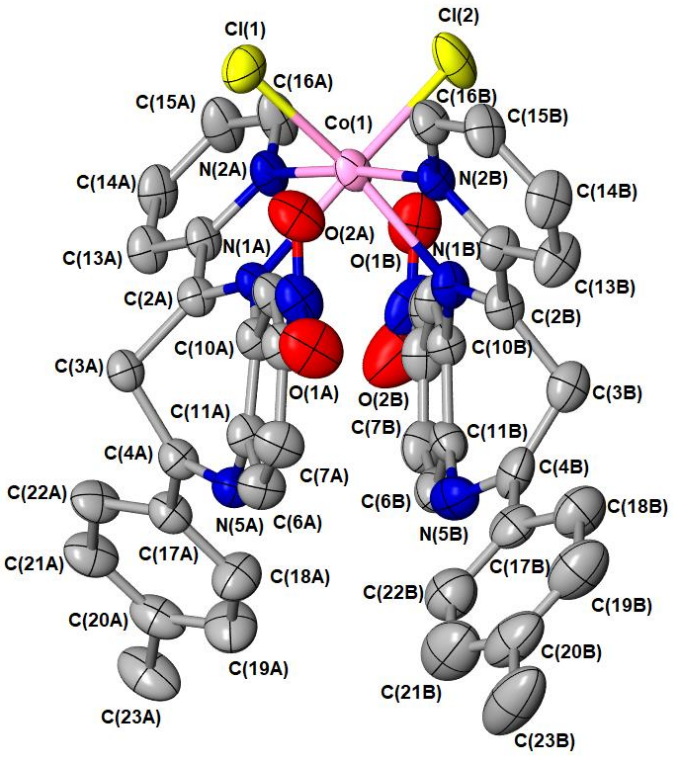

Figure 2.10 Crystal structure (50% probability thermal ellipsoids) of cobalt complex **7c** (hydrogen atoms omitted for clarity).

The pyridine to cobalt bond distance was 2.092(5) Å and the benzodiazepine to cobalt bond distance was 2.340(6) Å. Shown in Figure 2.3, b, a distorted trigonal bipyramid cobalt within a second cobalt/nickel compound (M1 = Ni, M2 = Co, R^1 = *i*-Pr, R^2 = H) has a Co–N_{py} bond distance of 2.146(1) and Co–N_{BZD} bond distance of 1.994(1) Å.[2]

The X-ray structures obtained from the nickel complexes also provide bond angle measurements (Table 2.3). One of the angles in **6a**–**c** (N1–Ni–N2) is in the range of 76.50° to 77.50°, whereas the analogous angle of cobalt complexes **7a**–**c** (N1–Co–N2) is in the range of 74.3° and 75.3°. The octahedral benzodiazepine nickel complexes shown

Table 2.2 Selected bond distances within nickel and cobalt complexes **6a**–**c** and **7a**–**c**.

Bond Distance (Å)	**6a**	**6b**	**6c**	**7a**	**7b**	**7c**
M—N2A	2.0705(17)	2.0807(11)	2.082(3)	2.144(4)	2.1675(13)	2.144(4)
M—N2B	2.0904(17)	2.0729(11)	2.081(3)	2.143(3)	2.1666(13)	2.143(3)
M—N1A	2.1416(16)	2.1416(11)	2.137(3)	2.198(3)	2.1916(12)	2.198(3)
M—N1B	2.1457(17)	2.1622(11)	2.165(19)	2.225(4)	2.1920(13)	2.225(4)
M—Cl1	2.4066(6)	2.4037(4)	2.4247(13)	2.4306(15)	2.4050(5)	2.4306(15)
M—Cl2	2.4231(6)	2.4013(4)	2.3684(11)	2.3655(13)	2.4035(4)	2.3655(13)

in Figure 2.3, a (R^1 = Me, R^2 = H)[2] had an average N_{BZD}–Ni–N_{py} angle of 76°, differing not more than 1° away from the nickel complexes **6a**–**c** (angles in Table 2.2). By comparison, the six-coordinate cobalt complex of Figure 2.3, b (M1 = M2 = Co, R^1 = *i*-Pr, R^2 = H, coordinated by a molecule of ethanol) had a N_{BZD}–Co–N_{py} bond angle of 71.9°, which was a slightly larger difference as compared to compounds **7a**–**c**. Upon inspection of the bond distances or angles, the nickel and cobalt complexes synthesized in this dissertation (compounds **6a**–**c** and **7a**–**c**) are similar in their metal coordination pattern to those produced in Sun's group. As evidenced by compounds **6a**–**c** and **7a**–**c**, the pyridine-substituted benzodiazepine ligand preferentially forms octahedral bischelate complexes even from 1:1 mixtures of ligand and metal chloride, in line with the nickel(II) and cobalt(II) chloride hexahydrate starting materials.

2.2.2. 1,5-Benzodiazepine manganese complexes

The benzodiazepine **2b** was used in the synthesis of manganese complexes, starting from manganese chloride tetrahydrate. Application of the reaction illustrated in Figure 2.5, using 1:1 ligand **2b**:manganese chloride tetrahydrate, furnished a distorted octahedral bischelate of manganese dichloride (**8**), as revealed by X-ray crystallography, in 52% yield. Using 2:1 ligand **2b**:manganese dichloride tetrahydrate also produced crystalline material of compound **8**, which was confirmed by elemental analysis of the product isolated from the reaction (52% yield, Table 2.4). Similar to the nickel and cobalt compounds, deviations of the elemental analysis of manganese complex **8** from the theoretical elemental content (C, N, and H) were attributed to the presence of water in the sample (confirmed by IR spectroscopy).

Table 2.3 Selected bond angles within nickel and cobalt complexes **6a**–**c** and **7a**–**c**.

Bond Angle (deg)	**6a**	**6b**	**6c**	**7a**	**7b**	**7c**
N1A—M—N2A	77.50(7)	77.50(4)	77.27(11)	74.82(5)	74.35(5)	75.25(13)
N1B—M—N2B	77.20(6)	76.84(4)	76.5(5)	74.80(5)	74.38(5)	74.52(13)
Cl1—M—Cl2	96.01(2)	93.95(13)	96.46(5)	97.72(16)	100.71(17)	99.98(6)

Table 2.4 Synthesized manganese complexes with analytical data.

Entry	Metal Complex	Elemental Analysis	Yield [%]
8	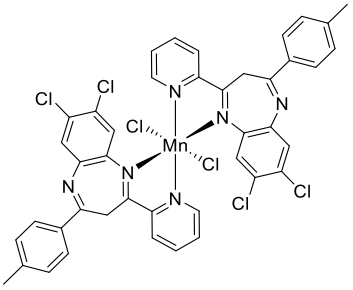	$C_{42}H_{34}N_6Cl_6Mn \bullet 1.5\ H_2O$ <u>Calculated</u> C: 55.23, H: 3.63, N: 9.20 <u>Found</u> C: 55.47, H: 3.39, N: 9.24	52[a]
9	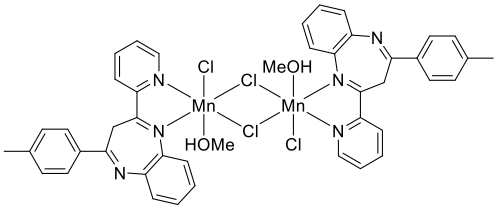	$C_{44}H_{42}Cl_4Mn_2N_6O_2$ <u>Calculated</u> C: 56.31, H: 4.51, N: 8.95 <u>Found</u> C: 56.40, H: 4.50, N: 9.00	n.d.

a) Elemental analysis / yield from crystalline material dried by an oil-pump vacuum.

To create a second manganese complex comparable to complex **8**, two equiv. of unsubstituted ligand **2a** were combined with manganese dichloride tetrahydrate. Subsequent crystallization did not provide crystals suitable for X-ray crystallography, and further analysis was not conducted. Additional experiments using 1:1 of **2a**:manganese dichloride tetrahydrate under various conditions were carried out. As had been inferred by other benzodiazepine metal complex preparations in the literature,[68] acetonitrile and methanol were applied in the crystallization of the metal complex. It was found that when combining equal equivalents of **2a** in dichloromethane and manganese chloride in methanol or ethanol, an orange precipitate formed that could be dissolved with a 1:1

solution of acetonitrile and methanol. Diffusion with diethyl ether furnished crystals of bridged chlorine complex **9**. The structure was confirmed by X-ray crystallography (Figure 2.11, bottom) and was supported by elemental analysis.

It was thought the precipitate from a 1:1 mixture of **2a**:manganese dichloride in dichloromethane and methanol would be representative of the crystallization experiment. Samples of the precipitate were expected to produce an assay of C: 56.31, H: 4.51, N: 8.95 by elemental analysis, but C: 65.00, H: 4.75, N: 10.94 was instead found. This result is not consistent with the bischelate of **2a** and manganese dichloride (calculated C: 67.39, H: 4.58, N: 11.23), the loss of one molecule of methanol in compound **9** (expected assay C: 56.97, H: 4.23, N: 9.27), nor the loss of both methanol molecules in **9** (expected assay C: 57.69, H: 3.92, N: 9.61). One possibility is that a mixture of bischelate and the bridged compound **9** formed. The expected assay for 4:1 of bischelate:compound **9** is C: 64.74, H: 4.56, N: 10.68. The experiment was repeated using the procedure that produced crystalline material, and the elemental analysis of the material was closer to the expected elemental analysis of **9** (Table 2.4), but analytical results discussed in section 2.2.3 suggest bischelate was still present in the crystalline material. A larger scale reaction for yield determination of **9** and attempts at purification were not successful; the preparation of complex **9** was not developed further.

The geometries of compounds **8** and **9** (Figure 2.11) were analyzed in terms of bond distances and bond angles around the metal center. The two X-ray crystal structures with *R*1 of 0.044 and 0.025 for **8** and **9** respectively. Complex **9** featured two six-coordinate manganese centers bridged by two chlorides. Two methanol molecules from the reaction solvent are bonded in terminal positions.

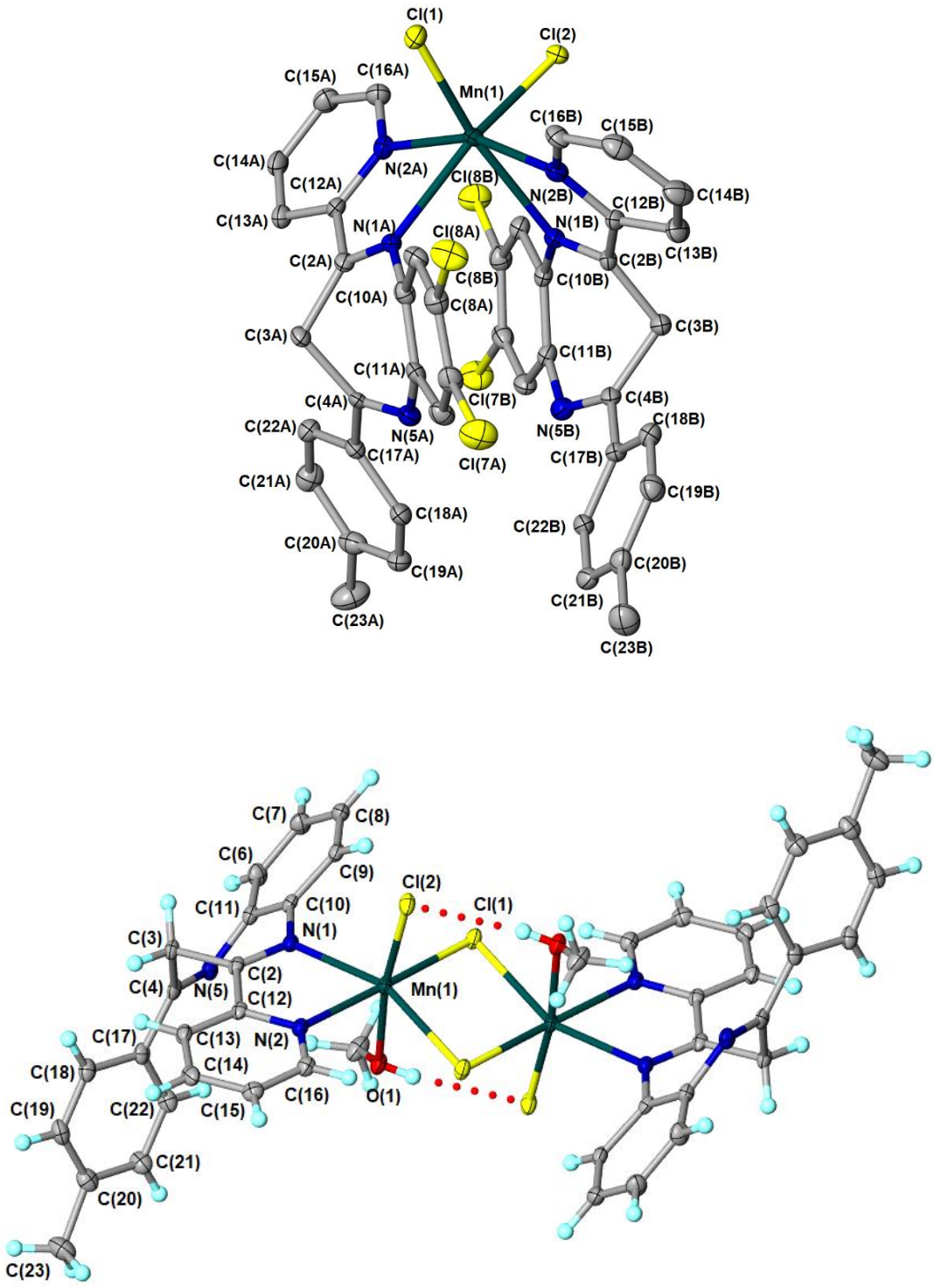

Figure 2.11 Crystal structures (50% probability thermal ellipsoids) of manganese bischelate complex **8** (top, hydrogen atoms omitted for clarity) and manganese bimetallic complex **9** (bottom).

Both complexes were compared in terms of bond angles and distances (Table 2.5). Between complexes **8** and **9**, the bond distance between the manganese and each nitrogen was not observed to differ by more than 0.09 Å, showing that the bond lengths in **9** were not influenced by the presence of fewer nitrogen-donors per metal ion. However, comparing **8** to **9**, the bond distances between the manganese chloride ligand, Mn1—Cl1, is elongated by *ca.* 0.07 Å in **9**, which could be attributed to the bridged nature of the chlorides (Figure 2.11, bottom). In addition, complex **9** featured coordinating molecules of methanol, and the distance from one of the manganese ions to the methanol oxygen (Mn1—O1) was 2.316(1) Å. In terms of bond angles, which are also shown in Table 2.5, the bischelate **8** had a larger angle between the benzodiazepine and pyridine nitrogen, N_{BZD}–Mn–N_{py}, as compared to complex **9** (see N1A–Mn–N2A and N1B–Mn–N2B of Table 2.5). Complex **8** has an average N_{BZD}–Mn–N_{py} angle of 69.85° as compared to the corresponding angle (72.36(5)°) in complex **9**. In contrast, the angle between the chloride ligands and the manganese ion are smaller in the bischelate (Table 2.5). For **8**, Cl1–Mn–Cl2 was 97.38(5)°, whereas complex **9** has three chloride angles with manganese as the apex, and they range between 91.0° and 94.5°. Presently, complex **9** is a unique benzodiazepine-manganese coordination system, albeit the nickel complexes of Sun's group (Figure 2.3, c)[59] and the copper complexes of Kojić-Prodić's group (Figure 3.2, Chapter 3)[68] contain bimetallic structures bridged by chloride ligands as well.

To further investigate the denticity of the manganese complexes formed using **2a**, EPR measurements were undertaken. Both 1 and 2 equiv. of *p*-tolyl benzodiazepine **2a** in dichloromethane were mixed with manganese chloride (in methanol). For a bimetallic

Table 2.5 Selected bond distances and angles within manganese complexes **8** and **9**.

Bond Distance [Å]	**8**	**9**	Bond Angle [deg]	**8**	**9**
Mn1—N1A	2.384(4)		N1A—Mn—N2A	69.35(15)	
		2.3128(13)			72.36(5)
Mn1—N1B	2.400(4)		N1B—Mn—N2B	70.35(16)	
Mn1—N2A	2.264(4)		Cl1—Mn—Cl2	97.38(5)	91.402(15)
		2.2425(13)			
Mn1—N2B	2.280(4)		Cl1′—Mn1—Cl2		94.273(15)
Mn1—Cl1	2.4379(15)	2.5043(4)	Cl1—Mn1—Cl1		91.259(14)
Mn1—Cl2	2.4615(13)	2.4549(4)	′		
Mn1—Cl1′		2.5282(4)			

manganese monochelate complex, an unpaired spin (I = 5/2) should provide six resonance lines, and indeed six lines are observed (see Figure 2.12). In these spectra, splitting of the signals by the ligated nitrogen atoms is resolved (A_N). The values for A_N in the spectra have a range of 25.6–28.8 G, with an average of 27.3 G in the case where 1:1 equivalents of manganese chloride tetrahydrate was combined with benzodiazepine ligand **2a** (Figure 2.12, top) and an average of 27.4 G in the case where 1:2 metal to ligand ratio was used (Figure 2.12, bottom). Moreover, both spectra indicate an electron-rich metal species as suggested by g-values greater than 2. In 1:1 equivalents of manganese to benzodiazepine, g-values of 2.004 and 4.309 were found alongside an average A_{Mn} coupling of 95.6 G. With 2 equiv. benzodiazepine, g-values of 2.002 and 3.806 were found alongside an average A_{Mn} coupling of 95.4 G. It is apparent by comparison that the spectra are almost identical.

The matching EPR spectral signatures suggest identical compounds formed in these batches. Though ligand **2a**, as demonstrated in nickel and cobalt compounds **6a**–**c** and **7a**–**c**, appears to preferentially form bischelates, these similar spectra imply that the compound in the 1:1 and 2:1 mixtures are identical. Given the crystal structure of compound **9** from one equiv. of **2a**, the EPR implies that the bimetallic bridged chlorine structure forms in both 2:1 and 1:1 starting material ratios in solution. Also, in the case of the 2:1 ratio, some precipitation was observed, which could be the bischelate that was found to contaminate the crystalline material of **9**.

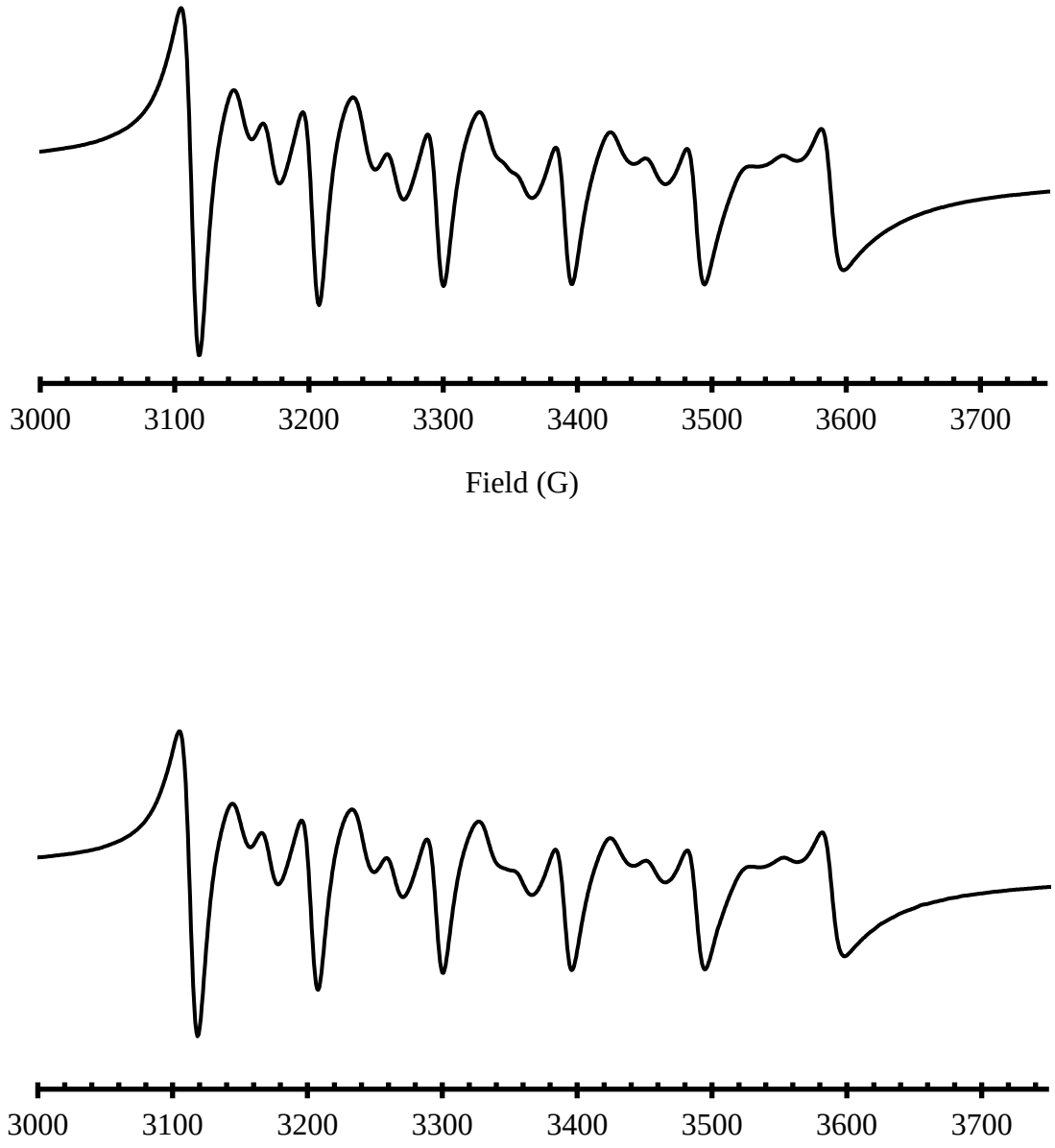

Figure 2.12 X-band EPR spectrum (77 K) of a 1:1 mixture of compound **2a** (2.5 mM) and anhydrous manganese dichloride (2.5 mM) in methanol glass (top) and of a 2:1 mixture of compound **2a** (9.8 mM) and anhydrous manganese dichloride (4.9 mM) in methanol glass (bottom). Spectrometer settings: microwave frequency 9.39 GHz; microwave power 0.2 mW; modulation frequency 100 kHz; modulation amplitude 0.80 mT; gain 30.

2.2.3. Comparison of nickel, cobalt, and manganese complexes

In comparing the bischelate compounds, the benzodiazepine ligand does not appear to undergo significant conformational changes in the different metal complexes (**6a**–**c**, **7a**–**c** and **8**). The conformation of the benzodiazepine 7-membered ring has been studied in the literature.[69] The distance of the tip of the benzodiazepine's half chair conformation (referred to as C–3) to the plane that contained the diazepine benzene ring was determined for each bischelate complex from the X-ray crystal structures (see Figure 2.13). Table 2.6 presents these distances, and on average, the complexes differ by no more than 0.3 Å. Compared to the crystal structure of the free *m*-tolyl ligand **2d** alone, there is only, at most, a *ca.* ±0.1 Å difference when examining metal complexes **6a**–**c**, **7a**–**c**, and **8**.

The observed HRMS spectra and DSC for compounds **6a**–**c**, **7a**–**c**, **8**, and **9** provided more information with regards to the structural assignments and homogeneity of samples. A peak corresponding to the complex's ionized molecular weight (M+H) in the HRMS spectra was consistently not detected. Instead, the ionized molecular mass by loss of a chloride (M–Cl) was observed. These observations are also similar to another study on benzodiazepine metal complexes where the authors reported a loss of multiple chlorides in the mass spectra for their metal complexes and characterized one compound by X-ray.[2] The observed HRMS of this class of metal complexes is scarcely reported in the literature.[56–58] Moreover, experiments to reproduce crystalline material of compound **9** showed the presence of another complex, which is potentially the bischelate derivative with benzodiazepine ligand **2a** (not illustrated) as evidenced by an $[M–Cl]^+$ of 712.1909 (calculated $[M–Cl]^+$ mass of $C_{42}H_{34}N_6ClMn$ 712.1914) in the HRMS spectrum of

compound **9** in solvent CH_2Cl_2:methanol (2:98) using a water and acetonitrile LC-MS mobile phase.

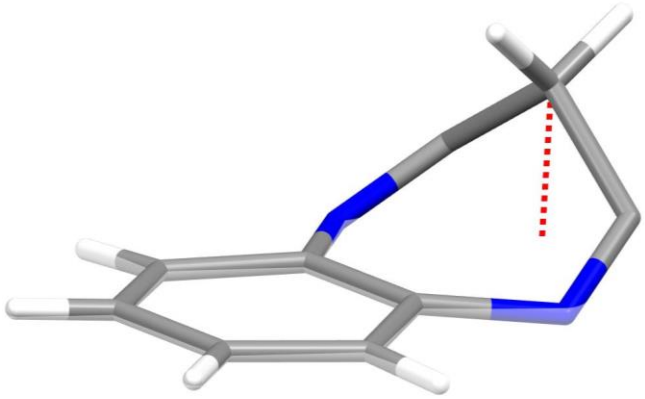

Figure 2.13 Distance from C–3 to the average plane of the benzodiazepine benzene ring.

Table 2.6 Distance between C–3 and the average plane containing the benzene carbons.

Compound	Ligand 1 [Å]	Ligand 2 [Å]
2d	1.500	n/a
2e	1.379	n/a
6a	1.616	1.482
6b	1.636	1.658
6c	1.469	1.490
7a	1.385	1.513
7b	1.608	1.609
7c	1.454	1.487
8	1.353	1.425

Regarding DSC, the complexes all demonstrated melting temperatures as opposed to decomposition exotherms. Nickel compounds **6a** and **6c** had relatively larger melting points at 330 °C and 303 °C, respectively, and were of higher melting point temperatures than their analogous cobalt complexes, **7a** (278 °C) and **7c** (225 °C). Nickel compound **6b** had a relatively lower melting point at 208 °C, which suggests intermolecular forces may be altered by the *m*-tolyl substituent. Manganese compound **8** had a melting point of 304 °C, which is comparable to those of the other complexes.

2.3. Summary

A simple method has been developed and applied for the synthesis of a variety of benzodiazepine bidentate coordination complexes (yields >80%, and a yield of 53% for compound **8**), namely bischelate nickel, cobalt, and manganese dichlorides. The method provides room-temperature access to a variety of metal-coordinated complexes using metal dichloride hydrates. Complex structures were confirmed by X-ray crystallography. They exhibit predominantly distorted octahedral geometry and possess two coordinating ligands per metal center, except for the bridged chloride manganese structure **9**. Their structural features were determined and were often in alignment with similar complexes reported in the literature. These results show that 1,5-benzodiazepines may potentially coordinate to metal ions in biological materials.

2.4. Experimental

2.4.1. Materials and methods

Unless otherwise noted, reagent grade solvents and starting materials were used without further purification. High-resolution mass spectra (HRMS) were recorded on a Synapt G2 S*i* mass spectrometer (Waters) equipped with an ESI source and quadrupole

time-of-flight mass analyzer. Data were collected in centroid mode and mass measurement was corrected during acquisition using leucine enkephalin solution as an external reference (Lock-SprayTM, reference ion at m/z 556.2771 Da ($[M+H]^+$) in ESI+ mode). FT-IR spectra were recorded on a Bruker Alpha-P ATR spectrometer. DSC was conducted on a TA Instruments model Q 1000 (rate 10 °C/min) equipped with the software Universal Analysis V4.5A for T_i, T_e, and T_p values. Samples for X-band EPR spectra were prepared from methanol solutions of **2a** and anhydrous manganese chloride, which were frozen (glass) to 77 K with liquid nitrogen. X-Band EPR spectra were recorded on glassy (77 K) samples using a Bruker EMX PremiumX EPR spectrometer (9.39 GHz), using 0.2 mW microwave power, 100 kHz field modulation, and 0.80 mT modulation amplitude.

2.4.2. Synthesis of nickel complexes **6a**–**6c**; general procedure

A reaction vessel (*i.e.*, a vial or round bottom flask, 10 mL) equipped with a stir bar was charged with benzodiazepine **2a**, **2d**, or **2e** (0.261 mmol), dichloromethane (4.0 mL), and the solution was stirred or sonicated until the benzodiazepine was fully dissolved. A second reaction vessel (25 mL) equipped with a stir bar was charged with nickel chloride hexahydrate (0.0313 g, 0.131 mmol) and methanol (1.5 mL). The mixture was stirred or sonicated until the metal salt was fully dissolved. The benzodiazepine solution was added dropwise to the metal salt solution, and the mixture was allowed to stir for *ca*. 2 h. The stir bar was removed, and the reaction vessel was placed uncapped into a sealed jar containing ether or n-pentane (vapor diffusion, 24–72 h). The resulting solution was decanted, and the remaining crystals were collected for X-ray

crystallography or dried by oil-pump vacuum for determination of yield and elemental analysis.

2.4.3. Nickel complex **6a**

From 2-(4-methylphenyl)-4-(pyridin-2-yl)-3*H*-1,5-benzodiazepine **2a** (0.0813 g, 0.261 mmol) and nickel chloride hexahydrate (0.0313 g, 0.131 mmol), yellow-green crystals (0.0936 g, 0.120 mmol; 92%), DSC ($T_i/T_e/T_p$) 278/330/335 °C. IR (ν, cm^{-1}): 3405 br w (H_2O), 3058 br w, 1585 m, 1563 w, 1436 br w, 1341 w, 1338 m, 1256 m, 1206 w, 1182 w, 1153 w, 1009 br w, 871 m, 762 s, 527 m, 436 m. HRMS (ESI-TOF): $[M–Cl]^+$ calcd for $C_{42}H_{34}N_6ClNi$ 715.1887, found 715.1894. Anal calcd for $C_{42}H_{34}N_6Cl_2Ni•1.5\ H_2O$ C, 64.72; H, 4.79; N, 10.79. Found C, 64.86; H, 4.69; N, 10.72.

2.4.4. Nickel complex **6b**

From 2-(3-methylphenyl)-4-(pyridin-2-yl)-3*H*-1,5-benzodiazepine **2d** (0.1123 g, 0.3606 mmol) and nickel chloride hexahydrate (0.0427 g, 0.180 mmol), gold crystals **6b** (0.1237 g, 0.1551 mmol, 86%), DSC ($T_i/T_e/T_p$) 200/208/214 °C. IR (ν, cm^{-1}): 3417 br w (H_2O), 3027 w, 1574 m, 1434 m, 1343 m, 1313 m, 1256 m, 1223 m, 1201 m, 768 s, 699 m. HRMS (ESI-TOF): $[M–Cl]^+$ calcd for $C_{42}H_{34}ClN_6Ni$ 715.1881, found 715.1898. Anal calcd for $C_{42}H_{34}Cl_2N_6Ni•2.5\ H_2O$ C, 63.26; H, 4.93; N, 10.54. Found C, 63.43; H, 4.73; N, 10.51.

2.4.5. Nickel complex **6c**

From 2-(4-methylphenyl)-7-nitro-4-(pyridin-2-yl)-3*H*-1,5-benzodiazepine **2e** (0.0680 g, 0.191 mmol) and nickel chloride hexahydrate (0.0227 g, 0.0954 mmol), yellow-green crystals dried to yellow-green solid **6c** (0.0778 g, 0.0904 mmol, 95%), DSC ($T_i/T_e/T_p$) 294/303/316 °C. IR (ν, cm^{-1}) 3073 br w, 1588 w, 1550 s, 1508 s, 1334 s, 1315

s, 1185 m, 1172 m, 1086 w, 1011 br w, 817 m, 799 m, 782 m, 746 m, 731 m, 703 m, 537 w, 518 w. HRMS (ESI-TOF) $[M–Cl]^+$ calcd for $C_{42}H_{32}ClN_8NiO_4$ 805.1583, found 805.1584. Anal calcd for $C_{42}H_{32}Cl_2NiN_8O_4$•1.5 H_2O C, 58.02; H, 4.06; N, 12.89, found C, 57.85; H, 4.07; N, 12.73.

2.4.6. Synthesis of cobalt complexes **7a**–**7c**; general procedure

To a reaction vessel (25 mL) equipped with a stir bar was added benzodiazepine **2a**, **2d**, or **2e** (0.260 mmol). Dichloromethane (5–10 mL) was added to the vial and the solution was stirred or sonicated until the benzodiazepine was fully dissolved. A reaction vessel equipped with a stir bar was charged with cobalt chloride hexahydrate (0.0146 g, 0.0614 mmol) and methanol (1.5 mL). The solution was stirred or sonicated until the metal salt was fully dissolved. The benzodiazepine solution was added to the metal salt solution, and the mixture was allowed to stir for ca 1 h. The mixture was transferred to an empty round-bottom flask (25 mL) and placed into a jar. The vial was partially filled with ether or *n*-pentane, surrounding the test tube (vapor diffusion) for at least 24 h.

2.4.7. Cobalt complex **7a**

From 2-(4-methylphenyl)-4-(pyridin-2-yl)-3*H*-1,5-benzodiazepine **2a** (0.0809 g, 0.260) and cobalt chloride hexahydrate (0.0310 g, 0.130 mmol), orange crystals dried to an orange solid **7a** (0.0843 g, 0.108 mmol, 83%), DSC ($T_i/T_e/T_p$) 264/278/280 °C. IR (ν, cm^{-1}): 3422 br w (H_2O), 3056 br w (H_2O), 1585 m, 1562 m, 1437 m, 1340 m, 1312 m, 1253 m, 1224 m, 1208 m, 1190 m, 1007 br w, 854 m, 815 m, 765 s, 752 m, 629 w, 542 m, 525 m, 502 m, 473 w, 433 m. HRMS (ESI-TOF) $[M–Cl]^+$ calcd for $C_{42}H_{34}N_6ClCo$ 716.1865, found: 718.1885. Anal calcd for $C_{42}H_{34}N_6Cl_2Co$•1.5 H_2O C, 64.70; H, 4.78; N, 10.78. Found C, 64.55; H, 4.78; N, 10.80.

2.4.8. Cobalt complex **7b**

From 2-(3-methylphenyl)-4-(pyridin-2-yl)-3*H*-1,5-benzodiazepine (0.0358 g, 0.115 mmol) **2d** and cobalt(II) chloride hexahydrate (0.0124 g, 0.0521 mmol), red crystals **7b** (0.0368 g, 0.0472 mmol, 91%). DSC ($T_i/T_e/T_p$) 267/273/275 °C; first transition endothermic peak at 29/34/76 °C. IR (ν, cm^{-1}): 3435 br w (H_2O), 3088 br w (H_2O), 1575 w, 1434 w, 1342 m, 1312 m, 1253 m, 1222 m, 1201 m, 767 s, 698 s. HRMS (ESI-TOF): $[M–Cl]^+$ calcd for $C_{42}H_{34}ClCoN_6$ 716.1860, found 716.1875. Anal calcd for $C_{42}H_{34}Cl_2N_6Co•1.5\ H_2O$ C, 64.71; H, 4.78; N, 10.78. Found C, 64.61; H, 4.57; N, 10.86.

2.4.9. Cobalt complex **7c**

From 2-(4-methylphenyl)-7-nitro-4-(pyridin-2-yl)-3*H*-1,5-benzodiazepine **2e** (0.0588 g, 0.164 mmol) and cobalt chloride hexahydrate (0.0200 g, 0.0840 mmol), orange crystals dried to an orange solid **6b** (0.0589 g, 0.0684 mmol, 81%), DSC ($T_i/T_e/T_p$) 205/225/230 °C. IR (ν, cm^{-1}): 3448 br w (H_2O), 3030 w, 1590 w, 1553 w, 1508 m, 1336 s, 1316 m, 1214 w, 1185, 1087 w, 1011 w, 800 w, 783 w, 746 w, 518 w. HRMS (ESI-TOF) $[M–Cl]^+$ calcd for $C_{42}H_{32}ClCoN_8O_4$ 806.1562, found 806.1575. Anal calcd for $C_{42}H_{32}Cl_2CoN_8O_4•H_2O$ C,58.61; H, 3.98; N, 13.02, found C, 58.61; H, 4.05; N, 12.88.

2.4.10. Manganese complex **8**

A round bottom flask (25 mL) equipped with a stir bar was charged with manganese chloride tetrahydrate (0.0261 g, 0.132 mmol) in methanol (5 mL). A solution of 7,8-dichloro-2-(4-methylphenyl)-4-(pyridin-2-yl)-3*H*-1,5-benzodiazepine **2b** (0.1001 g, 0.2630 mmol) in dichloromethane (10 mL) was added with stirring. The reaction was stirred for 2 h, and the mixture was transferred into a vial placed inside a jar filled with ether. Diffusion (24 h) gave orange crystals, the mother liquor was decanted off, and the

residue was dried over an oil-pump vacuum for 4 h to give **8** as an orange solid (0.0599 g, 0.0678 mmol, 52%), DSC ($T_i/T_e/T_p$) 278/304/308 °C. IR (ν, cm^{-1}) 3448 br w (H_2O), 3030 w, 1585 m, 1563 m, 1436 s, 1327 s, 1311 s, 1291 s, 1184 m, 1123 s, 1007 m, 857 m, 808 s, 788 s, 772 s, 746 m, 709 m, 569 w, 540 m, 525 m, 419 w. HRMS (ESI-TOF) $[M–Cl]^+$ calcd for $C_{42}H_{30}Cl_5MnN_6$ 848.0350, found 848.0367. Anal calcd for $C_{42}H_{34}N_6Cl_6Mn•1.5$ H_2O C, 55.23; H, 3.63; N, 9.20, found C, 55.47; H, 3.39; N, 9.24.

2.4.11. Manganese complex **9**

A round bottom flask (25 mL) equipped with a stir bar, was charged with manganese chloride tetrahydrate (0.0316 g, 0.160 mmol) in ethanol (1 mL). A solution of 2-pyridine-4-(4-methylphenyl)-3*H*-1,5-benzodiazepine **2a** (0.050 g, 0.160 mmol) in dichloromethane (1 mL) was added with stirring. An orange-colored solution was stirred for 2 h. Formation of an orange precipitate occurred within 20 min. The solid was filtered off using a fritted funnel (F porosity) and dissolved in acetonitrile/methanol (1:1, 4.0 mL total). A yellow-colored solution was placed into a test tube inside a vial containing ether. Diffusion (24 h) gave compound **9** as a light orange crystals. IR (ν, cm^{-1}) 3023 w, 2921 w, 1588 w, 1551 w, 1434 m, 1336 m, 1315 w, 1251 w, 1209 w, 1183 m, 1120 w, 1010 m, 854 m, 815 m, 784 w, 764 s, 624 w, 524 m, 423 w. HRMS (ESI-TOF) $[M–2CH_3OH–Cl]^+$ calcd for $C_{42}H_{34}Cl_3Mn_2N_6$ 837.0667, found 837.0676. In addition, HRMS (ESI-TOF) $[M–Cl]^+$ calcd for $C_{42}H_{34}N_6ClMn$ 712.1914, found 712.1909. Anal calcd for $C_{44}H_{42}Cl_4Mn_2N_6O_2$ C, 56.31; H, 4.51; N, 8.95, found C, 56.40; H, 4.50; N, 9.00.

2.4.12. EPR measurements related to formation of manganese complex **9**

EPR investigations were carried out combining **2a** (2.5 mM in methanol) and anhydrous manganese dichloride (2.5 mM in methanol) and freezing (77 K) the solution

as a glass with liquid nitrogen. Samples were kept in liquid nitrogen during measurement. The same protocol was applied in the measurement of the 2:1 mixture of compound **2a** (9.8 mM in methanol) and anhydrous manganese dichloride (4.9 mM in methanol) at 77 K.

CHAPTER THREE

1,5-BENZODIAZEPINE METAL COMPLEXES WITH FOUR- AND SIX-COORDINATE MONOCHELATES AND FIVE-COORDINATE BISCHELATES

3.1. Introduction

3.1.1. 1,5-Benzodiazepine monochelate complexes

Because coordination with metals can substantially alter the biological properties, electronic properties, and availability of a given molecule, understanding the interaction of biologically active or chelating molecules with metals is important for considerations with regards to biocatalysis and medicine. There is evidence that benzodiazepines can form both bischelate and monochelate metal complexes.[54]

A few monochelate benzodiazepine complexes have been reported in the literature. For example, Aversa *et al*. synthesized a monochelated platinum complex using a 1,4-benzodiazepine as the ligand (Figure 3.1, a).[70] Figure 3.1, b shows the first ruthenated benzodiazepine by Pérez *et al*.[71] Like other complexes in the literature, these examples demonstrate that the majority of this class of compounds are derived from 1,4-benzodiazepines. Though Haketa *et al*. synthesized a rhodium complex that incorporated a 1,5-benzodiazepine with two pyrrole units (Figure 3.1, c),[72,71] there have been many more investigations into the coordinating abilities of 1,4-benzodiazepines than 1,5-benzodiazepines. To further illustrate, Figure 3.1, d and e displays Zn(II) and Pd(II) 1,4-benzodiazepine metal complexes synthesized by Kojić-Prodić's group, which were characterized by X-ray crystallography.[73]

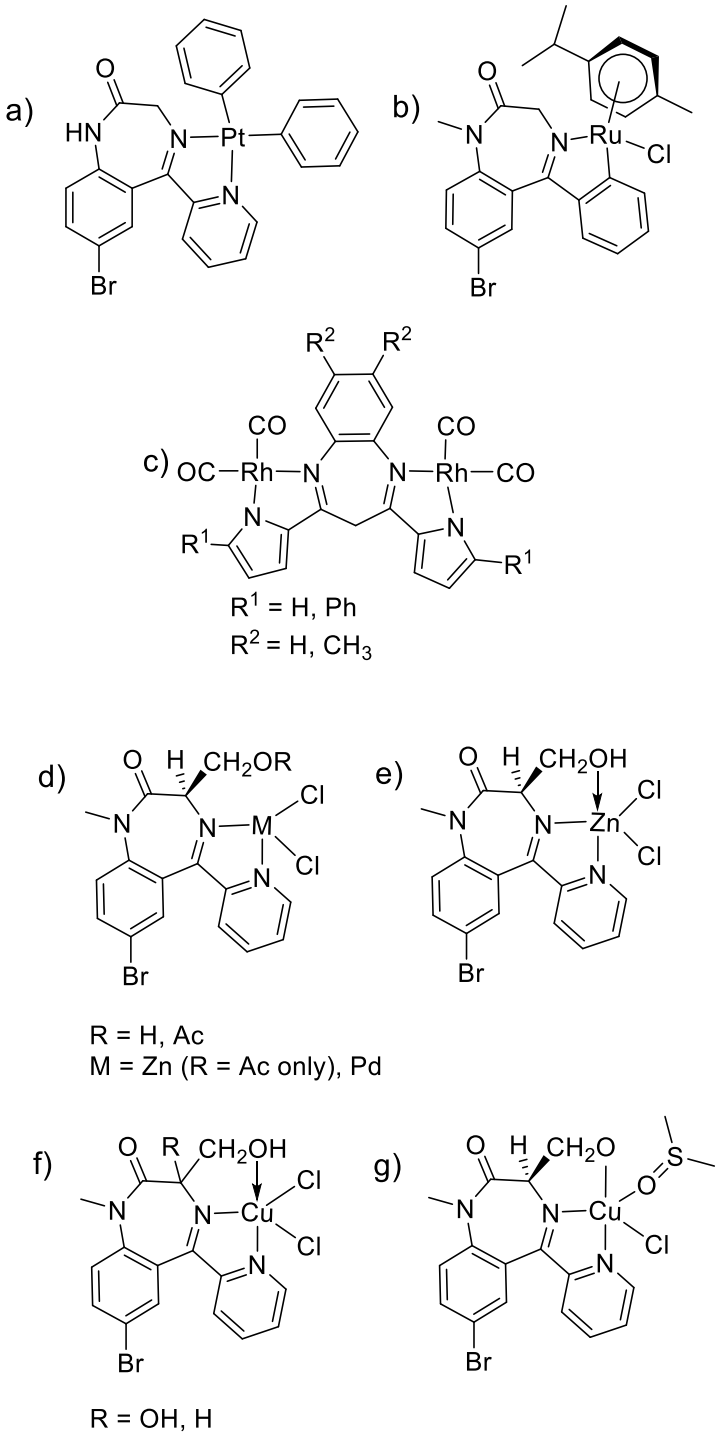

Figure 3.1 Examples of monochelated benzodiazepine metal coordinated complexes, see also Figure 2.4.

Kojić-Prodić's group[68] furthermore synthesized a variety of other 1,4-benzodiazepine metal complexes. The authors scope focused primarily on monochelated copper complexes with square-pyramidal and tetrahedral geometries (Figure 3.1, f and g), but it was also reported that bridged chloride copper complexes could form under similar conditions.[68] These copper compounds were subsequently studied by X-ray crystallography, which demonstrated the coordination ability of 1,4-benzodiazepines. Previous reports on 1,4-benzodiazepine copper dichloride complexes indicate that mono and bischelate compounds may form (structures not determined),[74] and that some monochloro copper complexes may be generated.[68] Furthermore, a protocol of similar complexes also implicated that changes in the crystallization solvent system may produce bis(μ-chloro) bridged complexes (Figure 3.2).[68] Like the aforementioned studies on bischelate complexes (Chapter 2), all of the complexes across Figures 3.1 and 3.2 demonstrate the feasibility of new coordination

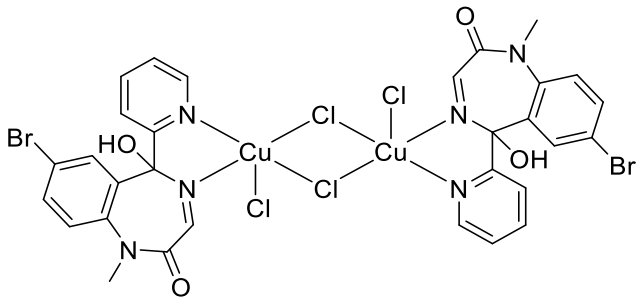

Figure 3.2 Chloride bridged copper complex reported by Kojić-Prodić's group.[68]

compounds using benzodiazepines, and these studies were extended into the synthesis and elucidation of new 1,5-benzodiazepine X-ray structures.[54,73] Herein is presented the investigation of new zinc, ruthenium, and copper 1,5-benzodiazepine metal complexes.

3.2. Results and discussion

3.2.1. Synthesis of zinc, ruthenium, and copper complexes

In a similar fashion to those complexes synthesized from nickel, cobalt, and manganese hydrated salts (Chapter 2), different metals were used in an attempt to form monochelate variants. Zinc chloride was chosen because it is known to form tetrahedral geometries.[73] Dichlorotris(triphenylphosphine)ruthenium(II) was also included because it has been characterized as a five-coordinate complex,[75] providing an interesting variant to investigate. Also copper chloride dihydrate[76] was included given previous reports of unique bridged-chlorine geometries.[68]

In applying a synthetic method similar to that described in Chapter 2, both monochelated and bischelated compounds were produced (Figure 3.3). The method illustrated in Figure 3.3 involved combining a metal salt with a benzodiazepine ligand in a mixture of two organic solvents, followed by vapor diffusion crystallization with a third, more volatile solvent. Application of this method produced several coordination complexes (**10a**–**b**, **11**, **12a**, and **13**) with yields >80%, with **12b** as one exception (63%, Table 3.1). As referred to the chelating ligand, two monochelated zinc complexes (**10a** and **10b**) and a monochelated ruthenium complex **11** (disregarding a coordinating triphenyl phosphine) were formed. Although prior reports by Kojić-Prodić's group[68] indicated monochelated copper complexes form with benzodiazepines (Figure 3.1, f and g), bischelated copper structures were formed using the synthesis outlined in Figure 3.3.

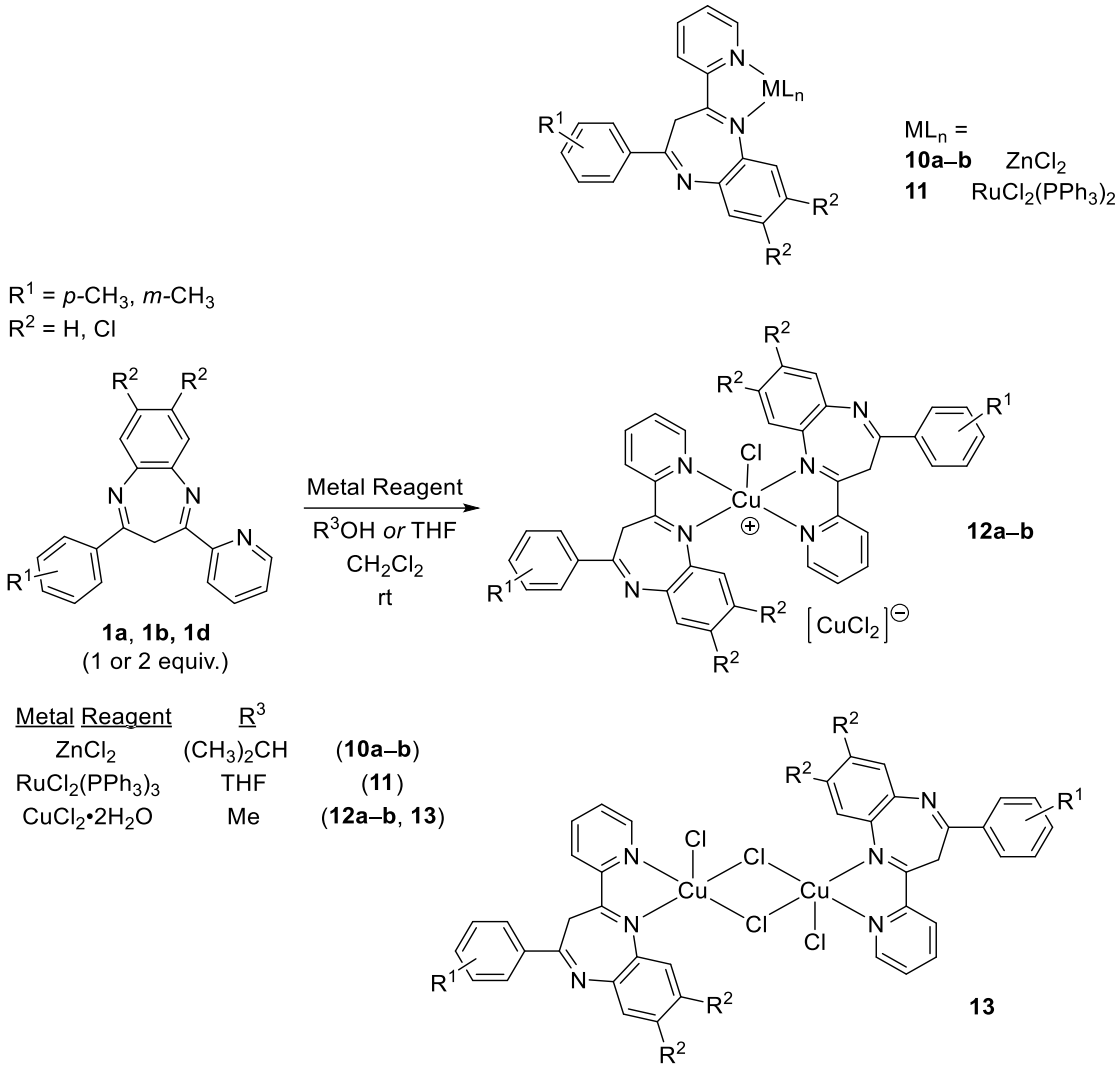

Figure 3.3 General synthesis of benzodiazepine mono- and bischelate complexes.

Elemental analysis of the oil-pump vacuum dried crystalline material gave evidence that the structures produced by X-ray analysis were representative of the entire sample, and deviations of the elemental analysis from the expected ratios was justified by the presence of the recrystallization solvent.

Table 3.1 Synthesized zinc, ruthenium, and copper complexes with analytical data.

Entry	Metal Complex	Elemental Analysis	Yield [%]
10a	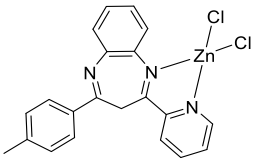	$C_{21}H_{17}Cl_2N_3Zn$ <u>Calculated</u> C: 56.34, H: 3.83, N: 9.39 <u>Found</u> C: 56.34, H: 3.88, N: 9.53	81
10b	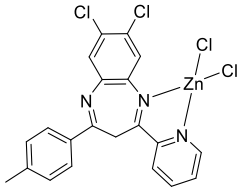	$C_{21}H_{15}Cl_4N_3Zn$ <u>Calculated</u> C: 48.83, H: 2.93, N: 8.13 <u>Found</u> C: 48.04, H: 2.90, N: 7.97	86[a]
11	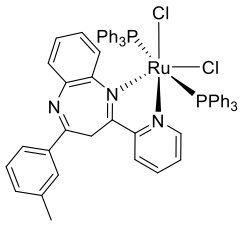	$C_{57}H_{47}Cl_2N_3P_2Ru•CH_2Cl_2$ <u>Calculated</u> C: 63.74, H: 4.52, N: 3.85 <u>Found</u> C: 63.64, H: 4.58, N: 3.90	86
12a	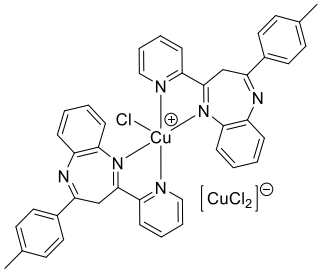	$C_{42}H_{34}Cl_3Cu_2N_6$ <u>Calculated</u> C: 58.92, H: 4.00, N: 9.82 <u>Found</u> C: 58.73, H: 3.93, N: 9.74	85
12b	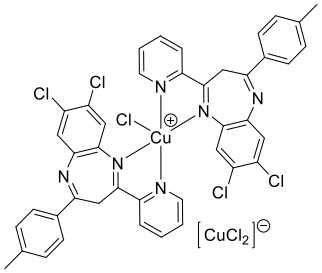	$C_{42}H_{30}Cl_7Cu_2N_6$ <u>Calculated</u> C: 50.75, H: 3.04, N: 8.46 <u>Found</u> C: 48.47, H: 2.91, N: 8.16	63

Table 3.1 Synthesized zinc, ruthenium, and copper complexes with analytical data —Continued

Entry	Metal Complex	Elemental Analysis	Yield [%]
13	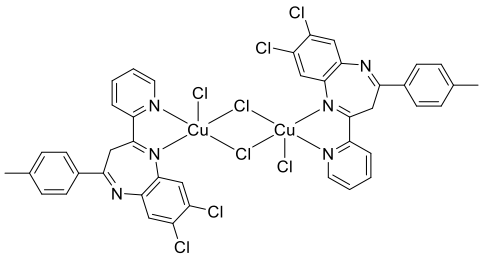	$C_{42}H_{30}Cl_8Cu_2N_6$•0.5 CH_2Cl_2 Calculated C: 47.62, H: 2.92, N: 7.84 Found C: 47.53, H: 2.76, N: 7.87	84[a]

a) Non-crystalline powder material.

3.2.2. Zinc monochelate benzodiazepine complexes

The X-ray structures and the corresponding crystallographic data of the monochelated zinc compounds **10a** and **10b** are shown in Figure 3.4 and Table 3.2. These structures were determined with high accuracy, with an *R*1 of 0.030 for **10a** and 0.028 for **10b** (Appendix A). To assess the geometry of the zinc coordination compounds (**10a** and **10b**), the geometric index for a 4-coordinate complex, τ_4,[77] was applied and found to be similar between the two molecules. τ_4 can be calculated using equation 3.1:

$$\tau_4 = \frac{360 - (\beta + \alpha)}{360° - 2\theta} \tag{3.1}$$

where θ is the interior angle of a tetrahedron (*i.e.*, $\theta = \cos^{-1}\left(\frac{1}{3}\right) \approx 109.5°$), and $\beta + \alpha$ is the sum of the two largest metal-containing angles in the complex, which happened to be N1—Zn—Cl2 and Cl1—Zn—Cl2, (Table 3.2). For compound **10a**, these two angles were 122.53(5)° and 117.29(2)°, respectively. For compound **10b**, the two angles were

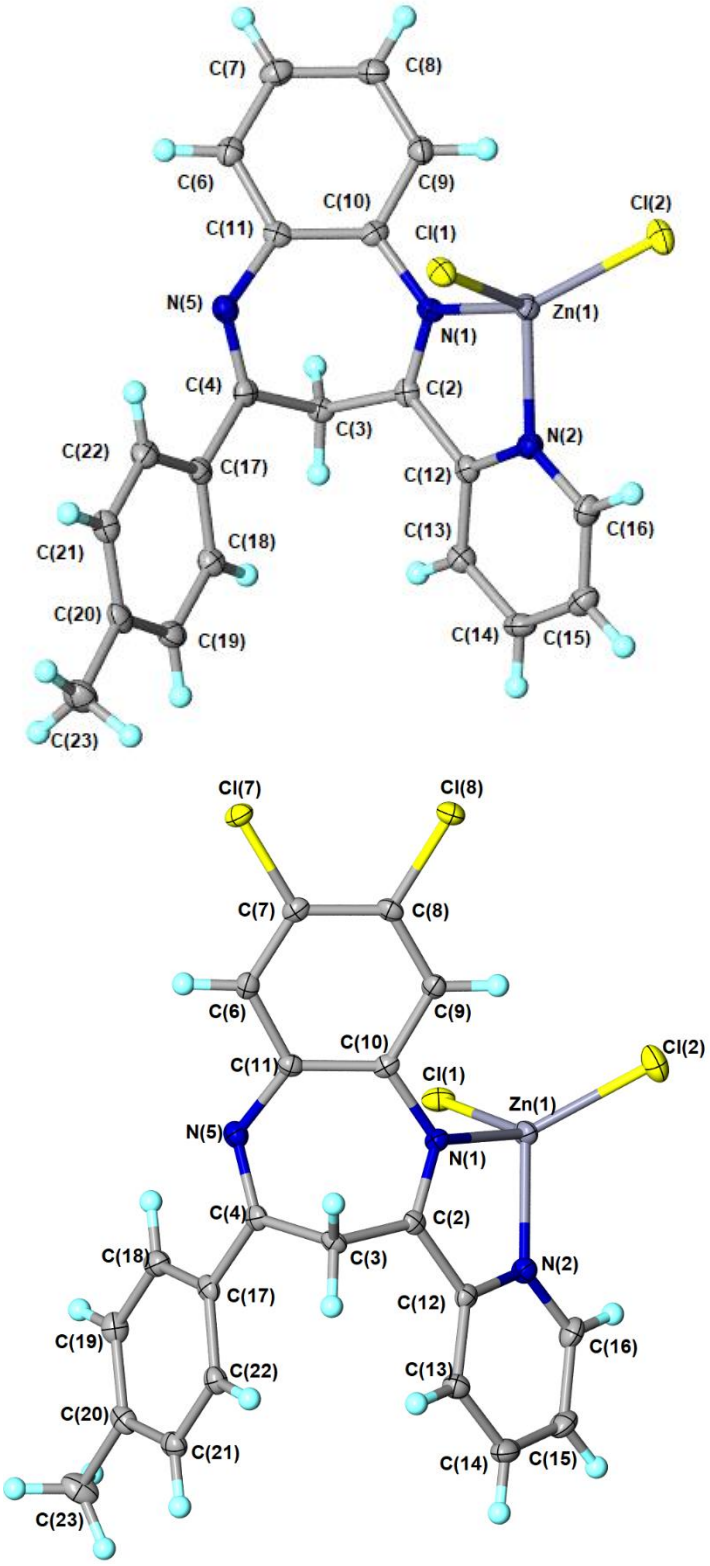

Figure 3.4 Crystal structures (50% probability thermal ellipsoids) of zinc complexes **10a** (top) and **10b** (bottom).

120.45(5)° and 118.55(2)°, respectively. For both **10a** and **10b** the value of τ_4 was found to be 0.9, which is in line with a tetrahedral geometry for the two compounds, as opposed to a square planar or seesaw geometry ($\tau_4 < 0.5$).

Table 3.2 Selected bond distances and angles of zinc complexes **10a** and **10b**.

Bond Distance [Å]			Bond Angle [deg]		
	10a	**10b**		**10a**	**10b**
Zn—N1	2.0651(19)	2.0820(17)	N1—Zn—N2	79.94(7)	80.26(7)
Zn—N2	2.0668(19)	2.0586(19)	N1—Zn—Cl2	122.53(5)	120.45(5)
			Cl1—Zn—Cl2	117.29(2)	118.55(2)

For zinc complexes **10a** and **10b**, the average distance between the metal and benzodiazepine nitrogen was 2.0736 Å and the average pyridine nitrogen to metal distance was 2.0627 Å. The structures were compared to those by Kojić-Prodić's group, which described two X-ray crystal structures of benzodiazepine zinc complexes (Figure 3.1).[73] One of these zinc complexes was tetra-coordinated (Figure 3.1, d), whereas the second was penta-coordinated (Figure 3.1, e). For these complexes, the metal to benzodiazepine nitrogen bond lengths average 2.10(2) Å and metal to pyridine bond lengths average 2.09(2) Å, slightly larger than those in **10a** and **10b**. The N1—Zn—N2 angle of **10a** and **10b** were 79.94(7)° and 80.26(7)°. Compared to Kojić-Prodić's group's tetra-coordinated zinc compound, the angle between the nitrogen atoms, with the metal as

the apex, was larger (Kojić-Prodić's group's structures' N1—Zn—N2 angle was on average 77.8(8)°). The two largest angles in compounds **10a** and **10b** were 122.53(5)° and 120.45(5)°, respectively, and these two angles both included a nitrogen and chloride. Kojić-Prodić's group's tetra-coordinated zinc compound's largest angle was 125.3(5)°, which is also a Cl—Zn—N_{BZD} angle.

3.2.3. Six-coordinate ruthenium benzodiazepine complex

With the presence of ruthenium in several anti-cancer compounds,[54] alongside the relatively few reports (refer to Figure 3.1, b) on the synthesis and X-ray analysis of its benzodiazepine coordination compounds,[56,71] the synthesis of ruthenium complexes was explored next. With literature precedence that a dimeric ruthenium precursor provides a suitable starting material for monochelated complexes,[71] a tris(triphenylphosphine)-ruthenium(II) dichloride was chosen, providing a five-coordinate starting material and a different type of metal starting material than those previously reported for benzodiazepine complexes.[56,71]

Synthesis of a monochelate complex of ruthenium was attempted under two conditions. Under ambient temperature (*ca.* 25 °C) and atmosphere, following the scheme depicted in Figure 3.3 with THF as solvent, a blue solution was obtained. Crystallizations attempts by diffusion using this solution were not successful and led to the precipitation of a black solid, suggesting decomposition of any ruthenium containing materials. There are experiments from the literature that implicate the necessity of an inert atmosphere, and therefore all following ruthenium experiments were carried out in a similar fashion to a method described in the literature.[72] Removal of THF by rotary evaporation, followed by vapor diffusion crystallization, produced X-ray quality crystals

of a distorted octahedral ruthenium complex whose X-ray structure was determined with high accuracy ($R1$ = 0.036, appendix A) and is shown in Figure 3.5.

The ruthenium compound's bond angles and bond distances are presented in Table 3.3. The bond distance between the chelating nitrogens and the metal center (2.093(2) Å for Ru1—N1 and 2.040(2) Å for Ru1—N2) were shorter than that of the phosphorous to metal distances (2.3748(7) for Ru1—P1 and 2.4202(7) Å for Ru1—P2), and the bond distances of compound **11** held similarities between those in the literature (see Figure 3.1, b)[71] and to compounds **10a** and **10b**.

Pérez *et al.*'s ruthenium compound (Figure 3.1, b) has a Ru—N_{BZD} distance of 2.055(4) Å, which is smaller than the analogous distance, Ru1—N1, in compound **11** and is closer in magnitude to the pyridine to metal bond distance in compound **11**, Ru1—N2. Pérez *et al.*'s compound consists of coordination by an *ortho*-carbon, which allowed for a five-membered chelate ring and this *ortho*-carbon to ruthenium bond distance is 2.038(5) Å, which is also surprisingly similar to that of the more electron-donating pyridine nitrogen to metal bond distance (Ru1—N2) in compound **11** (Table 3.3). Compound **11** had some similarities to the benzodiazepine nitrogen to zinc distance found in compounds **10a** and **10b** (2.0651(19) Å and 2.0820(17) Å, respectively, Table 3.2).

As opposed to similar studies of benzodiazepine metal complexes,[3] no d-d transitions were observed in the UV-vis spectra. This lack of convincing evidence can be attributed to the fact that the coordination complexes **6a**–**c**, **7a**–**c**, **8**, **9**, and **10a**–**b** did not withstand solvation in solution during the recording of the spectra. However, a transition

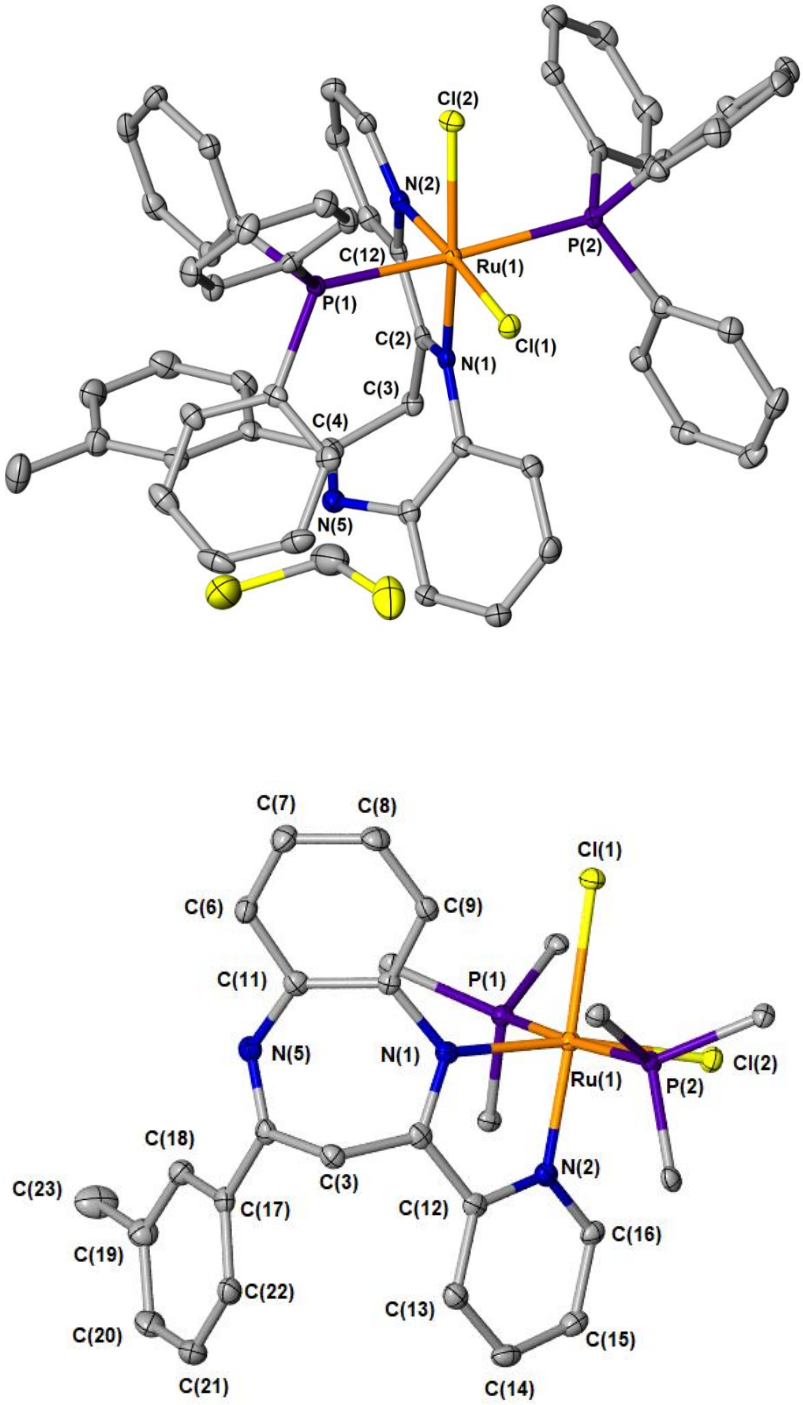

Figure 3.5 Crystal structure (50% probability thermal ellipsoids) of ruthenium complex **11** (top, full ORTEP and bottom, hydrogen atoms and triphenyl groups omitted for clarity).

Table 3.3 Selected bond distances and angles of ruthenium complex **11**.

Bond Distance [Å]		Bond Angle [deg]	
Ru1—N1	2.093(2)	N1—Ru1—N2	78.28(9)
Ru1—N2	2.040(2)	Cl1—Ru1—Cl2	90.46(2)
Ru1—P1	2.3748(7)	P1—Ru1—P2	174.73(3)
Ru1—P2	2.4202(7)		
Ru1—Cl1	2.4638(7)		
Ru1—Cl2	2.4205(7)		

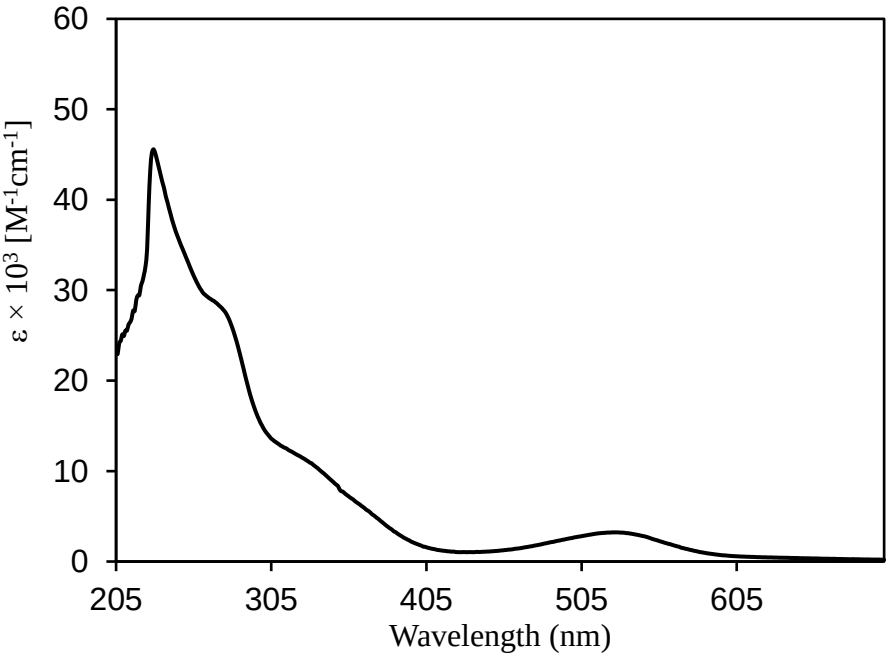

Figure 3.6 UV-vis of ruthenium compound **11** (CH_2Cl_2, 25 °C).

in the UV-vis spectrum of ruthenium complex **11** was observed at 527 nm (3,230 $M^{-1}cm^{-1}$, Figure 3.6). Moreover, a semi-reversible CV was only observed for the ruthenium compound **11** with $E_{1/2}$ = 0.4960 V (Figure 3.7).

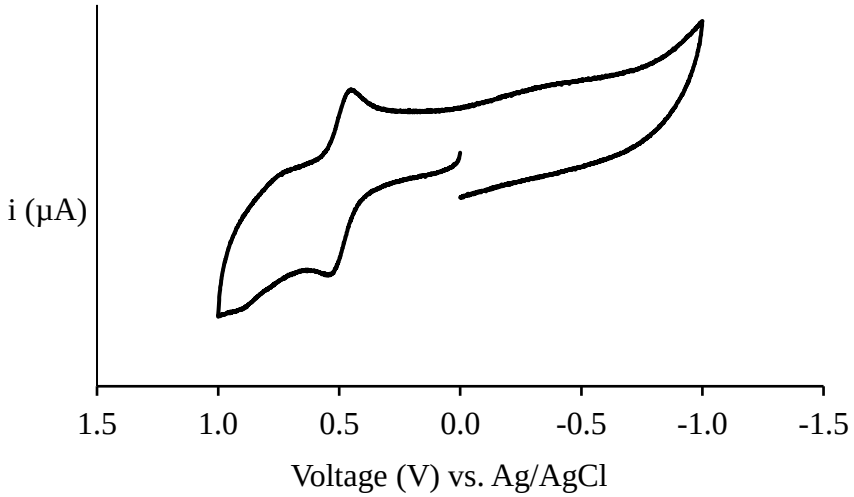

Figure 3.7 Cyclic voltammetry of ruthenium compound **11** (*ca.* 0.3 mM, CH_2Cl_2, 23 °C); supporting electrolyte: $TBAPF_6$ (0.1 M, CH_2Cl_2); working electrode Pt; reference electrode: Ag/AgCl; auxiliary electrode: Pt wire; scan rate: 100 mV/s.

3.2.4. Five-coordinate copper benzodiazepine complexes

Two copper benzodiazepine complexes (**12a** and **12b**) were obtained from ligands **2a** and **2b** in yields 85% and 63%, respectively (Table 3.1) through a preparation and X-ray analysis similar to that of zinc compounds **10a** and **10b** (Figure 3.8, top; and Table 3.4). These complexes were prepared from copper(II) chloride dihydrate and unique coordination behavior was observed (*e.g.*, bridged-chlorine structures).

Compared to compounds **6a**–**c**, **7a**–**c**, **8**, **9**, **10a**–**b**, and **11**, complexes **12a** and **12b** are unique in that their complexation is five-coordinate, contain a charged metal center balanced by a reduced form of the starting material, and feature two oxidation states of copper. Formation of the complex involved loss of one chloride from the metal center, forming a five-coordinate copper(II) complex as opposed to six-coordinate (*e.g.*, see Chapter 2) complexes. Within the literature, reports of similar benzodiazepine copper chloride complexes had also shown the loss of a chloride, with respect to the starting material, due to coordination of either a solvent molecule or a neighboring polar substituent (Figure 3.1, g),[68] but the X-ray crystal structures of **12a** and **12b** (Figure 3.8, top) do not contain coordinating solvents or the lost chloride anion. The other chloride appears to be bonded to a copper(II) cation that is balanced by a copper(I) dichloride anion. This means that half of the copper chloride was reduced, which has been observed in similar complexes derived from copper chloride dihydrate.[78]

It was thought that methanol may reduce copper(II) in the starting material and methanol would likely convert into a formaldehyde byproduct, which was also suggested in another study involving copper complexes.[78] The synthesis of **12b** was repeated and the crude reaction solution was sampled for solvent analysis by ^{1}H NMR. Analysis of the spectra in D_2O did not indicate any signals or appearance related to formaldehyde (9.7 ppm) or its hydrolysis products in aqueous solution (*i.e.*, methylene glycol at 4.9 ppm and dimethylene glycol at 5.0 ppm); experimental spectra were compared to spectra provided in the literature.[79] Formaldehyde would likely react with methanol, as opposed to any residual water, so the NMR was inspected for formaldehyde-derived products as suggested in the literature.[80] The original methanol peak appeared to widen downfield,

indicative of peaks forming in the vicinity of those of formaldehyde-methanol adducts (*ca.* 3.55 ppm),[80] so GC-MS was carried out after the copper complex **12b** crystalized from its solvent via vapor diffusion with ether. GC-MS analysis only detected methanol and dichloromethane. No formaldehyde, nor any larger adduct with water or methanol, were detected, though it is possible that it evaporated upon formation, or oxidized further into formic acid, and requires more sophisticated detection techniques.[81]

Chloride bridged species, compound **13**, was also obtained and was synthesized when only one equiv. of benzodiazepine **1b** ligand was reacted with copper(II) chloride dihydrate (Table 3.1), which is similar to those copper bridged species described in the literature.[68] Formation of complex **13** also excludes the reduction of copper(II), in contrast to **12a** and **12b**. X-ray crystallography determined the structures of all three copper compounds with relatively good accuracy (Figure 3.8; $R1 < 0.050$, appendix A), with compounds **12a** and **12b** having $R1 = 0.039$ and 0.045, respectively and compound **13** at 0.029.

Compounds **12a** and **12b** both consist of a geometry that appears to be between a square pyramidal or a trigonal bipyramidal geometry. A parameter was assessed to determine the predominant geometry in these complexes. For five-coordinate complexes, the geometry index (τ_5 in this case) is frequently used to assist in classifying the geometry.[82] Parameter τ_5 is calculated by equation 3.2:

$$\tau_5 = \frac{\beta - \alpha}{60°} \tag{3.2}$$

where α and β are the two largest angle measures in the given 5-coordinate complex.

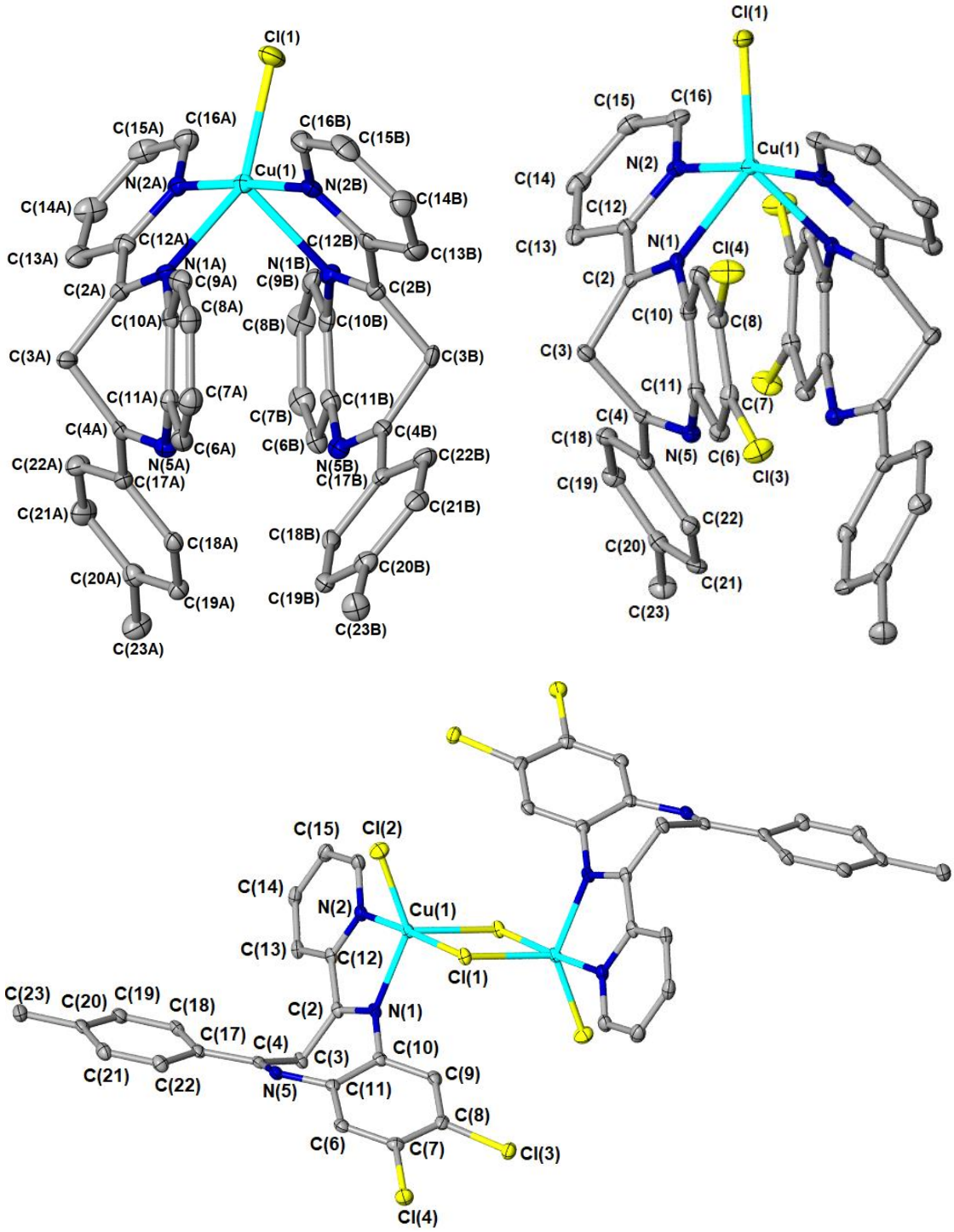

Figure 3.8 Crystal structures (50% probability thermal ellipsoids) of copper complexes **12a**, **12b**, and **13** (from top left to bottom, hydrogen atoms omitted for clarity).

Values of τ_5 closer to 1 are considered more trigonal bipyramidal in character, whereas those closer to 0 are considered more characteristic of square pyramidal.[83]

For copper compounds **12a** the largest angles were Cl1—Cu1—N1A, 150.68(13)° and N2A—Cu1—N2B, 176.0(2)° (Table 3.4) and this provides a τ_5 of 0.4, meaning the geometry is closer to a square pyramidal rather than trigonal bipyramidal. Likewise, the largest angles within compound **12b** are Cl1—Cu1—N1A, 135.11(7)° and N2A—Cu1—N2B, 173.15° (no ESD). The τ_5 of compound **12b** calculates to 0.6, which indicates this compound has more trigonal bipyramidal character than it has square pyramidal character, marking a difference between compounds **12a** and **12b**.

In terms of bond distances, compounds **12a** and **12b**. had a copper to benzodiazepine nitrogen distance (Cu1—N1) of 2.117(5) Å and 2.172(3) Å, respectively, which appeared to contrast bond distances of similar copper complexes.[68] In another study by Kojić-Prodić's group regarding penta-coordinated copper benzodiazepine complexes (Figure 3.1, f and g),[68] in contrast to compounds **12a** and **12b**, an average Cu—N_{BZD} distance of 1.98(1) Å and an average Cu—N_{py} distance of 2.00(1) Å was found. The shorter bond distances with the copper center and the chelating nitrogens could be attributed to the presence of only one ligand in the species. The copper compound **12b** is also unique in that, unlike compound **12a** and those from Kojić-Prodić's group, it was distorted trigonal bipyramidal in character.

Table 3.4 Selected bond distances and angles of copper complexes **12a** and **12b**.

Bond Distance [Å]	**12a**	**12b**	Bond Angle [deg]	**12a**	**12b**
Cu1—N1A	2.117(5)	2.172(3)	N1A—Cu1—N2A	79.62(19)	
					78.26(10)
Cu1—N1B	2.237(5)	2.172(3)	N1B—Cu1—N2B	77.63(19)	
Cu1—N2A	1.998(5)	1.987(3)	Cl1—Cu1—Cl2	n.a.	n.a.
Cu1—N2B	1.981(5)	1.987(3)	Cl1—Cu1—N1A	150.68(13)	135.11(7)
Cu1—Cl1	2.2662(15)	2.2589(12)	Cl1—Cu1—N2A	93.15(14)	93.42(8)
			N2A—Cu1—N2B	176.0(2)	173.15[a]

a) ESD is not available.

The crystallographic data for chloride-bridged compound **13** (Figure 3.8, bottom) is presented in Table 3.5. In considering the geometry of compound **13**, τ_5 was calculated using the two largest angles containing the copper ion as an apex (Table 3.5). These angles were N1—Cu1—Cl2 (138.23(5)°) and N2—Cu1—Cl1 (175.40(5)°), and these values meant τ_5 calculates out to 0.62, meaning that the bridged species **13** could be perceived as consisting of two trigonal bipyramidal units. This result is expected since **12b** was also trigonal bipyramidal and was also derived from ligand **2b**. In comparing the bond distances of compound **13**, to **12a** and **12b**, it was noticed that Cu—N_{BZD} was on average only slightly shorter in **13** by no more than 0.15 Å. As for Cu—N_{py}, compounds **12a** and **12b** were shorter on average by no more than 0.1 Å.

Table 3.5 Selected bond distances and bond angles from chloride bridged copper complex **13**.

Bond Distance [Å]		Bond Angle [deg]	
Cu1—N1	2.1070(17)	N1—Cu1—N2	78.73(7)
Cu1—N2	2.0017(18)	N1—Cu1—Cl2	138.23(5)
Cu1—Cl1	2.5803(5)	N2—Cu1—Cl1	175.40(5)
Cu1—Cl1′	2.2842(5)	Cl1—Cu1—Cl2	93.04(2)
Cu1—Cl2	2.2558(6)	Cl1′—Cu1—Cl2	119.46(2)
		Cl1—Cu1—Cl1′	86.518(18)

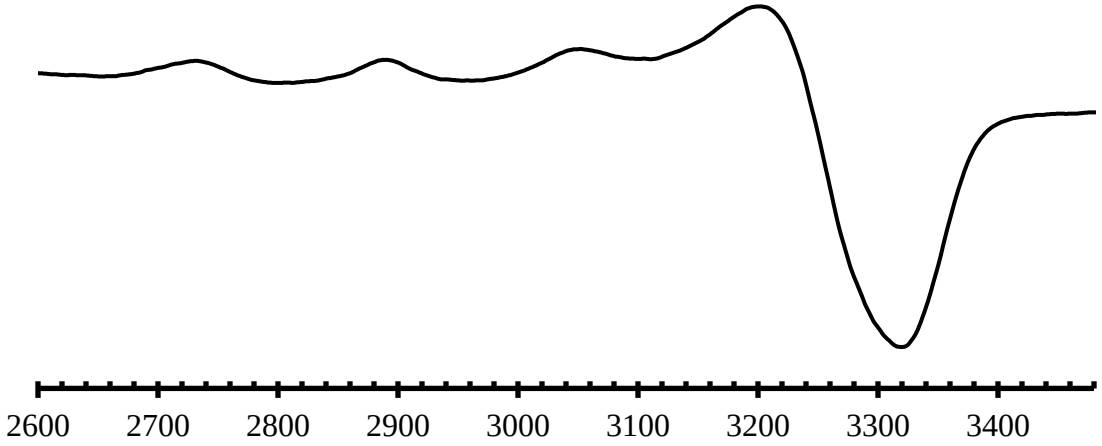

Figure 3.9 X-Band EPR spectrum (77 K) of copper complex **12a** at 23 °C prepared by combining compound **2a** (5.7 mM) with anhydrous copper chloride (2.5 mM) in methanol glass. Spectrometer settings: microwave frequency 9.39 GHz; microwave power 20 μW; modulation frequency 100 kHz; modulation amplitude 0.8 mT; gain 30.

EPR measurements of the copper bischelate complex (**12a**) formed *in situ* (methanol) as a methanol glass at 23 °C were performed to characterize any responsive coupling of the copper's electrons with its nucleus (Figure 3.9). The experimental EPR spectrum in Figure 3.9 has the four lines expected from a single-copper(II) complex. The $g_{\perp}$ was measured as 2.0678, and the $g_{\parallel}$ value was found to be 2.26786. The four lines split with an average $A_{\parallel}$ of 155.80 G. The hyperfine splitting and the corresponding A_N value are not present in the spectrum, and this can be attributed to the close relative abundances of the copper isotopes, ^{63}Cu and ^{65}Cu.

3.2.5. Comparison of zinc, ruthenium, and copper complexes

In examining zinc complexes **10a–b**, ruthenium complex **11**, copper complexes **12a–b**, and the bridged binuclear copper complex **13**, structural determinations and DSC

were compared. Structural measurement of the distance of C–3 from the aromatic diazepine ring and are shown in Table 3.6 (see Figure 2.13, Chapter 2). Irrespective of the ligand, the zinc complexes did not display a significant change in distance, whereas

Table 3.6 Distance between C–3 and the average plane containing the benzene carbons.

Structure	D1 [Å]	D2 [Å]
10a	1.457	n.a.
10b	1.437	n.a.
11	1.627	n.a.
12a	1.353	1.469
12b	1.604	1.604
13	1.386	1.386

copper bischelates **12a–b** differ by more than 0.2 Å, suggesting an effect of the benzodiazepine **2b** in complexation of a copper ion. DSC of the complexes showed that the monochelated zinc complexes (**10a–b**) had higher melting point temperatures, 325 °C and 328 °C respectively, as compared to the ruthenium complex **11** (223 °C), copper bischelates **12a–b** (229 °C and 216 °C respectively), and bridged copper complex **13** (219 °C), suggesting some enhancement of stability by either monochelate complexation or the zinc center.

3.3. Summary

A simple method has been developed for the synthesis of bischelate benzodiazepine metal complexes (see Chapter 2), and this method has been extended for the synthesis of a variety of benzodiazepine coordination complexes (yields >80%, and **12b** with a yield of 63%). The method provides room-temperature access to a variety of metal coordinated complexes using metal dichloride hydrates. Complex structures were confirmed by X-ray crystallography and the purity was supported by elemental analysis. As compared to Chapter 2, these complexes are either monochelate or are five-coordinate bischelates, with the unique example of bridged-chloride copper complex **13**. Their structural features were determined and were compared against one-another and with similar complexes reported in the literature. These results gave insight into how 1,5-benzodiazepines may coordinate to metal ions in solution.

3.4. Experimental

3.4.1. Materials and methods

Electronic absorbance was measured using a Cary-100 UV-vis spectrophotometer (Agilent) in double-beam mode (sample and solvent blank) using a 10 mm path quartz cuvette (Starna 23-Q-10 cell with a teflon stopper) and appropriate background subtraction to compensate for the solvent cutoff. For the electrochemical measurements, a Pt electrode was used as the working electrode. Pt wire and Ag/AgCl were used as counter electrode and reference electrode, respectively. Cyclic voltammograms were obtained with a Bioanalytical Systems, Inc. potentiostat controlled by Epsilon Electrochemical Workstation software with a scan rate of 100 mV/s. The supporting electrolyte was 0.1 M $TBAPF_6$ in CH_2Cl_2. All electrochemical measurements were

performed with bubbling dry dinitrogen into the sample. All other materials and methods were identical to those in Chapter 2.4.1.

3.4.2. Synthesis of zinc complex **10a**

A vial (25 mL) equipped with stir bar was charged with zinc chloride (0.0274 g, 0.201 mmol) and isopropanol (1.0 mL). A solution of 2-(4-methylphenyl)-4-(pyridin-2-yl)-3*H*-1,5-benzodiazepine **2a** (0.0626 g, 0.201 mmol) in dichloromethane (4.0 mL) was added while stirring. The reaction was stirred for 30 min; a small amount of precipitation formed within 15 min. The vial was placed inside a jar filled with ether. Diffusion over 24 h gave yellow crystals. The mother liquor was decanted, and the residue was dried by an oil-pump vacuum for 18 h at 40 °C to give **10a** as a yellow solid (0.0727 g, 0.163 mmol; 81%). DSC ($T_i/T_e/T_p$) 303/325/327 °C. IR (ν, cm^{-1}) 3105 w, 3060 w, 1587 m, 1559 w, 1435 m, 1336 m, 1313 m, 1255 m, 1208 m, 1182 m, 1115 br w, 1022 w, 959 w, 850 w, 815 w, 786 w, 764 s, 680 w, 629 w, 537 w, 517 w, 434 w. HRMS (ESI-TOF) $[M-Cl]^+$ calcd for $C_{21}H_{17}ClN_3Zn$ 410.0397, found 410.0398. Anal calcd for $C_{21}H_{17}Cl_2N_3Zn$ C, 56.34; H, 3.83; N, 9.39, found: C, 56.34; H, 3.88; N, 9.53.

3.4.3. Synthesis of zinc complex **10b**

A round bottom flask (25 mL) equipped stir bar was charged with zinc chloride (0.0439 g, 0.324 mmol) in isopropanol (2.0 mL). A solution of 7,8-dichloro-2-(4-methylphenyl)-4-(pyridin-2-yl)-3*H*-1,5-benzodiazepine **2b** (0.1116 g, 0.2935 mmol) in dichloromethane (6.0 mL) was added while stirring. The reaction was stirred for 1 h, a small sample was set aside, and the rest of the material was filtered off and dried with an oil-pump vacuum to give compound **10b** as a yellow solid (0.1300 g, 0.2516 mmol; 86%). The small sample was filtered, and the filtrate was transferred into a test tube

placed inside a vial containing ether. Diffusion (24 h) gave light yellow crystals suitable for X-ray crystallography. DSC ($T_i/T_e/T_p$) 307/328/333 °C. IR (ν, cm^{-1}): 3070 w, 3026 w, 1599 w, 1588 s, 1564 w, 1456 m, 1447 s, 1428 br w, 1331 m, 1310 s, 1294 m, 1271 br w, 1252 w, 1197 m, 1181 m, 1133 m, 1025 m, 902 w, 876 w, 859 w, 812 w, 792 m, 775 s, 723 w, 651 m, 539 m, 521 w. HRMS (ESI-TOF) $[M–Cl]^+$ calcd for $C_{21}H_{15}Cl_3N_3Zn$ 477.9618, found 477.9617. Anal calcd for $C_{21}H_{15}Cl_4N_3Zn$ C, 48.83; H, 2.93; N, 8.13, found: C, 48.04; H, 2.90; N, 7.97.

3.4.4. Synthesis of ruthenium complex **11**

A 25 mL round bottom flask was charged with dichlorotris(triphenylphosphine)-ruthenium(II) (0.159 g, 0.166 mmol) and a stir bar, and equipped with a septum. A separate 10 mL round bottom flask was charged with 2-(3-methylphenyl)-4-(pyridin-2-yl)-3*H*-1,5-benzodiazepine **2d** (0.0500 g, 0.161 mmol), a stir bar, and equipped with a septum. The flasks were evacuated and purged with nitrogen three times, and anhydrous THF (3.0 mL) was added to each flask. The benzodiazepine was stirred and sonicated until it fully dissolved, and then added via syringe to the ruthenium complex solution, which was stirred for 16 h. Solvent was removed by rotary evaporation and an oil-pump vacuum. The solid residue was flushed with nitrogen and was rinsed with ether (3 × 5.0 mL, decantation), while still in a closed flask, and was further dried with an oil-pump vacuum and subsequently flushed with nitrogen. Dichloromethane (3.0 mL) was added to the flask. The solution was transferred under nitrogen to an oven dried flask (25 mL), which was placed into a jar filled with n-pentane. Vapor diffusion (48 h) produced red violet crystals suitable for X-ray diffraction. Compound **11** was dried under an oil-pump vacuum for 24 h for elemental analysis and yield determination (0.1518 g, 0.1389 mmol,

86%). DSC ($T_i/T_e/T_p$) 176/223/229 °C. IR (ν, cm^{-1}): 3048 w, 1585 w, 1480 w, 1431 m, 1088 w, 788 w, 767 w, 734 m, 694 s, 511 s, 495 m, 406 w. UV-vis (CH_2Cl_2, 17.1 μM): λ_{max} 229 nm (45,600 $M^{-1}cm^{-1}$), 276 nm (sh, 27,400 $M^{-1}cm^{-1}$), 331 nm (sh, 10,900 $M^{-1}cm^{-1}$), 527 nm (3,230 $M^{-1}cm^{-1}$). HRMS (ESI-TOF): $[M–Cl]^+$ calcd for $C_{57}H_{47}ClN_3P_2Ru$ 972.1972, found 972.2001. Anal calcd for $C_{57}H_{47}Cl_2N_3P_2Ru•CH_2Cl_2$ C, 63.74; H, 4.52; N, 3.85. Found C, 63.64; H, 4.58; N, 3.90.

3.4.5. Synthesis of copper complex **12a**

A round bottom flask (25 mL) equipped with a stir bar, was charged with copper chloride dihydrate (0.0176 g, 0.103 mmol), methanol (2.0 mL), and dichloromethane (2.0 mL). A solution of 2-(4-methylphenyl)-4-(pyridin-2-yl)-3*H*-1,5-benzodiazepine **2a** (0.0633 g, 0.203 mmol) in methanol (2.0 mL) and dichloromethane (3.0 mL) was added with stirring. The reaction was stirred for 20 min, and the flask was transferred to a jar filled with ether. Diffusion (24 h) gave green crystalline material that was dried over an oil pump vacuum (24 h) to give compound **12a** as dark green crystals (0.0374 g, 0.0437 mmol, 85%), DSC ($T_i/T_e/T_p$) 187/229/238 °C; first transition endothermic peak at 140/155/167 °C. IR (ν, cm^{-1}): 3109 w, 3028 w, 1584 w, 1561 br w, 1538 w, 1434 m, 1332 w, 1311 w, 1257 m, 1205 br w, 1179 m, 1111 w, 1008 w, 962 w, 851 w, 817 w, 762 s, 625 m, 525 m, 477 br w, 409 br m. HRMS (ESI-TOF) $[M–Cl]^+$ calcd for $C_{42}H_{34}CuN_6$ 685.2135, found 685.2144, HRMS (ESI-TOF) $[M]^-$ calcd for Cl_2Cu 132.8679, found 132.8677. Anal calcd for $C_{42}H_{34}Cl_3Cu_2N_6$ C, 58.92; H, 4.00; N, 9.82, found C, 58.73; H, 3.93; N, 9.74.

3.4.6. Synthesis of copper complex **12b**

A 25 mL round bottom flask equipped with a stir bar was charged with copper chloride dihydrate (0.0064 g, 0.038 mmol), methanol (2.5 mL), and dichloromethane (2.5 mL). The mixture was allowed to stir for 5 min and a solution of 7,8-dichloro-2-(4-methylphenyl)-4-(pyridin-2-yl)-3*H*-1,5-benzodiazepine **2b** (0.0285 g, 0.0749 mmol) in methanol (2.5 mL) and dichloromethane (3.5 mL) was added dropwise while stirring. The reaction mixture was allowed to stir for 30 min and then the flask was transferred to a jar filled with ether. Diffusion over 24 h gave dark brown crystals. The material was dried over oil-pump vacuum to give **12b** as dark brown crystals (0.0111 g, 0.0106 mmol, 63%), DSC ($T_i/T_e/T_p$) 189/216/235 °C. IR (ν, cm^{-1}): 3102 w, 3071 w, 1581 w, 1558 m, 1436 s, 1336 w, 1310 m, 1290 m, 1261 m, 1182 m, 1124 m, 1024 w, 908 s, 851 m, 790 m, 773 s, 709 m, 647 m, 542 m, 524 m, 474 w, 416 w. HRMS (ESI-TOF) $[M–Cl]^+$ calcd for $C_{42}H_{30}Cl_4CuN_6$ $[M\text{-}Cl]^+$ 823.0553, found 823.0551. Anal calcd for $C_{42}H_{30}Cl_5CuN_6 \bullet CuCl_2$ C, 50.75; H, 3.04; N, 8.46, found C, 48.47; H, 2.91; N, 8.16.

3.4.7. Synthesis of copper complex **13**

A vial equipped with a stir bar was charged with copper chloride dihydrate (0.0292 g, 0.171 mmol), methanol (2.0 mL), and dichloromethane (2.0 mL). A solution of 7,8-dichloro-2-(4-methylphenyl)-4-(pyridin-2-yl)-3*H*-1,5-benzodiazepine **2b** (0.0650 g, 0.171 mmol) in methanol (1.0 mL) and dichloromethane (5.0 mL) was added while stirring. The reaction was stirred for 15 min and then the vial was placed inside a jar with ether (24 h) for vapor diffusion to give compound **13** as yellow needles. After decanting or filtering, the material was dried by an oil-pump vacuum for 18 h for to yield compound **12b** (0.0747 g, 0.0714 mmol, 84%). DSC ($T_i/T_e/T_p$) 193/219/238 °C. IR (ν,

cm^{-1}): 3073 w, 2922 w, 1581 w, 1558 m, 1438 m, 1337 m, 1311 m, 1290 m, 1263 m, 1184 m, 1125 m, 1024 w, 963 w, 909 m, 851 m, 820 br w, 790 w, 774 s, 746 w, 720 m, 709 m, 648 w, 569 m, 543 w, 524 w, 475 w, 416 w. Anal calcd for $C_{42}H_{30}Cl_8Cu_2N_6$•0.5 CH_2Cl_2 C, 47.62; H, 2.92; N, 7.84. Found C, 47.53; H, 2.76; N, 7.87.

3.4.8. Cyclic voltammetry measurements of ruthenium complex **11**

Cyclic voltammetry measurements were carried out on ruthenium compound **11** dissolved in CH_2Cl_2 (*ca.* 0.3 mM, 23 °C). The sample solution contained the supporting electrolyte $TBAPF_6$ (0.1 M in the CH_2Cl_2 sample solution), and nitrogen was purged through the solution prior to collection (100 mV/s scan rate). A platinum working electrode was used alongside a silver/silver chloride reference electrode and a platinum wire auxiliary electrode.

3.4.9. EPR measurements related to formation of copper complex **12a**

EPR investigations were carried out combining **2a** (5.7 mM in methanol) and anhydrous copper chloride (2.5 mM in methanol) and freezing (77 K) the solution as a glass with liquid nitrogen. Samples were kept in liquid nitrogen during measurement.

CHAPTER FOUR

CATALYST-FREE SYNTHESIS OF ISOQUINOLINE-FUSED BENZIMIDAZOLES

4.1. Introduction

4.1.1. Benzimidazo[2,1-*a*]isoquinolines

Another class of dinitrogen heterocycles that were investigated in this dissertation include benzimidazo[2,1-*a*]isoquinolines. These heterocycles are structurally composed of fused benzimidazole and isoquinoline moieties (Figure 4.1) and are potentially biologically active. Specifically, in 1996 Sun and LaVoie reported inhibitory effects on topoisomerase I and II from 3-methoxy-10-nitrobenzimidazo[2,1-*a*]isoquinoline.[84]

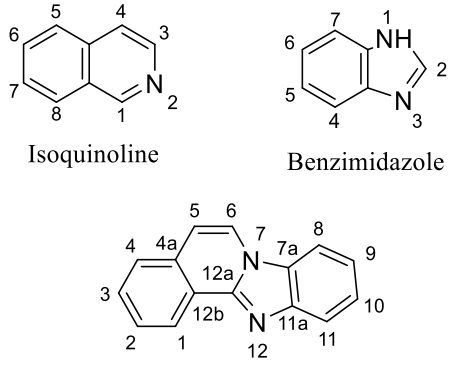

Figure 4.1 Structures of isoquinoline, benzimidazole, and benzimidazo[2,1-*a*]isoquinoline.

Synthetic protocols for this class of compounds have often included the use of a metal catalyst. From the standpoint of biological testing, metal catalysts usually are separated from the target compound to remove sources of auxiliary toxicity. Metal (*e.g.*, palladium) contaminants must also be beneath a specific threshold to meet pharmaceutical standards for medicinal drugs.[85] Minimizing the use of toxic reagents has value because it could lower the cost and time needed to produce new therapeutics. To develop a method that reduces costs and produces purer material, improvements of reported protocols for the synthesis of benzimidazo[2,1-*a*]isoquinoline were investigated.

4.1.2. Previous syntheses of benzimidazo[2,1-*a*]isoquinolines

In 1996, Sun and LaVoie described one of the earliest synthetic routes to benzimidazo[2,1-*a*]isoquinolines.[84] More recently, researchers have developed a variety of alternative means to form these molecules and these were reviewed by the author of this dissertation.[86] Substituted benzimidazoles can produce benzimidazo[2,1-*a*]isoquinolines through reactions with either diketones or acetylenes. Moreover, ethynylbenzaldehydes or benzimidamides can be used to produce the target compound through similar reactions with diamines and acetylenes, respectively.

In 2021, Liu and Li reported the application of calcium carbide, a low cost industrial starting material, for synthesizing benzimidazo[2,1-*a*]isoquinolines from haloaryl substituted benzimidazoles (Table 4.1).[87] The protocol can be used to prepare a variety of derivatives without substituents at C–5 and C–6.

In 2017, Miao *et al.*[88] and B.W. Yang *et al.*[89] independently published separate protocols to form benzimidazo[2,1-*a*]isoquinolines by reacting a phenyl substituted imidazole with a substituted 1,3-diketones (Table 4.2). Both protocols proceed by

Table 4.1 Selected experiments from a copper-catalyzed coupling protocol using bromo benzimidazoles and calcium carbide as substrates.

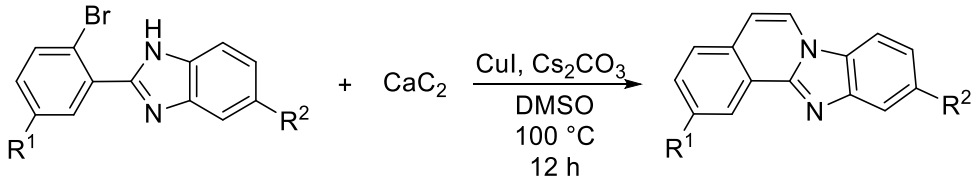

R^1	R^2	Yield [%]
H	H	82
F	H	84
Cl	H	85

Table 4.2 Selected experiments from a copper-catalyzed coupling protocol with benzimidazole and diketone as substrates.

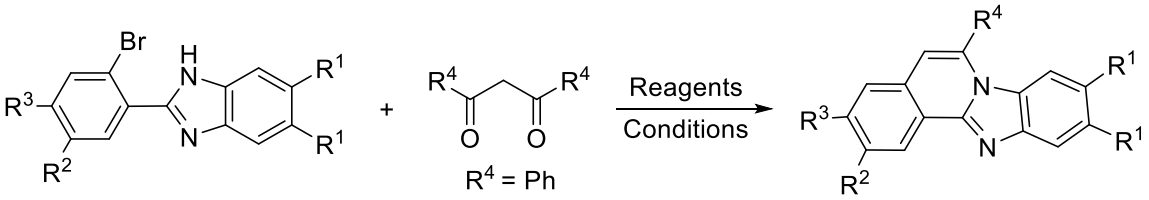

R^1	R^2	R^3	Catalyst/Solvent	Time [h]	T [°C]	Yield [%]	Ref
H	H	H	CuI, Cs_2CO_3, dioxane	n.d.	70	85	88
H	F	H	CuI, Cs_2CO_3, dioxane	n.d.	70	83	88
H	-OCH_2O-		CuI, Cs_2CO_3, dioxane	n.d.	70	75	88
Me	F	H	CuI, Cs_2CO_3, dioxane	n.d.	70	80	88
H	H	H	CuI, K_3PO_4, DMF	24	130	48	89
Me	H	H	CuI, K_3PO_4, DMF	24	130	52	89
H	F	H	CuI, K_3PO_4, DMF	24	130	45	89

copper-catalyzed coupling that is followed by a deacylation step. Miao *et al*. optimized reaction yields for the 2-(2-bromo-phenyl)-1*H*-benzo[*d*]imidazole and diphenyl 1,3-diketone using copper(I) iodide as the catalyst in the presence of cesium carbonate.[88] Yang *et al*. optimized a similar copper-catalyzed reaction but using potassium phosphate as a base.[89] These protocols produced several benzimidazo[2,1-*a*]isoquinolines. Products derived from diphenyl 1,3-diketone are shown in Table 4.2.

R. Yang *et al*. reported the synthesis of benzimidazo[2,1-*a*]isoquinolines through the annulation of 2-arylimidazoles and acetophenone derived sulfoxonium ylides (Table 4.3)[90] under aerobic conditions. Their procedure relies on catalysis using a rhodium(III) species that facilitates C–C coupling and formation of a C–N bond. The procedure includes catalytic amounts of silver hexafluoroantimonate and two equiv. of acetic acid in order to activate the rhodium precatalyst.

Table 4.3 Selected experiment from an annulation of benzimidazole with sulfoxonium ylides.

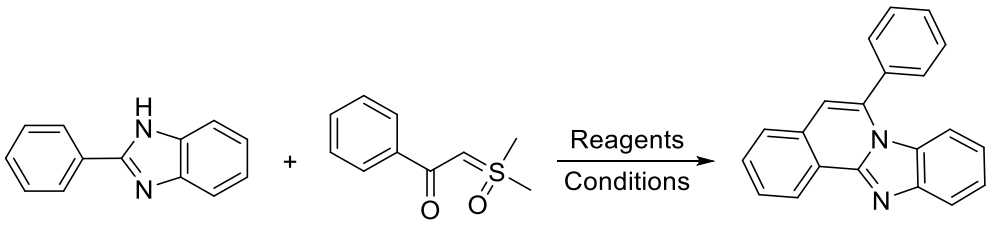

Catalyst/Solvent	Time [h]	T [°C]	Yield [%]
$[Cp^*RhCl_2]_2$, $AgSbF_6$, AcOH, DCE	18	130[a]	82

a) The reaction was carried out in a sealed Schlenk tube and was heated in an oil bath.

Xie *et al*.[91] reported the formation of benzimidazo[2,1-*a*]isoquinolines as a major product in the nickel-catalyzed annulation of 2-chloro-*N*-(2-halophenyl)benzimidamides with terminal acetylenes under anhydrous conditions (Table 4.4). The yield of the model compound in Table 4.4 was dependent on the choice of the halogen in the substrate. The corresponding benzimidazo[2,1-*a*]isoquinoline yields in Table 4.4 suggest that the fluoroaryl substrate is more reactive (66% yield) under the experimental conditions than the chloroaryl substrate (45% yield). Aside from the yields being lower than those of other protocols, another drawback is that the method proceeds at a higher temperature (140 °C).

Table 4.4. Nickel-catalyzed annulation of benzimidamides and terminal acetylenes.

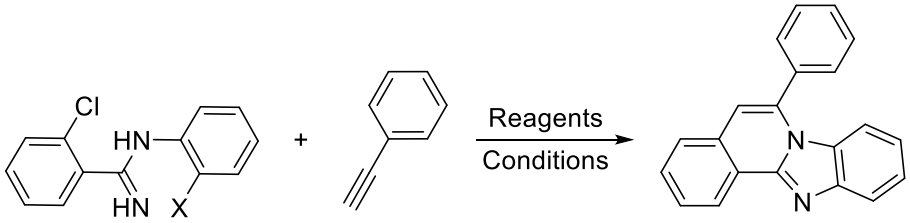

X	Catalyst	Solvent	Time [h]	T [°C]	Yield [%]
F	$Ni(dppp)Cl_2$, Zn	DMSO	24	140	66
Cl					45

In 2013, Peng *et al*.[92] reported a two-step synthesis that uses benzimidazoles and bromoacetylenes (Table 4.5). The first step involves nucleophilic addition to an alkynyl

halide. The benzimidazole, possessing nitrogen lone pairs, is thought to be the nucleophile that reacts with the triple bond of the haloalkyne. Hydroamination is followed by palladium-catalyzed C–H vinylation to form the final product (Table 4.5).

Table 4.5 Hydroamination of bromoacetylenes by benzimidazoles.

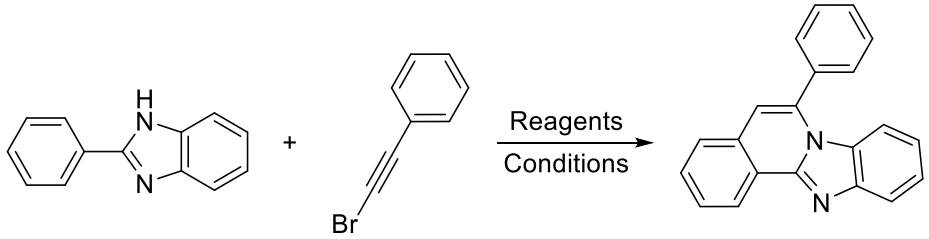

Reagents/Solvent by Step	Time [h]	T [°C]	Yield [%]
(1) K_2CO_3, DMF	2	120	n.d.
(2) $Pd(OAc)_2$, PCy_3	16–20	130	68

In 2012, Reddy *et al*.[93] reported a synthesis (Table 4.6) using oxidative cross-coupling involving two C–H bonds and a rhodium catalyst. The optimized protocol uses copper(II) acetate as an oxidant, pivalic acid as an additive, and mesitylene as solvent. The optimized conditions were applied to a phenyl substituted *N*-styrylbenzimidazole, comparing catalysts in two reactions, one with $Cu(OAc)_2$ and another with $Cu(OAc)_2•H_2O$.

In 2000, Dyker *et al*.[94] investigated the tandem cyclizations of substituted 2-ethynylbenzaldehydes with *o*-phenylenediamines (Figure 4.2, Pathway A). The authors reported the preparation of several benzimidazo[2,1-*a*]isoquinolines, 38–83% yields,

Table 4.6 Rhodium catalyzed intramolecular cross-coupling of *N*-styrylbenzimidazole.

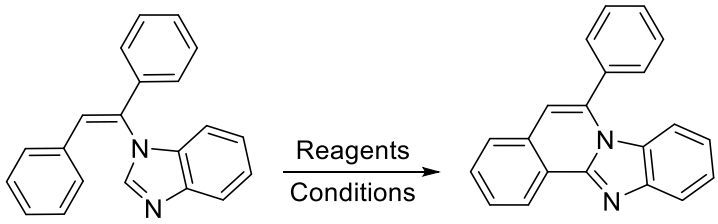

Reagents/Solvent	Oxidant	Time [h]	T [°C]	Yield [%]
$[Cp^*RhCl_2]_2$ Mesitylene/PivOH	$Cu(OAc)_2$	24	140	62
	or			
	$Cu(OAc)_2 \cdot H_2O$			68

using nitrobenzene as the solvent and oxidizing agent at an elevated temperature (150 °C, 2 d). Though not the first synthesis of benzimidazo[2,1-*a*]isoquinolines,[84] the authors developed a catalyst-free preparation.

The protocol described by Sun and LaVoie in 1996 described the synthesis of trimethylsilyl substituted 2-ethynylbenzaldehydes, which were used as substrates in two subsequent reactions to form a nitro-methoxy-substituted benzimidazo[2,1-*a*]isoquinoline (Figure 4.2, Pathway A).[84] The method was not studied beyond a reaction yielding two products, which were regioisomers of the same scaffold.

In 2009, Okamoto *et al*.[95] noted an improved yield (68%) compared to Dyker *et al*. (41%)[94] for the synthesis of an unsubstituted benzimidazo-[2,1-*a*]isoquinoline, which motivated the development of a protocol based on *o*-phenylenediamines. The improvement was carried out in a preliminary microwave protocol using palladium(II) acetate as a catalyst and DMF as solvent.

Okamoto *et al*.[95] also examined a synthesis combining a Sonogashira coupling with tandem cyclizations (Figure 4.2, Pathway B; Table 4.7). In the one-pot approach,

2-Ethynylbenzaldehydes form *in situ*, eliminating the need to prepare the precursor separately. To facilitate formation of 2-ethynylbenzaldehydes by the Sonogashira coupling, tetrabutylammonium acetate (Bu_4NOAc) was incorporated into the methodology as a base. The palladium(II) acetate catalyst remains in the reaction medium during the cyclization step following the Sonogarshira coupling. Okamoto *et al*.[95] did not determine if the cyclization step would still proceed without the catalyst in the experimental conditions used (DMF, 120 °C, microwave irradiation, 0.5–1 h). Table 4.8 presents substituted benzimidazo[2,1-*a*]isoquinolines reported in the literature and are the subject of this project (compare with Table 4.9). In work by Okamoto *et al*.[95] a variety of benzimidazo[2,1-*a*]isoquinolines were produced with yields ranging from 73–83% (Table 4.8, entries 2–5). The protocol's drawbacks are the stoichiometric amount of base, cumbersome to remove solvent (DMF), and the elevated temperature (120 °C) that potentially affects delicate functional groups.

Ouyang *et al*.[96] described the synthesis of iodine-substituted benzimidazo[2,1-*a*]isoquinolines (Figure 4.2, Pathway A, X = I). Ouyang *et al*.[96] reported a protocol involving a copper iodide catalyst (CuI) in the presence of iodine to produce iodobenzimidazo[2,1-*a*]isoquinolines. The authors synthesized a variety of iodobenzimidazo[2,1-*a*]isoquinolines (Figure 4.2, Pathway A).

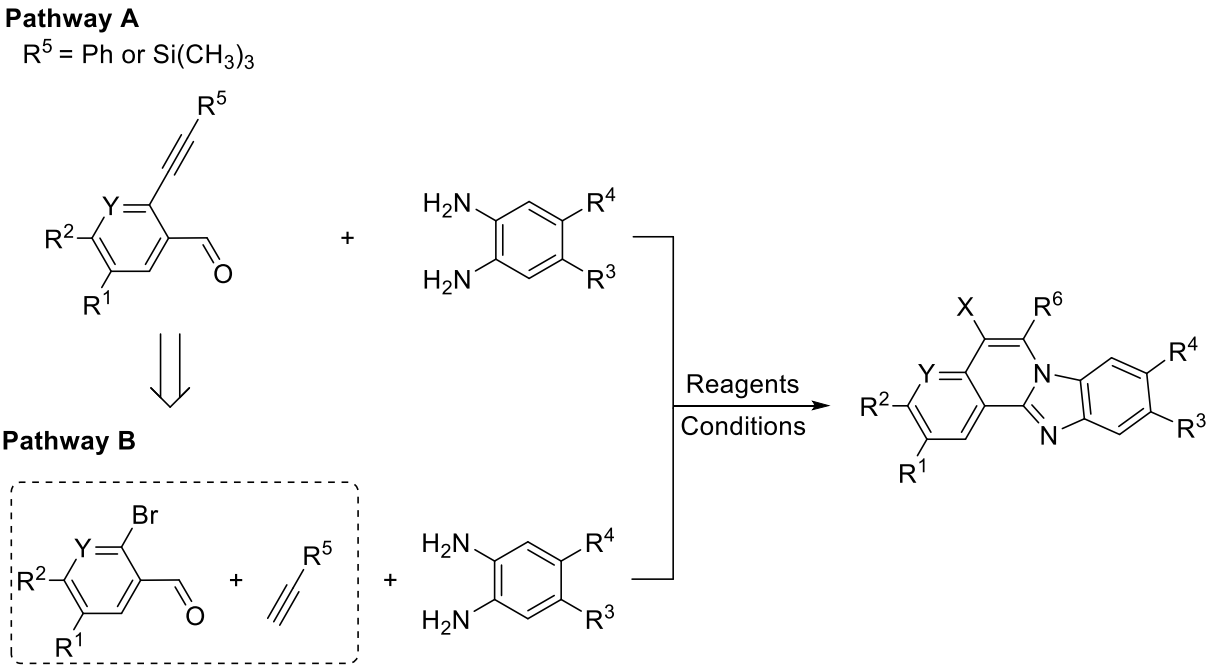

Figure 4.2 Synthesis of benzimidazo[2,1-*a*]isoquinolines by reaction of 2-ethynylbenzaldehydes and *o*-phenylenediamines (Pathway A) and by a one-pot reaction of bromobenzaldehydes, terminal acetylenes, and *o*-phenylenediamines (Pathway B).

Table 4.7 Reagents and conditions used previously for benzimidazo[2,1-*a*]isoquinoline synthesis from 2-ethynylbenzaldehydes and *o*-phenylenediamines (R^5 = Ph unless specified).

Reagents/Catalysts	Solvent	T [°C]	X	R^6	Time [h]	Ref
(1) 4-Nitro-*o*-phd	$PhNO_2$	150	H	H[c]	n.d.	84
(2) $Pd(OAc)_2$	DMF	100			Overnight	
-	$PhNO_2$	150[a]	H	Ph	48	94
$Pd(OAc)_2$, Bu_4NOAc	DMF	120[b]	H	Ph	0.5–1	95
I_2, CuI	DMSO	120[a]	I	Ph	24	96

a) Method of heating not specified; conventional heating assumed.
b) Microwave irradiation.
c) R^5 = $SiMe_3$.

Table 4.8 Representative benzimidazo[2,1-*a*]isoquinolines reported in the literature prepared by the reaction of 2-ethynylbenzaldehydes with *o*-phenylenediamines (Figure 4.2, X = H, $R^5 = R^6$ = Ph).

Entry[a]	R^1	R^2	$R^3 = R^4$	Y	Yield [%]	Ref
1	H	H	H	CH	83	94
2	H	H	H	CH	80	95
3	F	H	H	CH	79	95
4	H	H	H	N	73	95
5	H	H	Me	CH	76	95

a) Compare with Table 4.9

The available methods require high temperatures, metal catalysts, and/or the difficulty to remove the solvents. Given these drawbacks, an opportunity exists to develop a more environmentally friendly catalyst-free protocol that requires lower temperatures and/or less hazardous solvents.

4.2. Results and discussion

4.2.1. Hydroamination of 2-ethynylbenzaldehydes by *o*-phenylenediamines

The reactivity of alkynes with amines was investigated for some time in our laboratory. It was found that the synthesis of benzodiazepines proceeds through the reaction of *o*-phenylenediamines and alkynes in ethanol without a catalyst.[36] These experiments established that traditional, commonly acid-catalyzed, high-temperature protocols reported for the synthesis of heterocycles could, in fact, readily proceed at mild

temperatures and without the use of any catalyst. The present investigation is regarding the design of an environmentally friendly synthesis of benzimidazo[2,1-*a*]isoquinolines using substituted *o*-phenylenediamines (Figure 4.3).

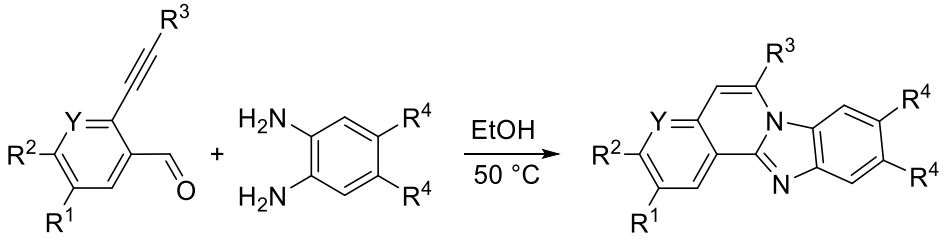

14a–f **15a–l**

Figure 4.3 Investigated synthesis of benzimidazo[2,1-*a*]isoquinolines.

Given earlier reports using 2-ethynylbenzaldehydes and catalysis to form heterocycles, 2-ethynylbenzaldehyde and *o*-phenylenediamine appeared as promising substrates. 2-Ethynylbenzaldehydes were synthesized from 2-bromobenzaldehydes and terminal acetylenes using a modified protocol from the literature (Figure 4.4).[97]

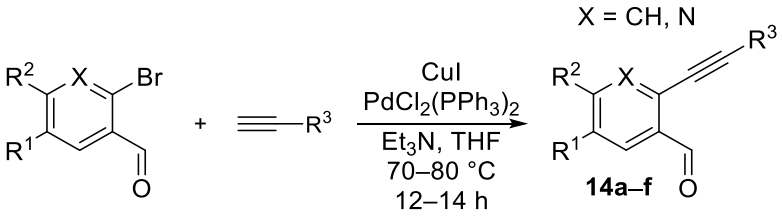

14a–f

Figure 4.4 Sonogashira coupling of 2-bromobenzaldehyde and terminal acetylene.

The unsubstituted substrates, 2-ethynylbenzaldehyde and *o*-phenylenediamine, were also stirred together in the presence of montmorillonite K-10, a well-known solid acid catalyst.[98] GC confirmed the corresponding benzimidazo[2,1-*a*]isoquinoline formed within 30 min after microwave irradiation at 50 °C. An experiment without the catalyst was carried out, and it was found that the reaction also proceeds without the catalyst.

As shown in Table 4.9, the catalyst-free reaction was further investigated using a variety of interesting, substituted substrates at 50 °C. Substituted 2-ethynylbenzaldehydes **14a**–**f** and *o*-phenylenediamines produced targeted products **15a**–**l** with isolated yields of 63–92% (Table 4.9). For each 2-ethynylbenzaldehyde, the experiments conducted with 4,5-dimethyl-phenylenediamine suggested both halves of the benzimidazo[2,1-*a*]isoquinoline can be modified with isolated yields remaining within 63–92%. The protocol was shown to tolerate electron-withdrawing substituents, such as fluorine (Table 4.9, entries 5–8, yields >70%). The presence of a cyclopropyl group at C–6 (entries 9 and 10) suggests that the presence of a phenyl substituent at the alkyne is not essential to the synthesis. The reaction of 2-ethynylpyridine-3-carbaldehyde (Table 4.9, entries 11 and 12) demonstrates the protocol's viability for additional heteroatoms.

4.2.2. Suggested mechanisms

The first step of the reaction sequence in Figure 4.3 may be the formation of an imine from the carbonyl group. Alternatively, the first step may include the creation of a C–N bond along the alkyne.[36,99] A plausible mechanistic outline where the carbonyl group reacts first is shown in Figure 4.5. In this first step, reaction of the aldehyde yields an imine, eliminating water. The imine's carbon then connects to the second amino group

Table 4.9 Synthesized benzimidazo[2,1-*a*]isoquinolines and their yields.

Entry	2-Ethynylbenzaldehyde		Diamine[a] R^4	Product		Yield [%]
1	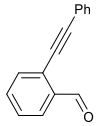	**14a**	H	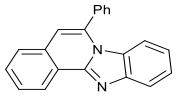	**15a**	88
2	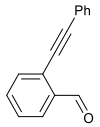	**14a**	Me	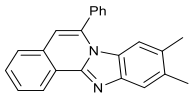	**15b**	63
3	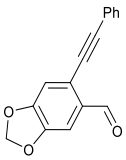	**14b**	H	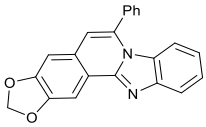	**15c**	82
4	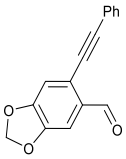	**14b**	Me	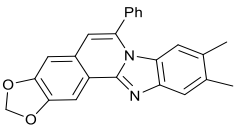	**15d**	92
5	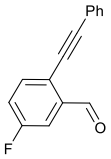	**14c**	H	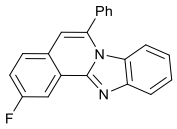	**15e**	80
6	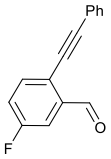	**14c**	Me	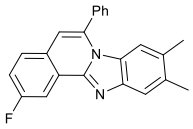	**15f**	85
7	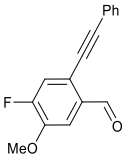	**14d**	H	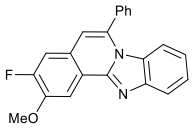	**15g**	79
8	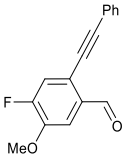	**14d**	Me	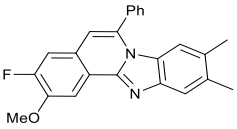	**15h**	89

a) Refer to Figure 4.3.

Table 4.9 Synthesized benzimidazo[2,1-*a*]isoquinolines and their yields—Continued

Entry	2-Ethynylbenzaldehyde		Diamine[a] R^4	Product		Yield [%]
9	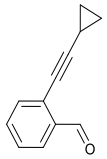	**14e**	H	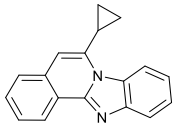	**15i**	92
10	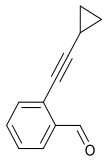	**14e**	Me	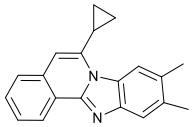	**15j**	88
11	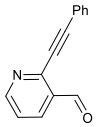	**14f**	H	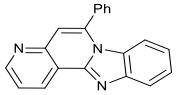	**15k**	88
12	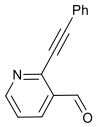	**14f**	Me	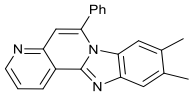	**15l**	90

a) Refer to Figure 4.3.

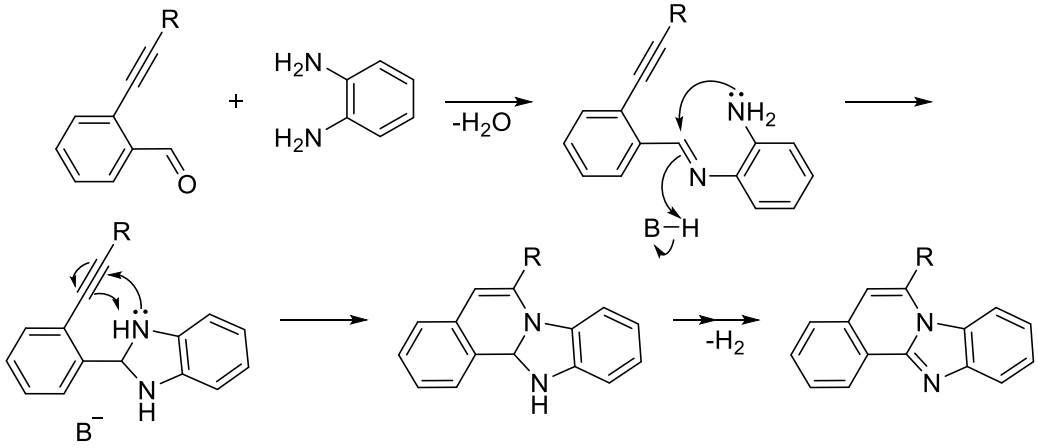

Figure 4.5 Plausible mechanism for the formation of benzimidazo[2,1-*a*]isoquinolines through reaction of the diamine and carbonyl group first.

of the phenylenediamine to form a dihydrobenzimidazole. Attack of the triple bond by a nitrogen, followed by oxidization by ambient oxygen, yields the final structure.

If the alkyne were to react first, an enamine forms adjacent to the aldehyde's carbonyl group (Figure 4.6). The remaining primary amine of the *o*-phenylenediamine could then attack the carbonyl group, forming an imine embedded within the heterocyclic scaffold. Subsequent ethanol-assisted proton transfers result first in a protonated imine intermediate and then in a cyclic structure. The cyclic structure is oxidized to the final product by ambient oxygen.

The isolation of intermediates supports the mechanism in Figure 4.5. The reaction of unsubstituted 2-ethynylbenzaldehyde with selected *o*-phenylenediamines results in an

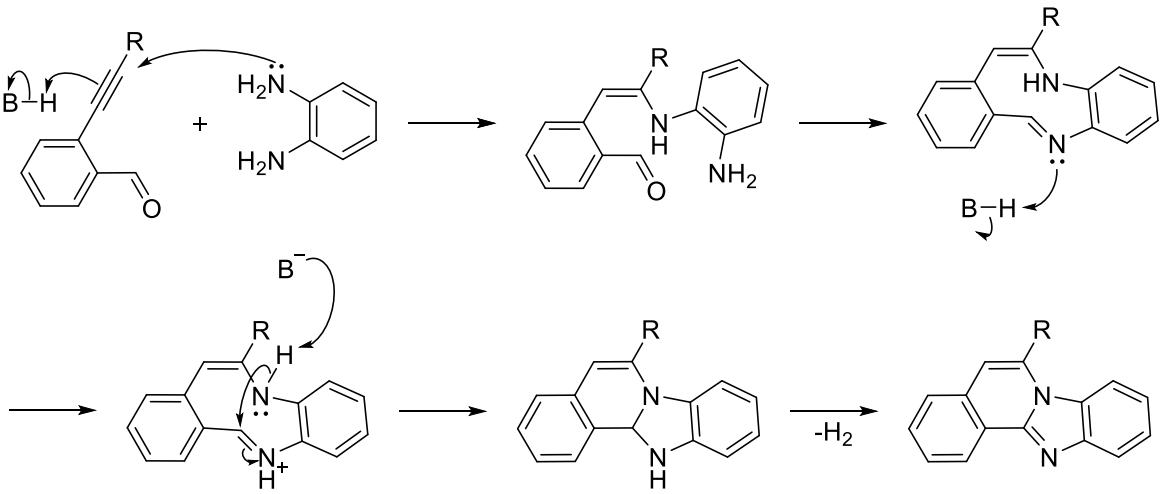

Figure 4.6 Alternative mechanistic outline for the formation of benzimidazo[2,1-*a*]isoquinolines; the diamine reacting with the alkyne first.

imine intermediate before reaction at the alkyne (Figure 4.7). The intermediate suggests reaction at the carbonyl group occurs first, implying that the *o*-phenylenediamine's amino group with the largest electron density reacts first. Isolation of compound **16a** suggests that the carbonyl group reacts before the alkyne. Since a nitro substituent is electron-withdrawing, **16a** also supports the hypothesis that the most electron-rich amino group reacts first. The isolation of halogen-containing compound **16b**, with strongly deactivating NO_2, also suggests that the most electron-rich amino group will attack the carbonyl group first.[a]

4.2.3. Electron donating substituents and crystallographic analysis

The amino group para to the methoxy group is expected to be more nucleophilic than the *meta*-amine; therefore, the *para*-amino group should attack the aldehyde's carbonyl group. Figure 4.8 illustrates the mechanism for 4-methoxy-*o*-phenylenediamine.

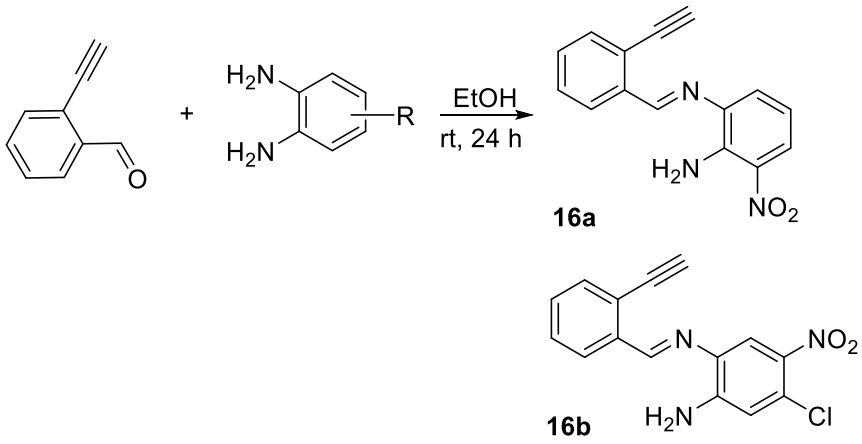

Figure 4.7 Isolation of mechanistically relevant intermediates.

a) Yields were not determined for compounds **16a** and **16b**. Compounds were characterized by NMR.

Attack of the carbonyl group and subsequent formation of an imidazole ring would produce intermediate **17**. The alkyne unit in intermediate **17** undergoes nucleophilic attack by the imidazole's nitrogen (para to the methoxy group). Subsequent oxidation by ambient oxygen forms the final benzimidazo[2,1-*a*]isoquinoline structure.

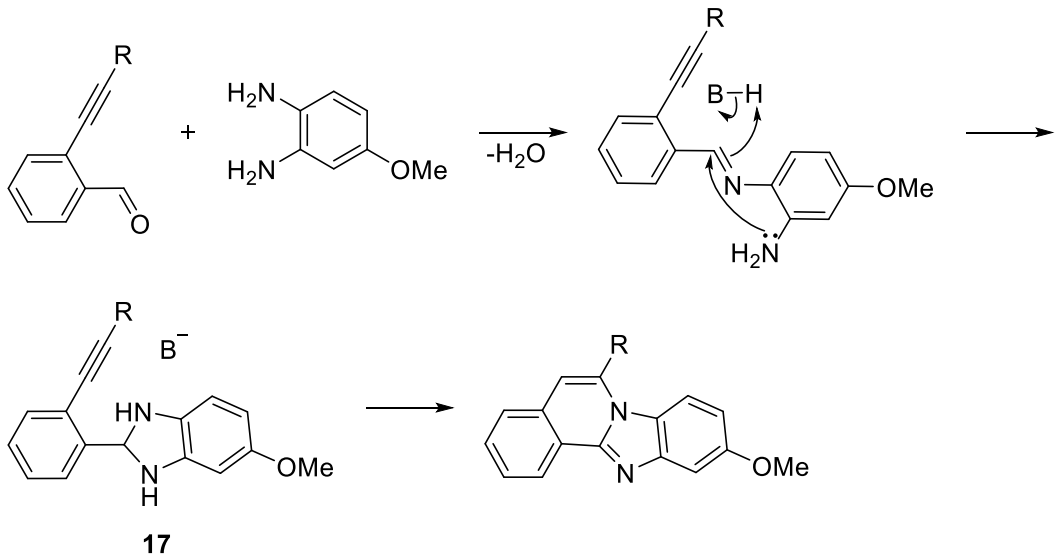

Figure 4.8 Proposed mechanistic outline illustrating regioselectivity of a reaction using 4-methoxy-*o*-phenylenediamine.

The results of the 4-methoxy-*o*-phenylenediamine substrate provide some support to the mechanism in Figure 4.5 and Figure 4.8. The isolation of the product in Figure 4.8, with exclusive regioselectivity (Table 4.10, entry 1), suggests that the electron donation by the methoxy substituent to the *para*-amino group may contribute to the regioselectivity observed. To find additional evidence, another experiment was carried out.

3,4-Dimethyl-*o*-phenylenediamine was also used as a substrate to determine the effect of nucleophilicity on regiochemistry. The lack of symmetry makes the formation of two regioisomers possible, and the two amino groups should have similar electron density profiles due to the position of the methyl groups. 3,4-Dimethyl-*o*-phenylenediamine produced two regioisomers of compound **15n** in comparable quantities (65:35), likely due to the similarity of the amino groups. Interestingly, the mixture was not equimolar, and this was potentially due to the position of the amino groups relative to their corresponding methyl group donors, *i.e.*, *ortho* versus *para*. The observed **15n** regioisomers are evidence that a difference in the nucleophilicity of the amino groups of the substrate underlies the regioselectivity observed in compound **15m**.

Table 4.10 Starting material and yields of benzimidazo[2,1-*a*]isoquinolines **15m** and **15n**.

Entry	Ethynylbenzaldehyde	Diamine	Product	Yield [%]
1	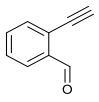 **14g**	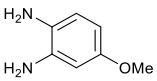	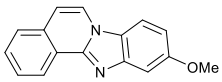 **15m**	91
2	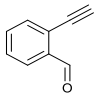 **14g**	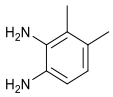	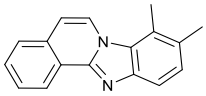 **15n**	95 (65:35)

The benzimidazo[2,1-*a*]isoquinolines **15m** and **15n** illustrated in Table 4.10 were crystalized and characterized by X-ray crystallography (Figure 4.9). The resulting crystallographic data in Table 4.11 provides evidence of resonance, as reflected in the

fluctuation of bond lengths along the outer six-membered rings (compare C2–C3 to C3–C4 in molecule A or molecule B). A similar pattern was observed for both crystallographically independent molecules, *i.e.* molecule A and molecule B. The crystal structures also reflect the double bond character of C5–C6 and N2–C7 (Table 4.11 and Figure 4.9). Between the two crystallographically independent molecules, A and B of **15m**, the average distances of C5–C6 and N2–C7 were determined as 1.35 and1.33 Å, respectively.

4.3. Summary

An environmentally friendly, catalyst-free method has been developed for the synthesis of isoquinoline-fused benzimidazoles. The method appears to have a broad substituent tolerance. The novelty and sustainable nature of the method includes: (i) no catalyst is needed, (ii) the reaction occurs at lower temperatures (50 °C) that those in the literature (Chapter 4.1), (iii) a renewable solvent (ethanol) is used, (iv) the cyclized products form in near quantitative yields, (v) high atom economy with one molecule of water lost as a byproduct, (vi) most of the reactants are commercially available and inexpensive.

4.4. Experimental

4.4.1. Materials and methods

Solvents, phenylenediamines, and 2-ethynylbenzaldehydes, commercially available from Sigma-Aldrich (currently MilliporeSigma), were used without further purification except where indicated. Triethylamine was distilled from calcium hydride, and THF was distilled from sodium-benzophenone ketyl under nitrogen.

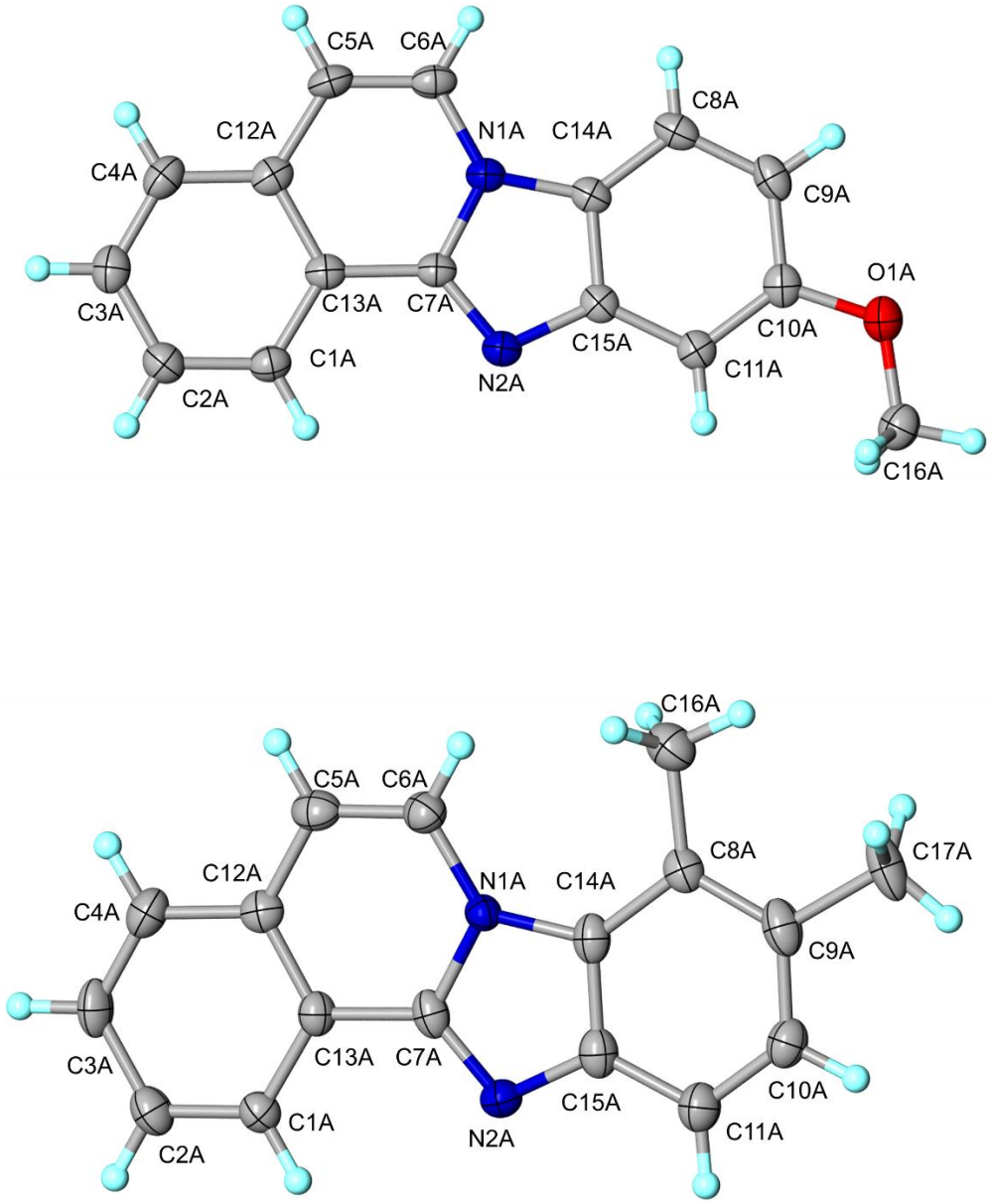

Figure 4.9 Crystal structures (50% probability thermal ellipsoids) of 10-methyoxybenzo[4,5]imidazo[2,1-*a*]isoquinoline **15m** (top) and 10,11-dimethylbenzo[4,5]imidazo[2,1-*a*]isoquinoline **15n** (major isomer, bottom).

Table 4.11 Selected bond distances in [Å] of compounds **15m** and **15n**.

Bond	**15m**		**15n**	
	Molecule A	Molecule B	Molecule A	Molecule B
N1–C6	1.393(4)	1.390(4)	1.398(3)	1.406(3)
N1–C7	1.397(4)	1.395(4)	1.410(4)	1.418(4)
N1–C14	1.397(4)	1.392(4)	1.398(4)	1.391(4)
N2–C7	1.334(4)	1.330(4)	1.344(3)	1.334(3)
N2–C15	1.393(4)	1.400(4)	1.372(4)	1.364(4)
C1–C2	1.379(4)	1.386(5)	1.364(4)	1.363(4)
C1–C13	1.404(5)	1.398(5)	1.420(5)	1.415(5)
C2–C3	1.405(5)	1.398(5)	1.427(5)	1.424(5)
C3–C4	1.388(5)	1.380(5)	1.356(5)	1.351(5)
C4–C12	1.409(5)	1.407(5)	1.441(5)	1.441(5)
C5–C6	1.351(4)	1.342(5)	1.369(5)	1.371(5)
C10–C11	1.384(5)	1.393(5)	1.369(5)	1.367(5)
C8–C9	1.386(5)	1.386(5)	1.406(4)	1.398(4)
C8–C14	1.396(5)	1.392(5)	1.433(4)	1.440(5)
C9–C10	1.421(5)	1.409(5)	1.418(6)	1.410(5)
C11–C15	1.411(4)	1.403(4)	1.406(5)	1.409(5)

The ^{1}H and ^{13}C NMR spectra were recorded on an Agilent MR400DD2 spectrometer in $CDCl_3$ or $(CD_3)_2SO$ at 20–25 °C, using the residual solvent signal for reference (400 MHz for ^{1}H and 100 MHz for ^{13}C). The mass spectrometric identification of the products has been carried out by an Agilent 6850 gas chromatograph with a 5973 mass spectrometer system (70 eV electron impact ionization) using a 30 m long DB-5 type column (J&W Scientific). LC-MS was recorded using an Agilent 2100 system with C18 (5.0 μm, 6.0 mm × 50 mm) LC column. FT-IR spectra were recorded using neat, dry samples by a Thermo Fisher Nicolet 380 FT-IR equipped with Smart Orbit in ATR mode.

4.4.2. Synthesis of alkynylbenzaldehydes **14a**–**f**; general procedure

A Schlenk flask (25 mL) equipped with a septum and a stir bar was charged with a 2-bromobenzaldehyde (1.0 equiv.), triethylamine (2.0 equiv.), terminal acetylene (1.2–1.4 equiv.), and freshly distilled THF (7–9 mL). The solution was purged with nitrogen via needle for at least 15 min. Another Schlenk flask (25 mL) equipped with a reflux condenser was charged with *trans*-dichlorobis(triphenylphosphine)palladium(II) (0.03 equiv.) and copper(I) iodide (0.05 equiv.). The flask was evacuated and refilled with nitrogen, and the 2-bromobenzaldehyde containing mixture was added via syringe. The reaction was heated for 12–14 h at 70–80 °C, except for **14e** and **14f**, which were heated to 50 °C. The mixture was then filtered through celite using a medium porosity fritted funnel, which was rinsed with dichloromethane. The filtrate was washed with saturated ammonium chloride. The water phase was extracted with dichloromethane (30 mL × 3). The combined organic layers were dried over magnesium sulfate, concentrated by rotary evaporation, and further dried by an oil-pump vacuum. Purification was performed by silica gel flash column (15 × 2 cm) chromatography using hexanes/ethyl

acetate 95:5 to 90:10[a]. The ^{1}H and ^{13}C spectra of 2-(phenylethynyl)benzaldehyde (**14a**),[94,100] 6-(phenylethynyl)benzo[*d*][1,3]dioxole-5-carbaldehyde (or 6-phenylethynylpiperonal, **14b**),[101] 5-fluoro-2-(phenylethynyl)benzaldehyde (**14c**),[102] 2-(cyclopropylethynyl)benzaldehyde (**14e**),[103] 2-(phenylethynyl)nicotinaldehyde (**14f**),[103] were in agreement with those reported in literature. 5-Fluoro-4-methoxy-2-(phenylethynyl)benzaldehyde was not previously reported.

4.4.3. 5-Fluoro-4-methoxy-2-(phenylethynyl)benzaldehyde (**14d**)

Recrystallization from ethyl acetate gave analytically pure material. Colorless solid (0.275 g, 1.08 mmol, 45%), mp: 121–125 °C. NMR (δ, ppm; $CDCl_3$): ^{1}H (400 MHz) 3.97 (3H, s), 7.35 (1H, d, *J* = 11.0 Hz), 7.37–7.41 (3H, m), 7.51 (1H, part of d, second line obscured), 7.53–7.57 (2H, m), 10.54 (1H, s); $^{13}C\{^{1}H\}$ (100 MHz) 56.51, 83.73 (d, *J* = 2.8 Hz), 95.98, 111.00 (d, *J* = 3.8 Hz), 120.38 (d, *J* = 20.5 Hz), 121.01 (d, *J* = 9.6 Hz), 122.33, 128.72(2C), 129.28, 131.78(2C), 133.26 (d, *J* = 2.9 Hz), 148.89 (d, *J* = 11.4 Hz), 155.71 (d, *J* = 258.1 Hz), 190.39. IR (*v*, cm^{-1}): 3369, 3081, 3020, 2973, 2939, 2852, 2760, 2393, 2213, 2081, 1782, 1692, 1610, 1566. HRMS (ESI-TOF): $[M + H]^+$ calcd for $C_{16}H_{12}FO_2^+$ 255.0816, found 255.0817.

4.4.4. Synthesis of benzimidazo[2,1-*a*]isoquinolines **15a**–**n**; general procedure

2-Ethynylbenzaldehyde or its substituted derivatives (1 mmol) and *o*-phenylenediamine or its substituted derivatives (1 mmol) were combined in a round bottom flask (25 mL) equipped with septum and a stir bar. The mixture was dissolved in ethanol (3–6 mL) and stirred at 50 °C. The reaction was monitored by TLC or GC-MS,

a) An isocratic system within the range or a gradient system was employed based on the compound's relative position to the starting materials on TLC.

and after reaching conversion, the crude material was filtered through silica gel (2 cm height pad) or purified by column chromatography. The spectral data of 6-phenylbenzo[4,5]imidazo[2,1-*a*]isoquinoline (**15a**),[100] 9,10-dimethyl-6-phenylbenzo[4,5]imidazo[2,1-*a*]isoquinoline (**15b**),[95,100] 2-fluoro-6-phenylbenzo[4,5]imidazo[2,1-*a*]isoquinoline (**15e**),[95] 6-phenylbenzo[4,5]imidazo[2,1-f][1,6]-naphthyridine (**15k**),[95] and 6-cyclopropylbenzo[4,5]imidazo[2,1-*a*]isoquinoline (**15i**)[104] were in agreement with those reported in the literature.

4.4.5. 6-Phenylbenzo[4,5]imidazo[2,1-*a*]isoquinoline (**15a**)[100]

From *o*-phenylenediamine (0.108 g, 1.00 mmol) and **14a** (0.206 g, 1.00 mmol), colorless crystal **15a** (0.259 g, 0.88 mmol, 88%), mp: 178 °C. NMR (δ, ppm; $CDCl_3$): ^1H (400 MHz) 6.47–6.50 (1H, m), 6.91 (1H, s), 7.00 (1H, m), 7.37–7.70 (9H, m), 7.98 (1H, m), 8.88–8.90 (1H, m); $^{13}C\{^1H\}$ (100 MHz) 112.53, 114.04, 119.69, 121.20, 122.94, 124.14, 125.09, 126.62, 127.85, 128.84, 128.96(2C), 129.38(2C), 129.85, 130.07, 131.39, 131.56, 134.65, 137.43, 148.31. IR (*v*, cm^{-1}): 2980, 1525, 1447, 1032, 758. HRMS (ESI-TOF): $[M + H]^+$ calcd for $C_{21}H_{15}N_2^+$ 295.1230, found 295.1232.

4.4.6. 9,10-Dimethyl-6-phenylbenzo[4,5]imidazo[2,1-*a*]isoquinoline (**15b**)[95,100]

From 4,5-dimethyl-*o*-phenylenediamine (0.136 g, 1.00 mmol) and **14a** (0.206 g, 1.00 mmol), colorless crystals **15b** (0.203 g, 0.630 mmol, 63%), mp: 210 °C. NMR (δ, ppm; $CDCl_3$): ^1H (400 MHz) 2.12 (3H, s), 2.36 (3H, s), 6.19 (1H, s), 6.89 (1H, s), 7.58–7.69 (8H, m), 7.75 (1H, s), 8.89–8.91 (1H, m); $^{13}C\{^1H\}$ (100 MHz) 20.37, 20.73, 112.44, 114.26, 119.13, 122.47, 125.10, 126.59, 127.89, 128.18, 128.27, 128.50, 128.87(2C), 129.43(2C), 129.82, 129.98, 130.61, 131.44, 133.71, 134.57, 137.33. IR (*v*, cm^{-1}): 3710,

2971, 1490, 1054, 1032. HRMS (ESI-TOF): $[M + H]^+$ calcd for $C_{23}H_{19}N_2^+$ 323.1543, found 323.1543.

4.4.7. Phenylbenzo[4,5]imidazo[2,1-*a*][1,3]dioxolo[4,5-*g*]isoquinoline (**15c**)

From *o*-phenylenediamine (0.108 g, 1.00 mmol) **14b** (0.250 g, 1.00 mmol), colorless crystal **15c** (0.278 g, 0.820 mmol, 82%), mp: 192–193 °C. NMR (δ, ppm; $CDCl_3$): ^1H (400 MHz) 6.16 (2H, s), 6.47–6.50 (1H, m), 6.89 (1H, s), 6.98–7.01 (1H, m), 7.10 (1H, s), 7.38–7.42 (1H, m), 7.59–7.65 (5H, m), 7.99 (1H, d, J = 8.1 Hz), 8.40 (1H, s); $^{13}C\{^1H\}$ (100 MHz) 102.01, 103.76, 104.69, 109.08, 114.26, 118.56, 121.23, 124.90, 127.70, 129.04(2C), 129.45(2C), 130.01, 135.96, 146.86, 148.46, 148.92. IR (ν, cm^{-1}): 2919, 1492, 1450, 1241, 1032. HRMS (ESI-TOF): $[M + H]^+$ calcd for $C_{22}H_{15}N_2O_2^+$ 339.1128, found 339.1129.

4.4.8. 9,10-Dimethyl-6-phenylbenzo[4,5]imidazo[2,1-*a*][1,3]dioxolo-[4,5-*g*]isoquinoline (**15d)**

From 4,5-dimethyl-*o*-phenylenediamine (0.1362 g, 1.00 mmol) **14b** (0.2503 g, 1.00 mmol), colorless crystals **15d** (0.337 g, 0.920 mmol, 92%), mp: 254–256 °C. NMR (δ, ppm; $CDCl_3$): ^1H (400 MHz) 2.12 (3H, s), 2.36 (3H, s), 6.12 (2H, s), 6.20 (1H, s), 6.74 (1H, s), 7.05 (1H, s), 7.57–7.64 (5H, m), 7.68 (1H, s), 8.19 (1H, s); $^{13}C\{^1H\}$ (100 MHz) 20.39, 20.66, 101.67, 103.30, 104.66, 111.77, 114.19, 118.56, 119.21, 127.83, 128.77(2C), 128.97, 129.45(2C), 129.61, 129.64, 133.25, 134.77, 136.07, 148.30, 149.87, 156.12. IR (ν, cm^{-1}): 2965, 1452, 1234, 1032, 700. HRMS (ESI-TOF): $[M + H]^+$ calcd for $C_{24}H_{19}N_2O_2^+$ 367.1441, found 367.1443.

4.4.9. 2-Fluoro-6-phenylbenzo[4,5]imidazo[2,1-*a*]isoquinoline (**15e**)[95]

From *o*-phenylenediamine (0.108 g, 1.00 mmol) and **14c** (0.224 g, 1.00 mmol), light brown solid **15e** (0.250 g, 0.800 mmol, 80%), mp: 182–184 °C. NMR (δ, ppm; $CDCl_3$): ^1H (400 MHz) 6.47–6.50 (1H, m), 6.95 (1H, s), 7.01–7.06 (1H, m), 7.39–7.48 (2H, m), 7.59–7.65 (7H, m), 8.00–8.02 (1H, m); $^{13}C\{^1H\}$ (100 MHz) 110.74 (d, J = 23.9 Hz), 112.44, 114.29, 119.33 (d, J = 23.7 Hz), 119.35, 121.98, 123.61, 124.84, 128.24 (d, J = 2.2 Hz), 128.86, 128.99, 129.08(2C), 129.41(2C), 130.10, 130.31, 131.36, 134.11, 136.76 (d, J = 2.6 Hz), 162.03 (d, J = 249.3 Hz). IR (ν, cm^{-1}): 2920, 1596, 1426, 1192, 862. HRMS (ESI-TOF): $[M + H]^+$ calcd for $C_{21}H_{14}FN_2^+$ 313.1136, found 313.1136.

4.4.10. 2-Fluoro-9,10-dimethyl-6-phenylbenzo[4,5]imidazo[2,1-*a*]isoquinoline (**15f**)

From 4,5-dimethyl-*o*-phenylenediamine (0.136 g, 1.00 mmol) and **14c** (0.224 g, 1.00 mmol), colorless crystals **15f** (0.289 g, 0.850 mmol, 85%), mp: 274–275 °C. NMR (δ, ppm; $CDCl_3$): ^1H (400 MHz) 2.13 (3H, s), 2.37 (3H, s), 6.20 (1H, s), 6.89 (1H, s), 7.36–7.40 (1H, m), 7.57–7.72 (6H, m), 7.75 (1H, s), 8.56 (1H, d, J = 8.2 Hz); $^{13}C\{^1H\}$ (100 MHz) 20.38, 20.75, 110.46 (d, J = 24.7 Hz), 111.71, 114.31, 117.28, 119.24, 127.98 (d, J = 2.0 Hz), 128.84, 128.91(2C), 128.93, 129.45(2C), 129.90, 131.07, 134.36, 136.71 (d, J = 3.0 Hz), 161.93 (d, J = 248.6 Hz); ^{19}F (376 MHz) −130.72. IR (ν, cm^{-1}): 2980, 1529, 1492, 953, 846, 703. HRMS (ESI-TOF): $[M + H]^+$ calcd for $C_{23}H_{18}FN_2^+$ 341.1449, found 341.1447.

4.4.11. 3-Fluoro-2-methoxy-6-phenylbenzo[4,5]imidazo[2,1-*a*]isoquinoline (**15g**)

From *o*-phenylenediamine (0.108 g, 1.00 mmol) and **14d** (0.254 g, 1.00 mmol), colorless crystals **15g** (0.270 g, 0.790 mmol, 79%), mp: 237–238 °C. NMR (δ, ppm; $CDCl_3$): ^1H (400 MHz) 4.15 (3H, s), 6.50 (1H, d, J = 8.5 Hz), 6.82 (1H, s), 6.99–7.03

(1H, m), 7.38–7.43 (3H, m), 7.59–7.68 (5H, m), 7.98 (1H, d, *J* = 8.2 Hz), 8.36 (1H, d, *J* = 8.3 Hz); $^{13}C\{^{1}H\}$ (100 MHz) 56.67, 107.82 (d, *J* = 2.3 Hz), 111.75 (d, *J* = 2.5 Hz), 112.92 (d, *J* = 19.2 Hz), 114.37, 119.69, 120.06 (d, *J* = 2.2 Hz), 121.35, 124.52, 126.19 (d, *J* = 8.6 Hz), 129.18(2C), 129.61(2C), 130.08, 130.93, 134.71, 136.88, 144.32, 147.77, 148.85 (d, *J* = 12.3 Hz), 154.53 (d, *J* = 252.6 Hz); ^{19}F (376 MHz) −131.48. IR (*v*, cm^{-1}): 2972, 1531, 1464, 1296, 1057. HRMS (ESI-TOF): $[M + H]^+$ calcd for $C_{22}H_{16}FN_2O^+$ 343.1242, found 343.1240.

4.4.12. 3-Fluoro-2-methoxy-9,10-dimethyl-6-phenylbenzo[4,5]-imidazo [2,1-*a*]isoquinoline (**15h**)

From 4,5-dimethyl-*o*-phenylenediamine (0.136 g, 1.00 mmol) and **14d** (0.254 g, 1.00 mmol), colorless crystals **15h** (0.330 g, 0.890 mmol, 89%), mp: 252–254 °C. NMR (δ, ppm; $CDCl_3$): ^{1}H (400 MHz) 2.12 (3H, s), 2.37 (3H, s), 4.12 (3H, s), 6.20 (1H, s), 6.75 (1H, s), 7.37 (1H, d, *J* = 11.2 Hz), 7.57–7.64 (5H, m), 7.71 (1H, s), 8.29 (1H, d, *J* = 8.4 Hz); $^{13}C\{^{1}H\}$ (100 MHz) 20.40, 20.68, 56.57, 107.64 (d, *J* = 2.5 Hz), 111.19 (d, *J* = 3.0 Hz), 112.82 (d, *J* = 19.2 Hz), 114.29, 119.35, 120.17 (d, *J* = 2.4 Hz), 125.94 (d, *J* 8.5 Hz), 128.82(2C), 129.18, 129.44(2C), 129.73, 130.20, 133.46, 134.60, 136.57, 142.81, 147.20 (d, *J* = 1.6 Hz), 148.68 (d, *J* = 12.2 Hz), 154.28 (d, *J* = 251.9 Hz). IR (*v*, cm^{-1}): 2971, 1496, 1962, 1032, 702. HRMS (ESI-TOF): $[M + H]^+$ calcd for $C_{24}H_{20}FN_2O^+$ 371.1554, found 371.1554.

4.4.13. 6-Cyclopropylbenzo[4,5]imidazo[2,1-*a*]isoquinoline (**15i**)[104]

From *o*-phenylenediamine (0.1081 g, 1.00 mmol) and **14e** (0.170 g, 1.00 mmol), colorless solid **15i** (0.238 g, 0.920 mmol, 92%), mp: 134–135 °C. NMR (δ, ppm; $CDCl_3$): ^{1}H (400 MHz) 1.00–1.17 (m, 2H), 1.27–1.33 (m, 2H), 2.50–2.62 (m, 1H), 6.84 (s, 1H),

7.37 (ddd, *J* = 8.3, 7.3, 1.1 Hz, 1H), 7.52 (ddd, *J* = 8.1, 7.2, 0.9 Hz, 1H), 7.58–7.70 (m, 3H), 8.05 (d, *J* = 8.1 Hz, 1H), 8.45 (d, *J* = 8.4 Hz, 1H), 8.81–8.86 (m, 1H); $^{13}C\{^{1}H\}$ (100 MHz) 7.96, 14.91, 109.74, 114.86, 119.85, 121.81, 122.54, 124.43, 125.26, 126.32, 127.65, 130.15, 131.22, 131.86, 139.79, 144.19, 148.41. IR (*v*, cm^{-1}): 3054, 2974, 1646, 1606, 1560, 1529, 1450, 1333, 1294. HRMS (ESI-TOF): $[M + H]^+$ calcd for $C_{18}H_{15}N_2^+$ 259.1230, found 259.1230.

4.4.14. 6-Cyclopropyl-9,10-dimethylbenzo[4,5]imidazo[2,1-*a*]isoquinoline (**15j**)

From 4,5-dimethyl-*o*-phenylenediamine (0.1362 g, 1.00 mmol) and **14e** (0.170 g, 1.00 mmol), yellow crystals **15j** (0.252 g, 0.880 mmol, 88%), mp: 209–212 °C. NMR (δ, ppm; $CDCl_3$): ^{1}H (400 MHz) 1.02–1.09 (2H, m), 1.25–1.34 (2H, m), 2.46 (6H, s), 2.49–2.57 (1H, m), 6.76 (1H, s), 7.56–7.64 (3H, m), 7.79 (1H, s), 8.17 (1H, s), 8.76–8.82 (1H, m); $^{13}C\{^{1}H\}$ (100 MHz) 7.88, 14.81, 20.61, 21.11, 109.02, 114.86, 119.74, 122.70, 124.99, 126.18, 127.35, 129.62, 129.72, 130.74, 131.60, 133.41, 139.68, 143.02, 147.84. IR (*v*, cm^{-1}): 3054, 2974, 2944, 1644, 1530, 1456, 1402, 1336, 848. HRMS (ESI-TOF): $[M + H]^+$ calcd for $C_{20}H_{19}N_2^+$ 287.1543, found 287.1547.

4.4.15. 6-Phenylbenzo[4,5]imidazo[2,1-*f*][1,6]naphthyridine (**15k**)[95]

From *o*-phenylenediamine (0.108 g, 1.00 mmol) **14f** (0.207 g, 1.00 mmol), pale yellow crystals **15k** (0.260 g, 0.880 mmol, 88%), mp: 235–236 °C. NMR (δ, ppm; $CDCl_3$): ^{1}H (400 MHz) 6.50 (1H, d, *J* = 8.5 Hz), 7.04–7.09 (1H, m), 7.24 (1H, s), 7.42–7.44 (1H, m), 7.62–7.68 (6H, m), 8.01 (1H, d, *J* = 8.2 Hz), 9.00 (1H, s), 9.26 (1H, d, *J* = 7.9 Hz); $^{13}C\{^{1}H\}$ (100 MHz) 114.36, 119.34, 122.32, 122.80, 125.06, 129.13(2C), 129.20(2C), 130.14, 130.41, 133.28, 133.69, 141.22, 148.50, 152.50. IR (*v*, cm^{-1}): 3059,

1555, 1118, 773, 426. HRMS (ESI-TOF): $[M + H]^+$ calcd for $C_{20}H_{14}N_3^+$ 296.1182, found 296.1182.

4.4.16. 9,10-Dimethyl-6-phenylbenzo[4,5]imidazo[2,1-*f*][1,6]naphthyridine (**15l**)

From 4,5-dimethyl-*o*-phenylenediamine (0.136 g, 1.00 mmol) and **14f** (0.207 g, 1.00 mmol), pale yellow crystals **15l** (0.291 g, 0.900 mmol, 90%), mp: 244–245 °C. NMR (δ, ppm; $CDCl_3$): ^1H (400 MHz) 2.15 (3H, s), 2.39 (3H, s), 6.22 (1H, s), 7.15 (1H, s), 7.55–7.68 (6H, m), 7.74 (1H, s), 8.95 (1H, d, J = 4 Hz), 9.12 (1H, d, J = 7.5 Hz); $^{13}C\{^1H\}$ (100 MHz) 20.55, 20.91, 113.61, 114.50, 119.17, 119.72, 122.53, 129.08, 129.17(2C), 129.36(2C), 130.28, 131.33, 132.84, 134.11, 134.36, 141.38, 143.14, 146.90, 148.64, 152.29. IR (ν, cm^{-1}): 3050, 2914, 1557, 998, 767, 427. HRMS (ESI-TOF): $[M + H]^+$ calcd for $C_{22}H_{18}N_3^+$ 324.1495, found 324.1496.

4.4.17. 10-Methoxybenzo[4,5]imidazo[2,1-*a*]isoquinoline (**15m**)

From 3,4-dimethyl-*o*-phenylenediamine (0.138 g, 1.00 mmol) and **14g** (0.130 g, 1.00 mmol), colorless crystal **15m** (0.226 g, 0.910 mmol, 91%), mp: 138 °C. NMR (δ, ppm; $CDCl_3$): ^1H (400 MHz) 3.91 (3H, s), 6.88–7.07 (m, 2H), 7.44 (1H, d, J = 2.2 Hz), 7.61–7.70 (4H, m), 8.03 (1H, d, J = 7.3 Hz), 8.73–8.76 (1H, m); $^{13}C\{^1H\}$ (100 MHz) 55.72, 101.25, 110.22, 111.09, 112.21, 121.22, 123.32, 124.61, 124.70, 126.96, 128.05, 129.66, 131.23, 144.80, 147.45, 157.87. IR (ν, cm^{-1}): 1520, 1436, 1270, 462, 452. HRMS (ESI-TOF): [M + H] calcd for $C_{16}H_{13}N_2O^+$ 249.1022, found 249.1027.

4.4.18. 10,11-Dimethylbenzo[4,5]imidazo[2,1-*a*]isoquinoline (**15n**)

From 3-methoxy-*o*-phenylenediamine (0.136 g, 1.00 mmol) and **14g** (0.130 g, 1.00 mmol), colorless crystal **15n** (0.234 g, 0.950 mmol, 95%, 65:35), mp: 189 °C. NMR (δ, ppm; $CDCl_3$): ^1H (400 MHz) 2.44 (3H, s), 2.67 (3H, s), 6.81 (1H, d, J = 7.5 Hz),

7.25–7.27 (1H, m), 7.60–7.62 (3H, m), 7.72 (1H, d, *J* = 8.2 Hz), 8.41 (1H, d, *J* = 7.5 Hz), 8.77 (1H, d, *J* = 6.7 Hz); $^{13}C\{^{1}H\}$ (100 MHz) 14.98, 20.06, 110.46, 116.79, 120.33, 123.67, 123.88, 124.81, 126.43, 127.20, 127.76, 129.54, 129.58, 130.25, 130.71, 142.39, 147.09. IR (ν, cm^{-1}): 3400, 2919, 1456, 1358, 755. HRMS (ESI-TOF): $[M + H]^+$ calcd for $C_{17}H_{15}N_2^+$ 247.1230, found 247.1236.

4.4.19. Synthesis of imines **16a–b**; general procedure

2-Ethynylbenzaldehyde (0.5 mmol) and substituted *o*-phenylenediamine (0.5 mmol) were dissolved in absolute ethanol (5 mL) and stirred at room temperature for 24 h. The solid precipitate was filtered off and characterized by NMR spectroscopy.

4.4.20. 5-Chloro-2-((2-ethynylbenzylidene)amino)-4-nitroaniline (**16a**)

NMR (δ, ppm; $CDCl_3$): ^{1}H (400 MHz) 3.48 (1H, s), 4.97 (2H, s), 6.78 (1H, s), 7.45–7.49 (2H, m), 7.59–7.61 (1H, m), 7.92 (1H, s), 8.17–8.19 (1H, m), 9.10 (1H, s); $^{13}C\{^{1}H\}$ (100 MHz) 80.28, 84.17, 115.66, 115.86, 124.26, 126.82, 128.48, 129.14, 131.55, 133.63, 134.24, 136.47, 136.96, 147.52, 158.40. LC-MS for $C_{15}H_{11}N_3O_2Cl^+$ $[M + H]^+$ 300.1.

4.4.21. 2-((2-Ethynylbenzylidene)amino)-6-nitroaniline (**16b**)

NMR (δ, ppm; $CDCl_3$): ^{1}H (400 MHz) 3.45 (s, 1H), 6.68 (dd, *J* = 8.7, 7.5 Hz, 1H), 6.81 (bs, 2H), 7.27 (m, 1H), 7.47–7.49 (m, 2H), 7.60–7.62 (m, 1H), 8.04–8.07 (1H, m), 8.21–8.24 (m, 1H), 9.08 (s, 1H); $^{13}C\{^{1}H\}$ (100 MHz) 80.45, 83.72, 115.15, 121.94, 124.03, 124.32, 126.85, 129.03, 131.28, 132.06, 133.55, 136.67, 139.60, 141.48, 157.65. LC-MS for $C_{15}H_{12}N_3O_2^+$ $[M + H]^+$ 266.1.

	6a	**6b**	**6c**
Empirical formula	$C_{43}H_{34}Cl_2N_6Ni$•MeOH •Et_2O	$C_{42}H_{34}Cl_2N_6Ni$•MeOH •H_2O	$C_{42}H_{32}Cl_2N_8NiO_4$ •$(MeOH)_2$•CH_2Cl_2
Formula weight	784.40	802.42	991.369
Temperature	100(2) K	100(2) K	100(2)K
Wavelength	0.71073 Å	0.71073 Å	1.54178Å
Crystal system	triclinic	monoclinic	monoclinic
Space group	P-1	P21/c	Pc
a, α	12.0621(7) Å, 85.144(2)°	15.2499(8) Å, 90°	10.4519(5) Å, 90°
b, β	12.8495(7) Å, 71.808(2)°	15.9814(8) Å, 96.472(2)°	12.9464(6) Å, 95.486(2)°
c, γ	14.6993(8) Å, 73.451(2)°	15.8678(8) Å, 90°	16.8469(7) Å, 90°
Volume	2074.7(2)	3842.6(3)	2269.19(18)
Z	2	4	2
Density (calculated)	1.256 g/cm^3	1.387 g/cm^3	1.451 g/cm^3
Absorption coefficient	0.636 mm^{-1}	0.690 mm^{-1}	3.261 mm^{-1}
F(000)	816	1672	1022
Crystal size	0.261×0.158×0.113 mm^3	0.295×0.232×0.102 mm^3	0.464×0.086×0.060 mm^3
θ range	26.02 – 2.20 °	26.39 – 2.34°	74.42 – 3.41°
Index ranges	h = -14→14, k = -15→15, l = -18→18	h = -19→19, k = 19→19, l = -19→19	h = -13→11, k = -16→16, l = -21→21
No. Reflections	9761	7868	9836
Independent reflections	8197	9800	8576
Completeness Absorption	99.9%	99.9%	93%
Correction	multi-scan	mutli-scan	multi-scan
Max. and min. trans.	0.7453 and 0.6876	0.7454 and 0.7087	0.7538 and 0.5787
Data / restraints / param.	8197 / 11 / 497	7868 / 0 / 463	8576 / 711 / 648
GOF on F^2	1.030	1.031	1.041
Final R indices [I>2σ(I)]	R1: 0.0357, wR2: 0.0794	R1: 0.0277, wR2: 0.0594	R1: 0.0399, wR2: 0.1097
R indices (all data)	R1: 0.0510, wR2: 0.0869	R1: 0.0241, wR2: 0.0618	R1: 0.0420, wR2: 0.1115
Largest diff. peak and hole	0.278 and -0.469 e•$Å^{-3}$	0.308 and -0.301 e•$Å^{-3}$	0.549 and -0.386 e•$Å^{-3}$

	7a	**7b**	**7c**
Empirical formula	$C_{42}H_{34}Cl_2CoN_6$	$C_{42}H_{34}Cl_2CoN_6 \bullet (MeOH)_{1.5}$	$C_{42}H_{32}Cl_2N_8CoO_4 \bullet (MeOH)_2 \bullet CH_2Cl_2$
Formula weight	900.82	887.78	991.59
Temperature	100(2) K	100(2) K	100(2)K
Wavelength	0.71073 Å	0.71073 Å	1.54178Å
Crystal system	monoclinic	triclinic	monoclinic
Space group	C2/c	P-1	Pc
a, α	20.2682(7) Å, 90°	9.2497(7) Å, 115.919(2)°	10.3629(3) Å, 90°
b, β	23.6744(9) Å, 110.651(1)°	16.2387(10) Å,100.190(3)°	13.0048(4) Å, 95.240(2)°
c, γ	19.7440(7) Å, 90°	16.3041(11) Å, 102.345(3)°	16.9026(4) Å, 90 °
Volume	8864.2(6)	2047.3(2)	2268.40(11)
Z	8	2	2
Density (calculated)	1.350 g/cm^3	1.440 g/cm^3	1.452 g/cm^3
Absorption coefficient	0.556 mm^{-1}	0.600 mm^{-1}	5.611 mm^{-1}
F(000)	3784	928	1022
Crystal size	0.224×0.218×0.20 mm^3	0.345×0.152×0.093 mm^3	0.311×0.095×0.081 mm^3
θ range	26.35 – 2.25 °	26.66 – 2.54°	74.40 – 4.28°
Index ranges	h = -25→25, k = -29→29, l = - 24→24	h = -11→11, k = -20→20, l = -20→20	h = -12→10, k = -16→16, l = - 21→21
No. Reflections	9766	9955	9887
Independent reflections	9136	8721	8230
Completeness Absorption	99.6%	99.9%	89%
Correction	multi-scan	multi-scan	multi-scan
Max. and min. trans.	0.7454 and 0.7158	0.7454 and 0.7119	0.7538 and 0.5884
Data / restraints / param.	9136 / 121 / 527	8721 / 52 / 556	8230 / 691 / 981
GOF on F^2	1.036	1.046	1.015
Final R indices [I>2σ(I)]	R1: 0.0291, wR2: 0.0692	R1: 0.0297, wR2: 0.0510	R1: 0.0416, wR2: 0.1133
R indices (all data)	R1: 0.0397, wR2: 0.0741	R1: 0.0647, wR2: 0.0697	R1: 0.0478, wR2: 0.1181
Largest diff. peak and hole	0.220 and -0.251 e•Å^{-3}	0.265 and -0.275 e•Å^{-3}	0.357 and -0.525 e•Å^{-3}

	8	**9**
Empirical formula	$C_{42}H_{30}Cl_6N_6Mn•C_5H_{12}$	$(C_{22}H_{21}Cl_2MnN_3O)_2$
Formula weight	957.55	938.52
Temperature	100(2) K	100(2) K
Wavelength	1.54178 Å	0.71073 Å
Crystal system	monoclinic	triclinic
Space group	Cc	P-1
a, α	27.3160(14) Å, 90°	8.3552(4) Å, 81.136(2)°
b, β	9.4602(5) Å, 108.628(3)°	16.2387(10) Å, 100.190(3)°
c, γ	17.7854(8) Å, 90°	16.3041(11) Å, 102.345(3)°
Volume	4355.2(4)	2047.3(2)
Z	4	2
Density (calculated)	1.462 g/cm^3	1.440 g/cm^3
Absorption coefficient	6.184 mm^{-1}	0.600 mm^{-1}
F(000)	1972	928
Crystal size	0.235×0.141×0.049 mm^3	0.345×0.152×0.093 mm^3
θ range	74.73 – 4.98 °	26.66 – 2.54°
Index ranges	h = -34→34, k = -11→11, l = -22→22	h = -11→11, k = -20→20, l = -20→20
No. Reflections	9991	9955
Independent reflections	8495	8721
Completeness Absorption	99.8%	99.9%
Correction	multi-scan	multi-scan
Max. and min. trans.	0.754 and 0.548	0.7454 and 0.7119
Data / restraints / param.	8495 / 2 / 499	8721 / 52 / 556
GOF on F^2	0.998	1.046
Final R indices [I>2σ(I)]	R1 = 0.0440, wR2 = 0.1012	R1 = 0.0297, wR2 = 0.0510
R indices (all data)	R1 = 0.0561, wR2 = 0.1075	R1 = 0.0647, wR2 = 0.0697
Largest diff. peak and hole	0.698 and -0.266 e•Å^{-3}	0.265 and -0.275 e•Å^{-3}

	10a	**10b**	**11**
Empirical formula	$C_{21}H_{17}Cl_2N_3Zn$	$C_{21}H_{15}Cl_4N_3Zn$	$C_{57}H_{47}Cl_2N_3P_2Ru{\bullet}CH_2Cl_2$
Formula weight	447.64	516.53	1092.81
Temperature	100(2) K	100(2) K	100(2) K
Wavelength	0.71073 Å	0.71073 Å	0.71073 Å
Crystal system	monoclinic	monoclinic	monoclinic
Space group	P21/n	P21/c	P21/n
a, α	13.1469(7) Å, 90°	13.1094(6) Å, 90°	20.517(1) Å, 90°
b, β	10.1572(5) Å, 106.758°	10.2261(4) Å, 107.213(2)°	10.9607(5) Å, 103.321(2)°
c, γ	15.2069(7) Å, 90°	16.9095(8) Å, 90°	22.2621(9) Å, 90°
Volume	1944.42(17)	2165.32(17)	4871.6(4)
Z	4	4	4
Density (calculated)	1.529 g/cm^3	1.584 g/cm^3	1.490 g/cm^3
Absorption coefficient	1.548 mm^{-1}	1.641 mm^{-1}	0.651 mm^{-1}
F(000)	912	1040	2240
Crystal size	0.235×0172×0.061 mm^3	0.230×0.158×0.084 mm^3	0.356×0.092×0.040 mm^3
θ range	26.03 – 2.42°	26.35 – 2.36 °	26.03 – 2.41°
Index ranges	h = -16→16, k = -12→12, l = -18→18	h = -16→16, k = -12→12, l = - 21→20	h = -25→25, k = -13→13, l = -27→27
No. Reflections	9895	9008	9634
Independent reflections	3844	4431	9885
Completeness Absorption	99.9%	100%	99.8%
Correction	multi-scan	multi-scan	mutli-scan
Max. and min. trans.	0.754 and 0.668	0.7454 and 0.6518	0.7453 and 0.6556
Data / restraints / param.	3844 / 0 / 244	4431 / 0 / 263	9634 / 0 / 614
GOF on F^2	1.029	1.033	1.025
Final R indices [I>2σ(I)]	R1: 0.0297, wR2: 0.0606	R1: 0.0281, wR2: 0.0580	R1: 0.0358, wR2: 0.0750
R indices (all data)	R1: 0.0447, wR2: 0.0658	R1: 0.0435, wR2: 0.0634	R1: 0.0531, wR2: 0.0836
Largest diff. peak and hole	0.319 and -0.386 e•Å^{-3}	0.306 and -0.305 e•Å^{-3}	0.413 and -0.557 e•Å^{-3}

	12a	**12b**	**13**
Empirical formula	$C_{42}H_{34}ClCuN_6$•$CuCl_2$	$C_{42}H_{30}Cl_5CuN_6$•$CuCl_2$	$(C_{21}H_{15}Cl_4CuN_3)_2$
Formula weight	856.18	993.95	1029.4
Temperature	100(2) K	100(2) K	100(2) K
Wavelength	0.71073 Å	0.71073 Å	1.54178 Å
Crystal system	triclinic	monoclinic	monoclinic
Space group	P1	C2/c	P21/c
a, α	8.7269 (9) Å, 89.790°	12.9845(11) Å, 90°	10.8071(5) Å, 90°
b, β	9.1324 (10) Å, 77.537°	12.1905(9) Å, 99.004(3)°	15.5975(7) Å, 103.827(2)°
c, γ	11.8003 (12) Å, 79.714°	24.998(2) Å, 90°	11.9494(5) Å, 90°
Volume	902.94	3908.1(5)	1955.87(15)
Z	1	4	4
Density (calculated)	1.575 g/cm^3	1.689 g/cm^3	1.748 g/cm^3
Absorption coefficient	1.441 mm^{-1}	1.610 mm^{-1}	6.718 mm^{-1}
F(000)	437	2004	1036
Crystal size	0.262×0.203×0.060 mm^3	0.212×0.166×0.034 mm^3	0.125×0.043×0.032 mm^3
θ range	26.25 – 2.27°	26.30 – 2.36°	69.97 – 4.21°
Index ranges	h = -10→10, k = -11→11, l = -14→14	h = -16→16, k = -15→15, l = - 31→31	h = -13→13, k = -19→19, l = - 14→14
No. Reflections	9927	9946	9896
Independent reflections	3707	4026	3702
Completeness Absorption	100%	99.0%	99.9%
Correction	mutli-scan	multi-scan	mutli-scan
Max. and min. trans.	0.7454 and 0.6696	0.7457 and 0.6713	70.109 and 67.679
Data / restraints / param.	3707 / 3 / 481	4026 / 0 / 261	3702 / 0 / 263
GOF on F^2	1.069	1.080	1.073
Final R indices [I>2σ(I)]	R1: 0.0388, wR2: 0.0890	R1: 0.0445, wR2: 0.0624	R1: 0.0286, wR2: 0.0745
R indices (all data)	R1: 0.0440, wR2: 0.0915	R1: 0.0871, wR2: 0.0949	R1: 0.0332, wR2: 0.0771
Largest diff. peak and hole	0.456 and -0.677 e•Å^{-3}	0.384 and -0.779 e•Å^{-3}	0.392 and -0.540 e•Å^{-3}

APPENDIX B: COPYRIGHT PERMISSION

As indicated by the Royal Society of Chemistry[105] (RSC), no permission requests are needed to reproduce material I have jointly authored in *Green Chemistry*.[48]

For works I jointly authored in *Molecules*[86] "copyright is retained by the authors. Articles are licensed under an open access Creative Commons CC BY 4.0 license" and "in addition, the article may be reused and quoted provided that the original published version is cited. These conditions allow for maximum use and exposure of the work, while ensuring that the authors receive proper credit."[106]

REFERENCES

(1) Boa, A. N.; McPhillie, M. J. In *Comprehensive Heterocyclic Chemistry IV*; 2022; Vol. 13, pp 243–268. doi.org/10.1016/b978-0-12-818655-8.00110-4

(2) Zhang, S.; Xing, Q.; Sun, W. H. *RSC Adv.* **2016**, *6*, 72170–72176. doi.org/10.1039/c6ra13048h

(3) Hernández-Méndez, J.; González-Pérez, C.; González-Martín, M. I. *Microchem. J.* **1985**, *31*, 94–101.

(4) Kim, J. J.; Gharpure, A.; Teng, J.; Zhuang, Y.; Howard, R. J.; Zhu, S.; Noviello, C. M.; Walsh, R. M.; Lindahl, E.; Hibbs, R. E. *Nature* **2020**, *585*, 303–308. doi.org/10.1038/s41586-020-2654-5

(5) Olfson, M.; King, M.; Schoenbaum, M. *JAMA Psychiatry* **2015**, *72*, 136–142. doi.org/10.1001/jamapsychiatry.2014.1763

(6) Shinfuku, M.; Kishimoto, T.; Uchida, H.; Suzuki, T.; Mimura, M.; Kikuchi, T. *International Clinical Psychopharmacology* **2019**, *34*, 211–221. doi.org/10.1097/YIC.0000000000000276

(7) Schmitz, A. *Mental Health Clinician* **2016**, *6*, 120–126. doi.org/10.9740/mhc.2016.05.120

(8) National Collaborating Centre for Mental Health. *Generalised Anxiety Disorder in Adults: The NICE Guideline on Management in Primary, Secondary and Community Care*; The British Psychological Society and The Royal College of Psychiatrists, 2011.

(9) *Practice Guideline for the Treatment of Patients with Panic Disorder*, 2nd ed.; American Psychiatric Association, 2010.

(10) Tan, K. R.; Brown, M.; Labouébe, G.; Yvon, C.; Creton, C.; Fritschy, J. M.; Rudolph, U.; Lüscher, C. *Nature* **2010**, *463*, 769–774. doi.org/10.1038/nature08758

(11) Borda, M. G.; Jaramillo-Jimenez, A.; Oesterhus, R.; Santacruz, J. M.; Tovar-Rios, D. A.; Soennesyn, H.; Cano-Gutierrez, C. A.; Vik-Mo, A. O.; Aarsland, D. *International Journal of Geriatric Psychiatry* **2021**, *36*, 917–925. doi.org/10.1002/gps.5494

(12) Billioti, S.; Bégaud, B.; Bazin, F.; Verdoux, H.; Dartigues, J. F.; Pérès, K.; Kurth, T.; Pariente, A. *BMJ* **2012**, *345*, 1–12. doi.org/10.1136/bmj.e6231

(13) Arora, N.; Dhiman, P.; Kumar, S.; Singh, G.; Monga, V. *Bioorg. Chem.* **2020**, *97*, 103668. doi.org/10.1016/j.bioorg.2020.103668

(14) National Institutes of Health (U.S.). Office of Communications and Public Liaison. Benzodiazepine Often Used in Older People Despite Risks https://www.nih.gov/news-events/nih-research-matters/benzodiazepine-often-used-older-people-despite-risks (accessed Feb 28, 2021).

(15) Consumer medicine information. https://www.nps.org.au/ medicine-finder/lexotan-tablets (accessed Nov 24, 2021).

(16) Bastide, A.; de Codt, A.; Monhonval, P.; Bongaerts, X.; Tecco, J. M. *Psychiatria Danubina* **2016**, *28*, 154–158.

(17) Shoar, N. S.; Bistas, K. G.; Saadabadi, A. *Flumazenil*; StatPearls Publishing: Treasure Island, 2021

(18) American Psychiatric Association. *The American Psychiatric Association Practice Guideline for the Treatment of Patients With Schizophrenia*, 3rd ed.; American Psychiatric Association, 2020.

(19) Jamil, A.; Levinson, N.; Gelfand, M.; Hill, C. E.; Khankhanian, P.; Davis, K. A. *Neurology Clinical Practice* **2021**, *11*, e669–e676. doi.org/10.1212/cpj.0000000000000992

(20) An, Y. S.; Hao, Z. F.; Zhang, X. J.; Wang, L. Z. *Chem. Biol. Drug Des.* **2016**, 110–121. doi.org/10.1111/cbdd.12739

(21) Fader, L. D.; Bethell, R.; Bonneau, P.; Bös, M.; Bousquet, Y.; Cordingley, M. G.; Coulombe, R.; Deroy, P.; Faucher, A. M.; Gagnon, A.; Goudreau, N.; Grand-Maître, C.; Guse, I.; Hucke, O.; Kawai, S. H.; Lacoste, J. E.; Landry, S.; Lemke, C. T.; Malenfant, E.; Mason, S.; Morin, S.; O'Meara, J.; Simoneau, B.; Titolo, S.; Yoakim, C. *Bioorg. Med. Chem. Lett.* **2011**, *21*, 398–404. doi.org/10.1016/j.bmcl.2010.10.131

(22) Roberts, K.; Ursini, A.; Barnaby, R.; Cassar, P. G.; Corsi, M.; Curotto, G.; Donati, D.; Feriani, A.; Finizia, G.; Marchioro, C.; Niccolai, D.; Oliosi, B.; Polinelli, S.; Ratti, E.; Reggiani, A.; Tedesco, G.; Tranquillini, M. E.; Trist, D. G.; Van Amsterdam, F. T. M. *Bioorg. Med. Chem.* **2011**, *19*, 4257–4273. doi.org/10.1016/j.bmc.2011.05.057

(23) National Center for Information Biotechnology. PubChem Compound Summary for CID 4463. https://pubchem.ncbi.nlm.nih.gov/compound/Nevirapine (accessed Dec 14, 2021). doi.org/10.5517/ccpt3wg

(24) Lloyd, D.; McNab, H. *Adv. Heterocycl. Chem.* **1998**, *71*, 1–56. doi.org/doi.org/10.1016/S0065-2725(08)60830-2

(25) Essassi, E. M.; Lamkadem, A.; Zniber, R. *Bull. Soc. Chim. Belg.* **1991**, *100*, 277–286. doi.org/doi.org/10.1002/bscb.19911000313

(26) Qomi, H. R.; Habibi, A.; Shahcheragh, S. M. *Spectrochim. Acta - Part A Mol. Biomol. Spectrosc.* **2017**, *174*, 164–170. doi.org/10.1016/j.saa.2016.11.028

(27) Aquino, C. J.; Armour, D. R.; Berman, J. M.; Birkemo, L. S.; Carr, R. A. E.; Croom, D. K.; Dezube, M.; Dougherty, R. W. J.; Ervin, G. N.; Grizzle, M. K.; Head, J. E.; Hirst, G. C.; James, M. K.; Johnson, M. F.; Miller, L. J.; Queen, K. L.; Rimele, T. J.; Smith, D. N.; Sugg, E. E. *J. Med. Chem.* **1996**, *39*, 5236–5245. doi.org/10.1021/jm9601664

(28) Hirst, G. C.; Aquino, C.; Birkemo, L.; Croom, D. K.; Dezube, M.; Dougherty, R. W.; Ervin, G. N.; Grizzle, M. K.; Henke, B.; James, M. K.; Johnson, M. F.; Momtahen, T.; Queen, K. L.; Sherrill, R. G.; Szewczyk, J.; Willson, T. M.; Sugg, E. E. *J. Med. Chem.* **1996**, *39*, 5236–5245. doi.org/10.1021/jm9601664

(29) Ursini, A.; Capelli, A. M.; Carr, R. A. E.; Cassarà, P.; Corsi, M.; Curcuruto, O.; Curotto, G.; Cin, M. D.; Davalli, S.; Donati, D.; Feriani, A.; Finch, H.; Finizia, G.; Gaviraghi, G.; Marien, M.; Pentassuglia, G.; Polinelli, S.; Ratti, E.; Reggiani, A.; Tarzia, G.; Tedesco, G.; Tranquillini, M. E.; Trist, D. G.; Van Amsterdam, F. T. M. *J. Med. Chem.* **2000**, *43*, 3596–3613. doi.org/10.1021/jm990967h

(30) Hadac, E. M.; Dawson, E. S.; Darrow, J. W.; Sugg, E. E.; Lybrand, T. P.; Miller, L. J. *J. Med. Chem.* **2006**, *49*, 850–863. doi.org/10.1021/jm049072h

(31) Taylor, A. M.; Vaswani, R. G.; Gehling, V. S.; Hewitt, M. C.; Leblanc, Y.; Audia, J. E.; Bellon, S.; Cummings, R. T.; Coîté, A.; Harmange, J. C.; Jayaram, H.; Joshi, S.; Lora, J. M.; Mertz, J. A.; Neiss, A.; Pardo, E.; Nasveschuk, C. G.; Poy, F.; Sandy, P.; Setser, J. W.; Sims, R. J.; Tang, Y.; Albrecht, B. K. *ACS Med. Chem. Lett.* **2016**, *7*, 145–150. doi.org/10.1021/ml500411h

(32) Gümüş, M. *J. Heterocycl. Chem.* **2021**, *58*, 1943–1954. doi.org/10.1002/jhet.4320

(33) Vaddula, B. R.; Varma, R. S.; Leazer, J. *Tetrahedron Lett.* **2013**, *54*, 1538–1541. doi.org/10.1016/j.tetlet.2013.01.029

(34) Nájera, C.; Sydnes, L. K.; Yus, M. *Chem. Rev.* **2019**, *119*, 11110–11244. doi.org/10.1021/acs.chemrev.9b00277

(35) Willy, B.; Dallos, T.; Rominger, F.; Schönhaber, J.; Müller, T. J. J. *Eur. J. Org. Chem.* **2008**, 4796–4805. doi.org/10.1002/ejoc.200800619

(36) Solan, A.; Nişanci, B.; Belcher, M.; Young, J.; Schäfer, C.; Wheeler, K. A.; Török, B.; Dembinski, R. *Green Chem.* **2014**, *16*, 1120–1124. doi.org/10.1039/c3gc41898g

(37) Young, J.; Schäfer, C.; Solan, A.; Baldrica, A.; Belcher, M.; Nişanci, B.; Wheeler, K. A.; Trivedi, E. R.; Török, B.; Dembinski, R. *RSC Adv.* **2016**, *6*, 107081–107093. doi.org/10.1039/c6ra24291j

(38) Braun, R. U.; Zeitler, K.; Müller, T. J. J. *Org. Lett.* **2000**, *2*, 4181–4184. doi.org/10.1021/ol006721k

(39) Palimkar, S. S.; Lahoti, R. J.; Kumar, S. V. *Green Chem.* **2007**, *9*, 146–152. doi.org/10.1039/b610523h

(40) Atobe, S.; Masuno, H.; Sonoda, M.; Suzuki, Y.; Shinohara, H.; Shibata, S.; Ogawa, A. *Tetrahedron Lett.* **2012**, *53*, 1764–1767. doi.org/10.1016/j.tetlet.2012.01.105

(41) Vanitcha, A.; Gontard, G.; Vanthuyne, N.; Derat, E.; Mouriès-Mansuy, V.; Fensterbank, L. *Adv. Synth. Catal.* **2015**, *357*, 2213–2218. doi.org/10.1002/adsc.201500345

(42) Friel, D. K.; Snapper, M. L.; Hoveyda, A. H. *J. Am. Chem. Soc.* **2008**, *130*, 9942–9951. doi.org/10.1021/ja802935w

(43) Pithadia, A. S.; Kochi, A.; Soper, M. T.; Beck, M. W.; Liu, Y.; Lee, S.; Detoma, A. S.; Ruotolo, B. T.; Lim, M. H. *Inorg. Chem.* **2012**, *51*, 12959–12967. doi.org/10.1021/ic302084g

(44) Nishigaya, Y.; Umei, K.; Saito, Y.; Watanabe, H.; Kondo, T.; Kondo, A.; Kawamura, N.; Tatani, K.; Kohno, Y.; Tanaka, N.; Seto, S. *Bioorg. Med. Chem. Lett.* **2017**, *27*, 4044–4050. doi.org/10.1016/j.bmcl.2017.07.055

(45) Rajkiewicz, A. A.; Wojciechowska, N.; Kalek, M. *ACS Catal.* **2020**, *10*, 831–841. doi.org/10.1021/acscatal.9b04394

(46) Cox, R. J.; Ritson, D. J.; Dane, T. A.; Berge, J.; Charmant, J. P. H.; Kantacha, A. *Chem. Commun.* **2005**, 1037–1039. doi.org/10.1039/b414826f

(47) Obulesu, O.; Murugesh, V.; Harish, B.; Suresh, S. *J. Org. Chem.* **2018**, *83*, 6454–6465. doi.org/10.1021/acs.joc.8b00746

(48) Mishra, M.; Twardy, D.; Ellstrom, C.; Wheeler, K. A.; Dembinski, R.; Török, B. *Green Chem.* **2019**, *21*, 99–108. doi.org/10.1039/c8gc02520g

(49) Gazvoda, M.; Virant, M.; Pinter, B.; Košmrlj, J. *Nat. Commun.* **2018**, *9*, 1–9. doi.org/10.1038/s41467-018-07081-5

(50) Willy, B.; Müller, T. *Curr. Org. Chem.* **2009**, *13*, 1777–1790. doi.org/10.2174/138527209789630479

(51) Steed, J. W.; Atwood, J. L. *Supramolecular Chemistry*, 2nd ed.; John Wiley & Sons: Southern Gate, Chichester, West Sussex, U.K., 2009.

(52) Sniady, A.; Morreale, M. S.; Dembinski, R. *Org. Synth.* **2007**, *84*, 199–208; Coll. **2009**, *11*, 794-801. doi.org/10.15227/orgsyn.084.0199

(53) Spectral Database for Organic Compounds Triethylamine Hydrochloride https://sdbs.db.aist.go.jp/sdbs/cgi-bin/direct_frame_top.cgi (accessed Dec 2, 2021).

(54) da Silva, A. V.; Meneghetti, S. M. P.; Meneghetti, M. R. *Molecules* **2021**, *26*. doi.org/10.3390/molecules26092796

(55) Mosset, A.; Tuchagues, J. P.; Bonnet, J. J.; Haran, R.; Sharrock, P. *Inorg. Chem.* **1980**, *19*, 290–294. doi.org/10.1021/ic50204a003

(56) Mansour, A. M.; Shehab, O. R. *Appl. Organomet. Chem.* **2017**, *31*, 28–34. doi.org/10.1002/aoc.3635

(57) Zhang, S.; Vystorop, I.; Tang, Z.; Sun, W. H. *Organometallics* **2007**, *26*, 2456–2460. doi.org/10.1021/om070062z

(58) Zhang, S.; Sun, W. H.; Kuang, X.; Vystorop, I.; Yi, J. *J. Organomet. Chem.* **2007**, *692*, 5307–5316. doi.org/10.1016/j.jorganchem.2007.08.020

(59) Tang, X.; Cui, Y.; Sun, W. H.; Miao, Z.; Yan, S. *Polym. Int.* **2004**, *53*, 2155–2161. doi.org/10.1002/pi.1646

(60) Furuhashi, A.; Komatsu, S.; Ouchi, A. *Bull. Chem. Soc. Jpn.* **1972**, *45*, 2942–2943.

(61) Basavaraju, B.; Bhojya Naik, H. S.; Prabhakara, M. C. *Bioinorg. Chem. Appl.* **2007**. doi.org/10.1155/2007/42587

(62) Sharma, N. N. N.; Sharma, N. N. N. *Orbital Electron. J. Chem.* **2010**, *2*, 277–287.

(63) Stiefel, E.; Valentine, J.; Gray, H.; Bertini, I. *Biological Inorganic Chemistry, Structure and Reactivity*; University Science Books: Saulsalito, 2007.

(64) Zalkin, A.; Ruben, H.; Templeton, D. H.; *Acta Crystallogr.* **1964**, *17*, 235–240. doi.org/10.1107/S0365110X64000603

(65) Bleackley, M. R.; MacGillivray, R. T. A. *BioMetals* **2011**, *24*, 785–809. doi.org/10.1007/s10534-011-9451-4

(66) Benoit, S. L.; Miller, E. F.; Maier, R. J. *Infect. Immun.* **2013**, *81*, 580–584. doi.org/10.1128/IAI.00858-12

(67) Talukder, M. M.; Cue, J. M. O.; Miller, J. T.; Gamage, P. L.; Aslam, A.; McCandless, G. T.; Biewer, M. C.; Stefan, M. C. *ACS Omega* **2020**, *5*, 24018–24032. doi.org/10.1021/acsomega.0c03415

(68) Višnjevac, A.; Tušek-Božić, L.; Majerić-Elenkov, M.; Šunjić, V.; Kojić-Prodić, B. *Eur. J. Inorg. Chem.* **2001**, 2647–2654. doi.org/10.1002/1099-0682(200109)2001:10%3C2647::AID-EJIC2647%3E3.0.CO;2-D

(69) Claramunt, R. M.; Alkorta, I.; Elguero, J. *Comput. Theor. Chem.* **2013**, *1019*, 108–115. doi.org/10.1016/j.comptc.2013.07.002

(70) Aversa, M. C.; Bonaccorsi, P.; Cusumano, M.; Giannetto, P.; Minniti, D. *J. Chem. Soc., Dalton Trans.* **1991**, 3431–3434. doi.org/doi.org/10.1039/DT9910003431

(71) Pérez, J.; Riera, V.; Rodríguez, A.; Miguel, D. *Organometallics* **2002**, *21*, 5437–5438. doi.org/10.1021/om0205288

(72) Haketa, Y.; Miyasue, M.; Kobayashi, Y.; Sato, R.; Shigeta, Y.; Yasuda, N.; Tamai, N.; Maeda, H. *J. Am. Chem. Soc.* **2020**, *142*, 16420–16428. doi.org/10.1021/jacs.0c07751

(73) Višnjevac, A; Tušek-Božić, L; Majerić-Elenkov, M; Hameršak, Z.; Kooijman, H.; De Clercq, E.; Kojić-Prodić, B. *Polyhedron* **2002**, *21*, 2567–2577. doi.org/10.1016/S0277-5387(02)01251-2

(74) Correia Dos Santos, M. M.; Famila, V.; Simões Gonçalves, M. L. *Anal. Biochem.* **2002**, *303*, 111–119. doi.org/10.1006/abio.2002.5580

(75) La Placa, S. J.; Ibers, J. A. *Inorg. Chem.* **1965**, *4*, 778–783. doi.org/10.1021/ic50028a002.

(76) Pickering, I. J.; George, G. N. *Inorg. Chem.* **1995**, *34*, 3142–3152. doi.org/10.1021/ic00116a004

(77) Addison, A. W.; Rao, T. N.; Reedijk, J.; Rijn, J. van; Verschoor, G. C. *J. Chem. Soc. Dalt. Trans.* **1984**, 1349–1356. doi.org/10.1039/DT9840001349

(78) Grau, J.; Caubet, A.; Roubeau, O.; Montpeyó, D.; Lorenzo, J.; Gamez, P. *ChemBioChem* **2020**, *21*, 2348–2355. doi.org/10.1002/cbic.202000154

(79) Rivlin, M.; Eliav, U.; Navon, G. *J. Phys. Chem. B* **2015**, *119*, 4479–4487. doi.org/10.1021/jp513020y

(80) Hahnenstein, I.; Hasse, H.; Kreiter, C. G.; Maurer, G. *Ind. Eng. Chem. Res.* **1994**, *33*, 1022–1029. doi.org/10.1021/ie00028a033

(81) Jafari, N.; Zeinali, S. *ACS Omega* **2020**, *5*, 4395–4402. doi.org/10.1021/acsomega.9b03124

(82) Blackman, A. G.; Schenk, E. B.; Jelley, R. E.; Krenske, E. H.; Gahan, L. R. *Dalt. Trans.* **2020**, *49*, 14798–14806. doi.org/10.1039/d0dt02985h

(83) Yang, L.; Powell, D. R.; Houser, R. P. *J. Chem. Soc. Dalt. Trans.* **2007**, 955–964. doi.org/10.1039/b617136b

(84) Sun, Q.; LaVoie, E. J. *Heterocycles* **1996**, *43*, 737–743. doi.org/10.3987/Com-95-7338

(85) Garrett, C. E.; Prasad, K. *Adv. Synth. Catal.* **2004**, *346*, 889–900. doi.org/10.1002/adsc.200404071

(86) Twardy, D. J.; Wheeler, K. A.; Török, B.; Dembinski, R. *Molecules* **2022**, *27*, 2062. doi.org/10.3390/molecules27072062

(87) Liu, H.; Li, Z. *Org. Lett.* **2021**, *23*, 8407–8412. doi.org/10.1021/acs.orglett.1c03133

(88) Miao, W.-Q.; Liu, J.-Q.; Wang, X.-S. *Org. Biomol. Chem.* **2017**, *15*, 5325–5331. doi.org/10.1039/c7ob01022b

(89) Yang, B. W.; Dao, P. D. Q.; Yoon, N. S.; Cho, C. S. *J. Organomet. Chem.* **2017**, *851*, 136–142. doi.org/10.1016/j.jorganchem.2017.09.025

(90) Yang, R.; Wu, X.; Sun, S.; Yu, J.-T.; Cheng, J. *Synthesis (Stuttgart).* **2018**, *50*, 3487–3492. doi.org/10.1055/s-0037-1610124

(91) Xie, H.; Xing, Q.; Shan, Z.; Xiao, F.; Deng, G.-J. *Adv. Synth. Catal.* **2019**, *361*, 1896–1901. doi.org/10.1002/adsc.201801635

(92) Peng, J.; Shang, G.; Chen, C.; Miao, Z.; Li, B. *J. Org. Chem.* **2013**, *78*, 1242–1248. doi.org/10.1021/jo302471z

(93) Reddy, V. P.; Iwasaki, T.; Kambe, N. *Org. Biomol. Chem.* **2013**, *11*, 2249–2253. doi.org/10.1039/c3ob27396b

(94) Dyker, G.; Stirner, W.; Henkel, G. *Eur. J. Org. Chem.* **2000**, 1433–1441. doi.org/10.1002/(SICI)1099-0690(200004)2000:8<1433::AID-EJOC1433>3.0.CO;2-7

(95) Okamoto, N.; Sakurai, K.; Ishikura, M.; Takeda, K.; Yanada, R. *Tetrahedron Lett.* **2009**, *50*, 4167–4169. doi.org/10.1016/j.tetlet.2009.04.126

(96) Ouyang, H.-C.; Tang, R.-Y.; Zhong, P.; Zhang, X.-G.; Li, J.-H. *J. Org. Chem.* **2011**, *76*, 223–228. doi.org/10.1021/jo102060j

(97) Zhu, S.; Huang, H.; Zhang, Z.; Ma, T.; Jiang, H. *J. Org. Chem.* **2014**, *79*, 6113–6122. doi.org/10.1021/jo500838x

(98) Landge, S. M.; Török, B. *Catal. Lett.* **2008**, *122*, 338–343. doi.org/10.1007/s10562-007-9385-1

(99) Borkin, D. A.; Puscau, M.; Carlson, A.; Solan, A.; Wheeler, K. A.; Török, B.; Dembinski, R. *Org. Biomol. Chem.* **2012**, *10*, 4505–4508. doi.org/10.1039/c2ob25580d

(100) Roesch, K. R.; Larock, R. C. *J. Org. Chem.* **2002**, *67*, 86–94. doi.org/10.1021/jo010579z

(101) Cikotiene, I.; Buksnaitiene, R.; Sazinas, R. *Tetrahedron* **2011**, *67*, 706–717. doi.org/10.1016/j.tet.2010.11.073

(102) Chai, Z.; Xie, Z. F.; Liu, X. Y.; Zhao, G.; Wang, J.-D. *J. Org. Chem.* **2008**, *73*, 2947–2950. doi.org/10.1021/jo800029m

(103) Park, J. H.; Bhilare, S. V.; Youn, S. W. *Org. Lett.* **2011**, *13*, 2228–2231. doi.org/10.1021/ol200481u

(104) Liu, X.; Deng, G.; Liang, Y. *Tetrahedron Lett.* **2018**, *59*, 2844–2847. doi.org/10.1016/j.tetlet.2018.06.030

(105) Licences, copyright & permissions https://www.rsc.org/journals-books-databases/author-and-reviewer-hub/authors-information/licences-copyright-permissions/ (accessed Jun 5, 2022).

(106) Copyrights https://www.mdpi.com/authors/rights (accessed Jun 5, 2022).